POLITECNICO DI MILANO

*3º Encontro Nacional de **Pesquisa-Projeto-Produção** em Concreto Pré-Moldado*

ELEMENTOS PRÉ-MOLDADOS DE PEQUENAS ESPESSURAS PARA COBERTURAS: EXPERIÊNCIA ACUMULADA EM MAIS DE 20 ANOS

M. di Prisco
Department of Civil and Environmental Engineering
Politecnico di Milano

The Politecnico di Milano net

Pier Luigi Nervi

Architecture as challenge

✓A long history ... ***Ferrocement***

"We wondered if, increasing significantly the diffusion of the steel and its percentage (i.e. reinforcement ratio), it could not be possible to create a new material characterized by a higher strength and especially a larger elasticity and elongation ...".

Pier Luigi Nervi, 1940

t = 38 mm!

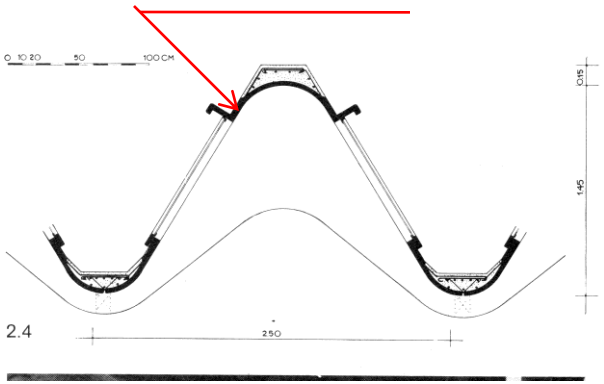

Vault span 94 m!

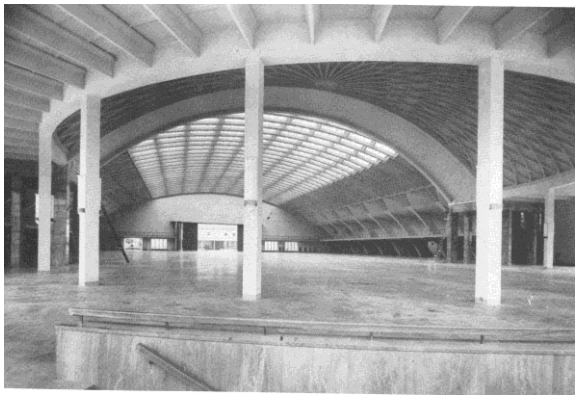

Exposition Palace: B Pavilion, Torino, 1949-50

Why fibres in the precast industry?

The connection as the weak point of the structure

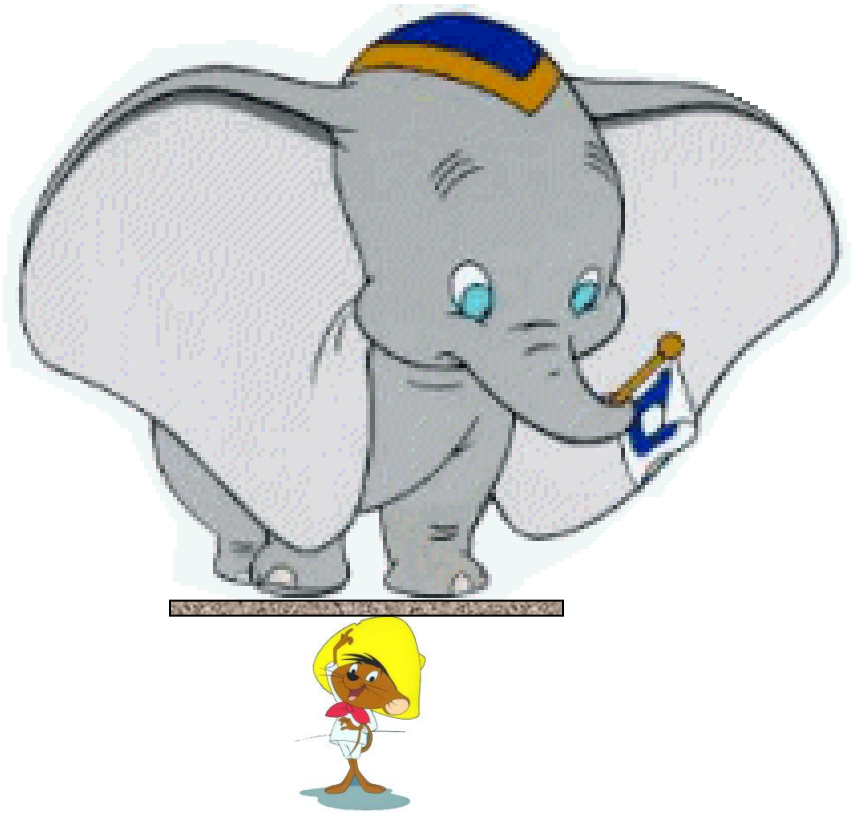


© ReLUIS 2012

Research in progress at JRC ISPRA

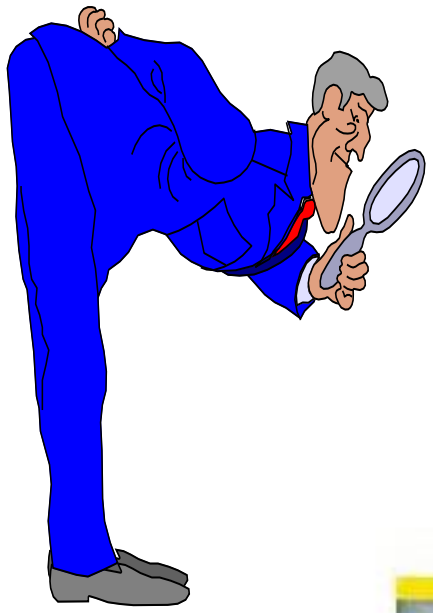

researcher

belt and braces…

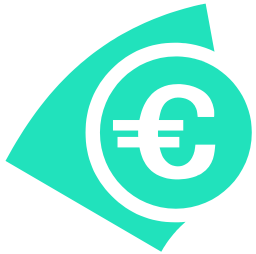

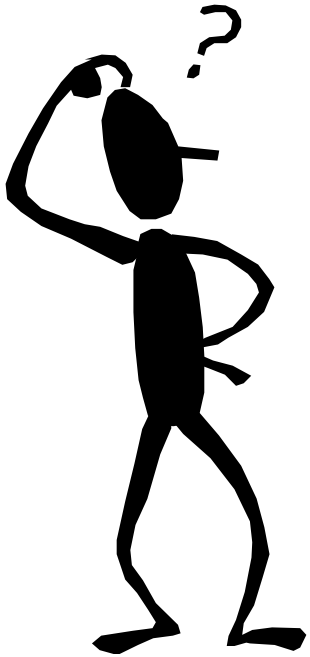

or

designer

Model Code: material and structure design

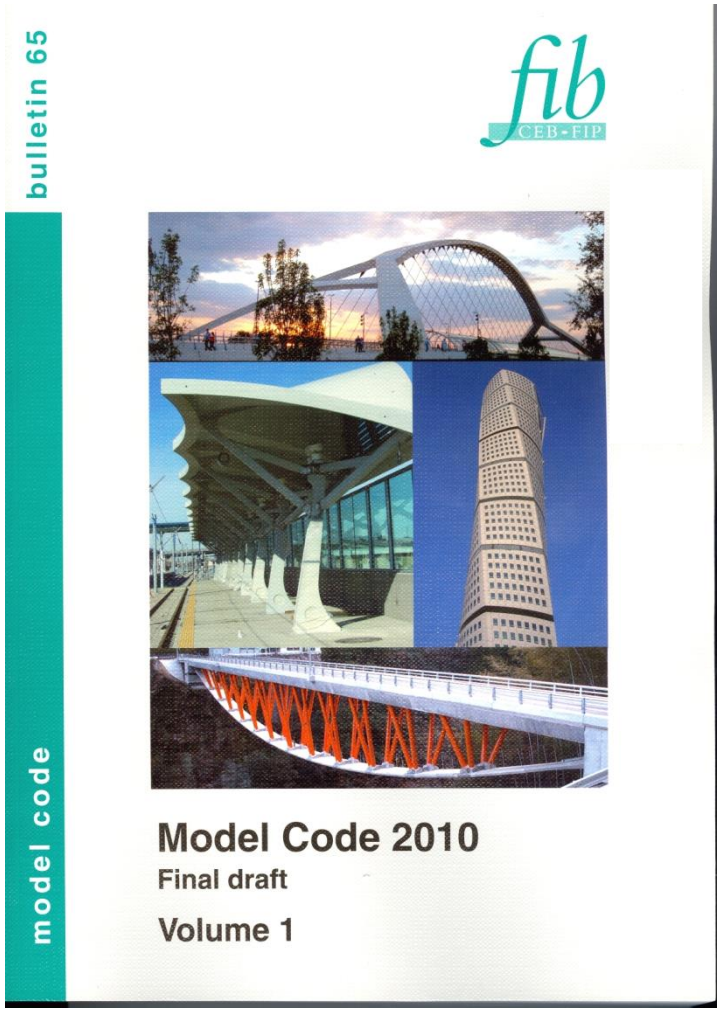

Chapter §5.6

Chapter §7.7

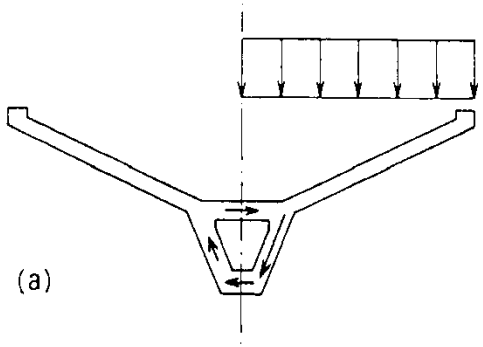
(a)

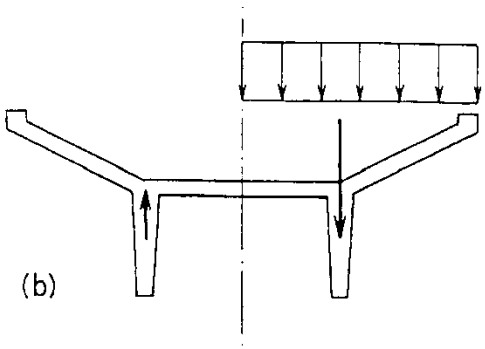
(b)

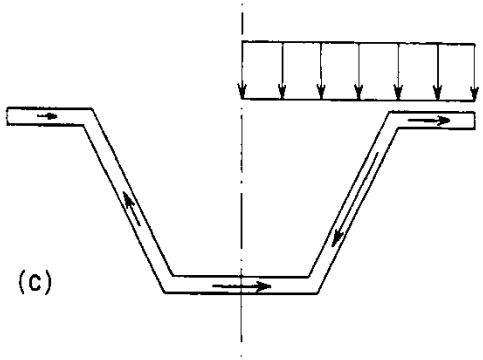
(c)

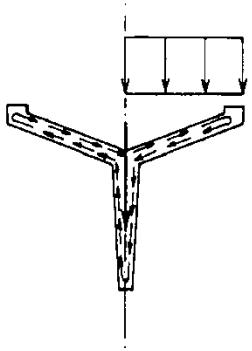
(d)

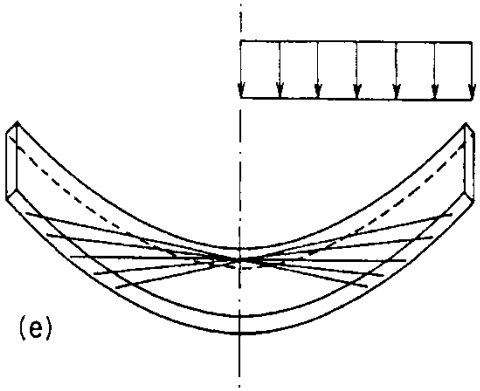
(e)

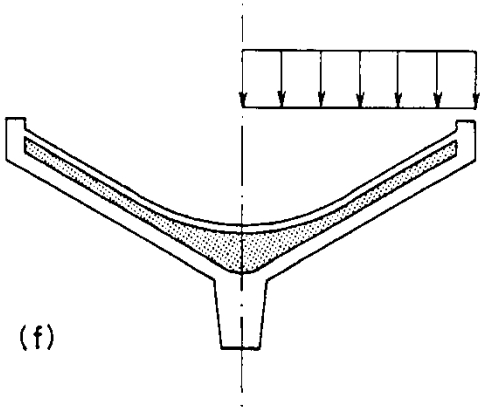
(f)

Longitudinal bending

Plane section check

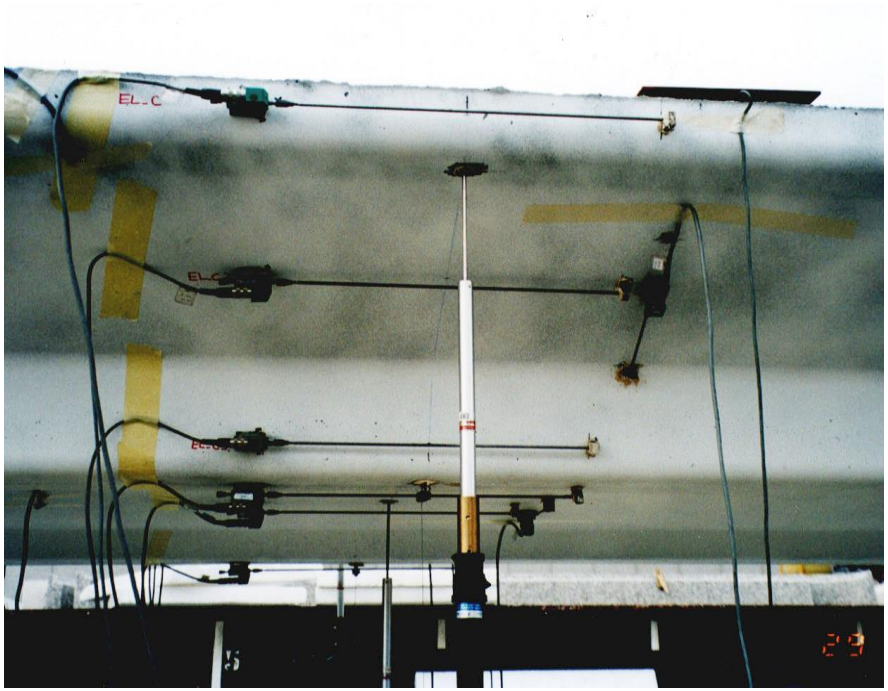

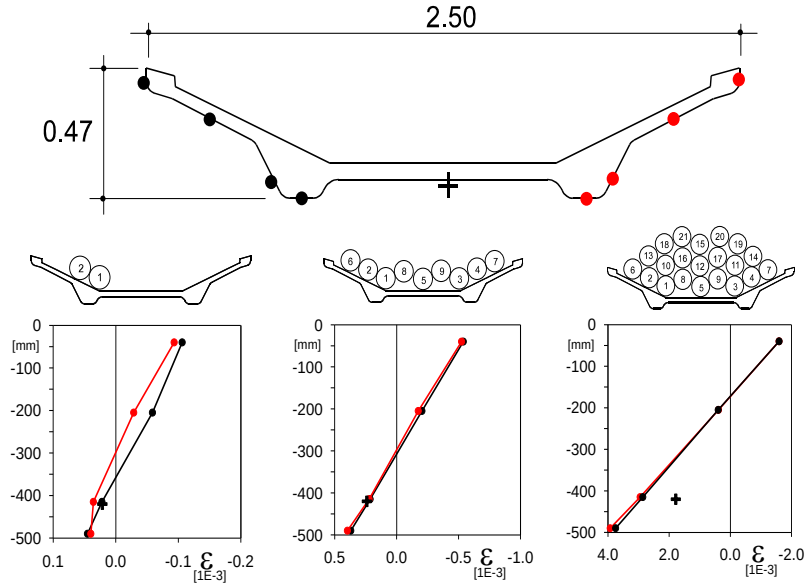

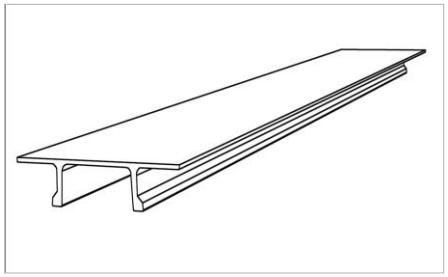

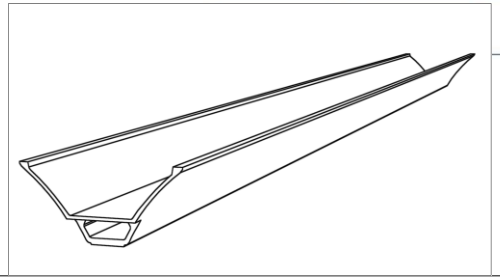

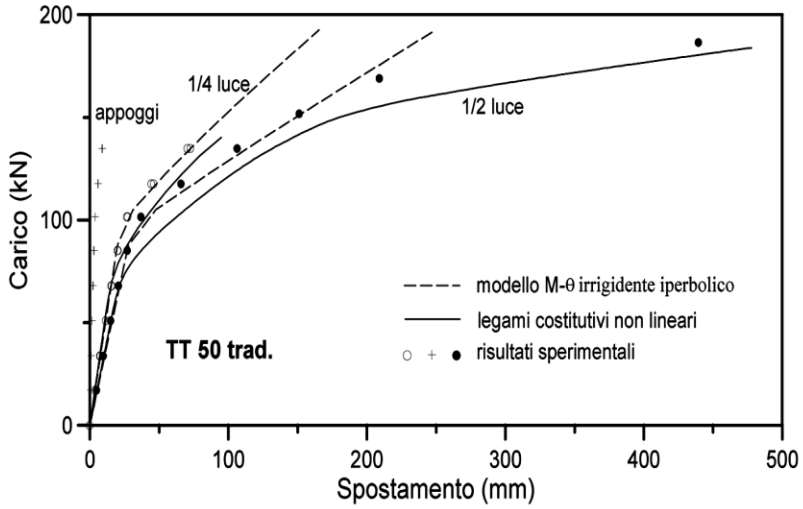
200
100
0
Carico (kN)
0
100
200
300
400
500
Spostamento (mm)
appoggi
1/4 luce
1/2 luce
TT 50 trad.
modello M-θ irrigidente iperbolico
legami costitutivi non lineari
risultati sperimentali

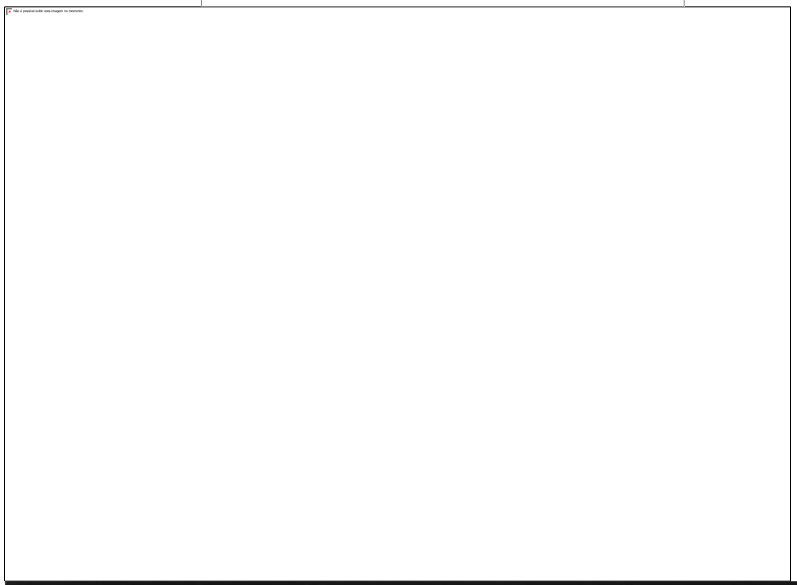

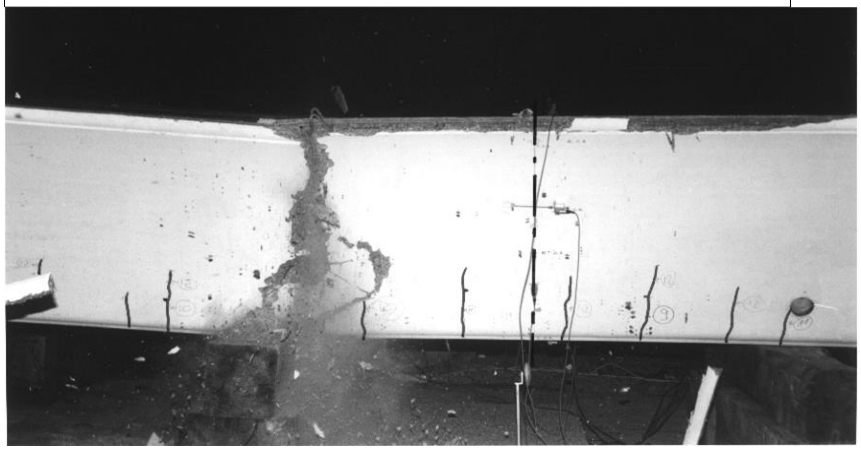

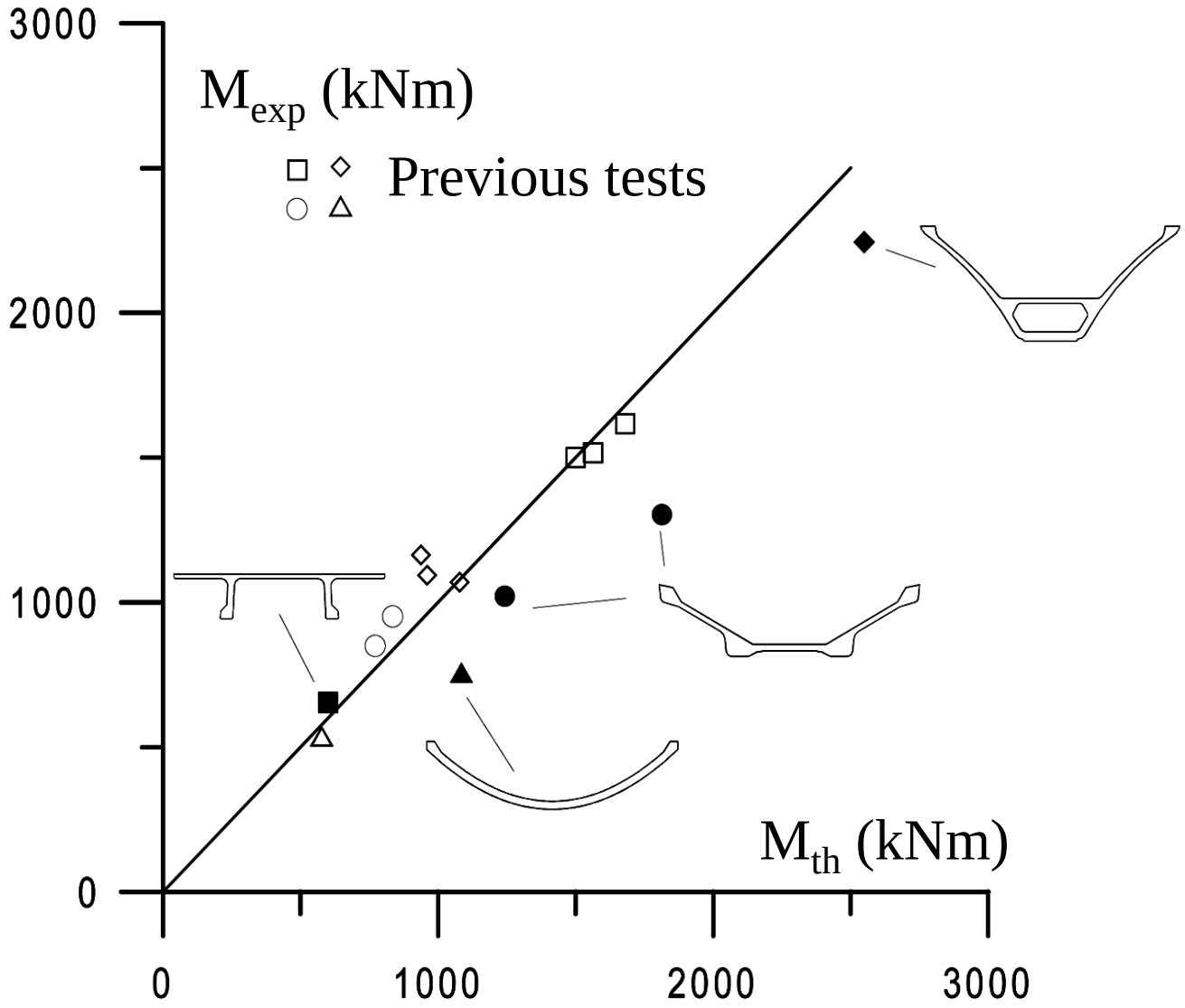
3000
2000
1000
0
M_{exp} (kNm)
Previous tests
M_{th} (kNm)
0
1000
2000
3000

Real-size tests

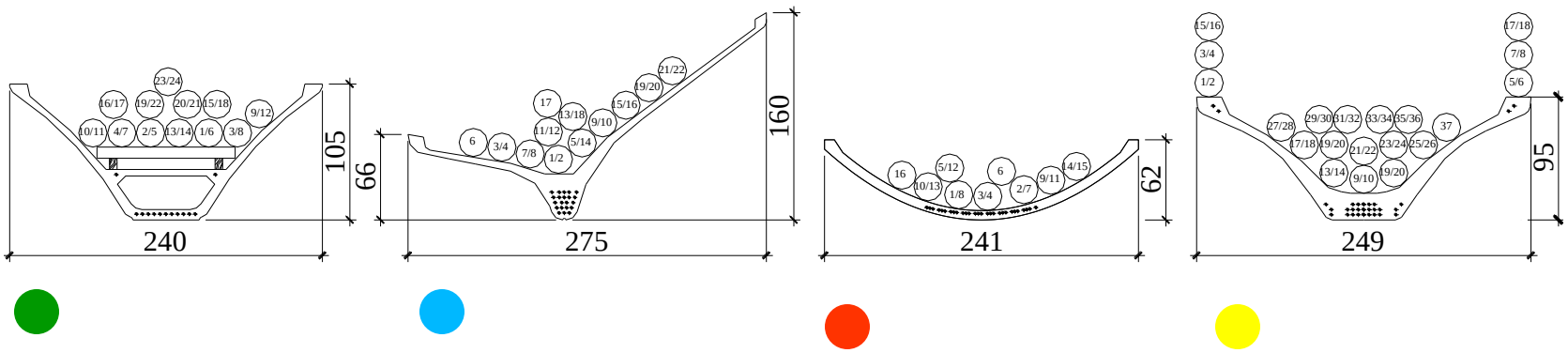

Precast Element	P_{max} [kN]	M_{CEB} [kNm]	M_{PRP} [kNm]	M_{EXP} [kNm]	Failure
T/50	502	2548.5 (+13.5%)	2484 (+10.7%)	2245	Longitudinal failure
P/60	419	2565 (+26.8%)	2461 (+20.3%)	2023	Local instability of a wing
S/50	209	1084.3 (+45.5%)	1057 (+41.8%)	745.3	Cross-section shape loss
A/50	703	2935 (-4.6%)	2905 (-5.7%)	3070	Wing failure in transversal bending

Simplified model

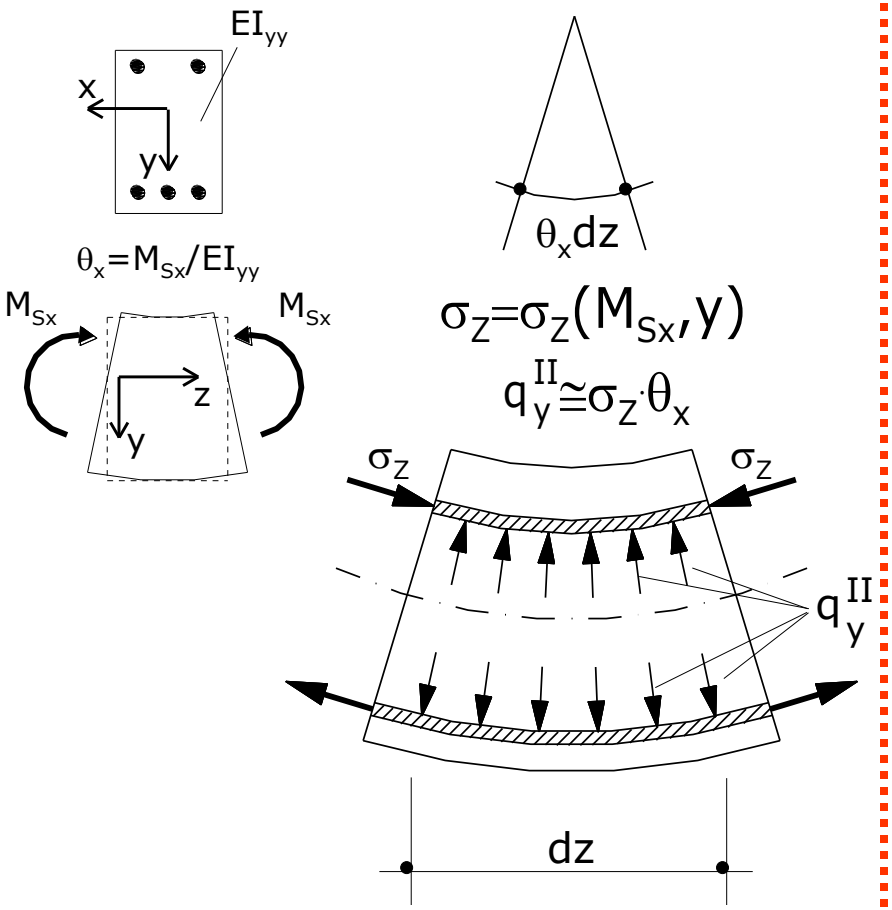

II order equilibrium

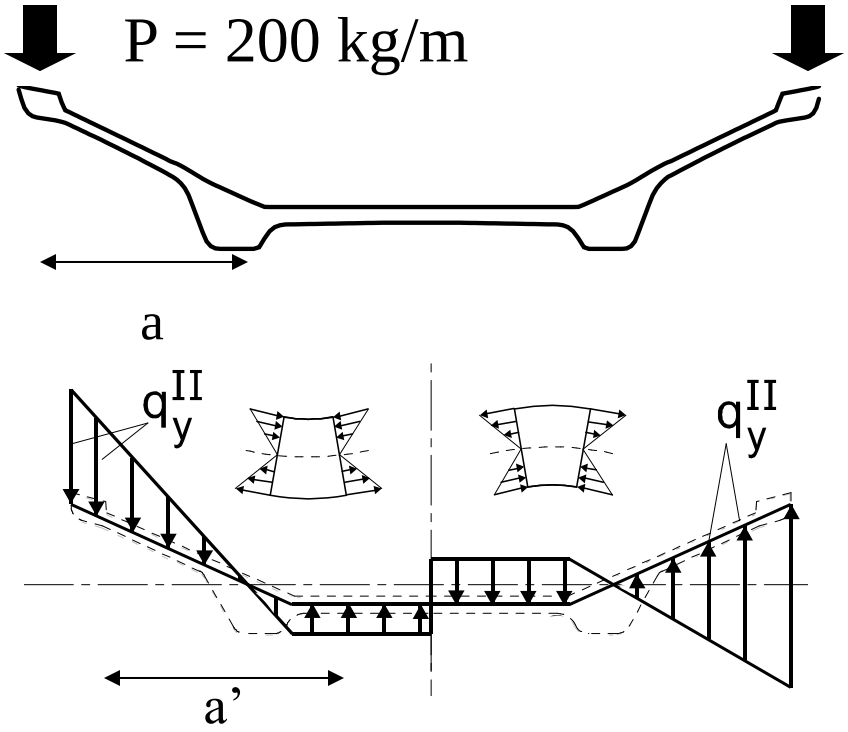

$M^I = Pa \approx 2$ N/mm*a

$M^{II} = \sigma_z * 10^4 mm^2 * 10^{-5} mm^{-1} * a' =$

$= 40 N/mm^2 * 0.1 mm * a' = 4$ N/mm*a'

Simplified model

• By assuming plane-section model compute longitudinal stresses related to longitudinal bending (mechanical non-linearity) and the longitudinal curvature in the middle section

• Compute $q^{II} = \sigma\theta$ (geometrical non-linearity)

• By considering the cross-section perfectly stiff in its plane, compute by equilibrium the transverse stresses, taking into account also q^{II}

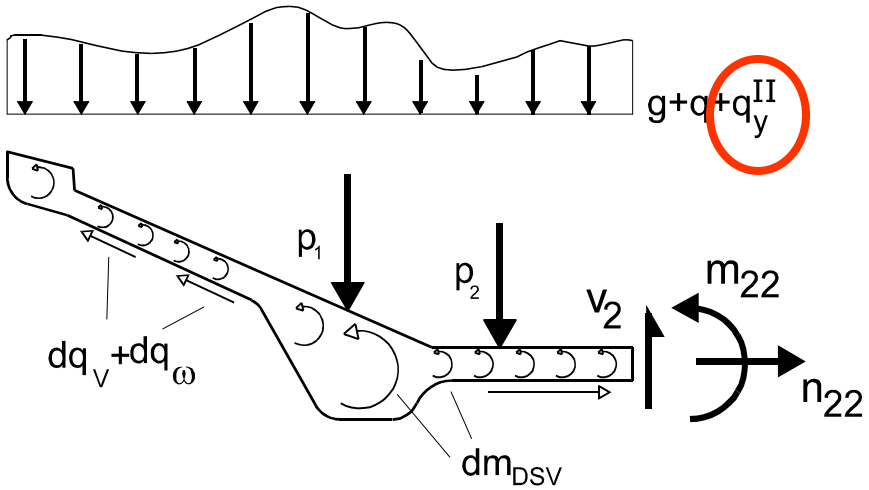

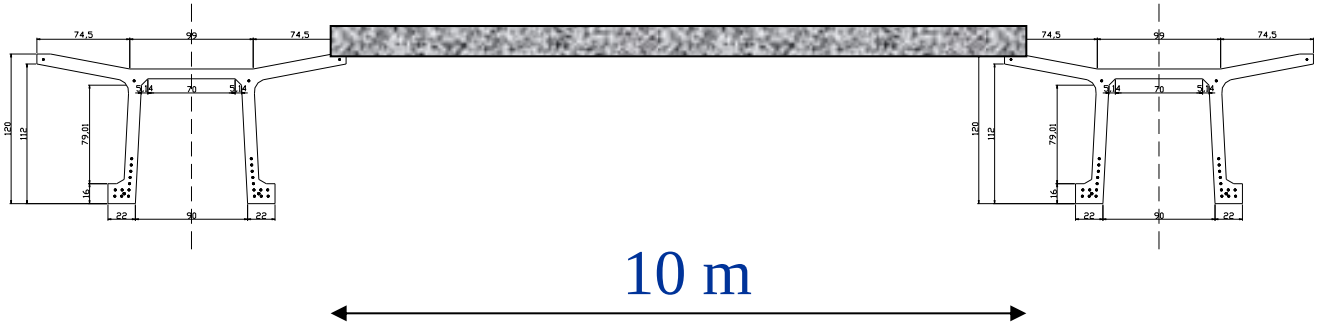
74,5
99
74,5
5,14
70
5,14
120
112
79,01
16
22
90
22

10 m

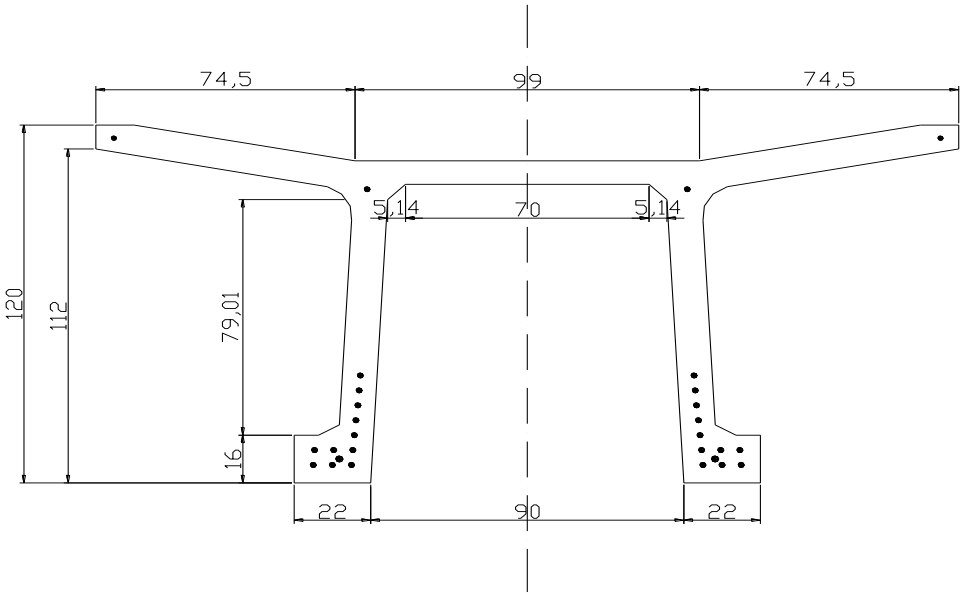
74,5
99
74,5
5,14
70
5,14
120
112
79,01
16
22
90
22

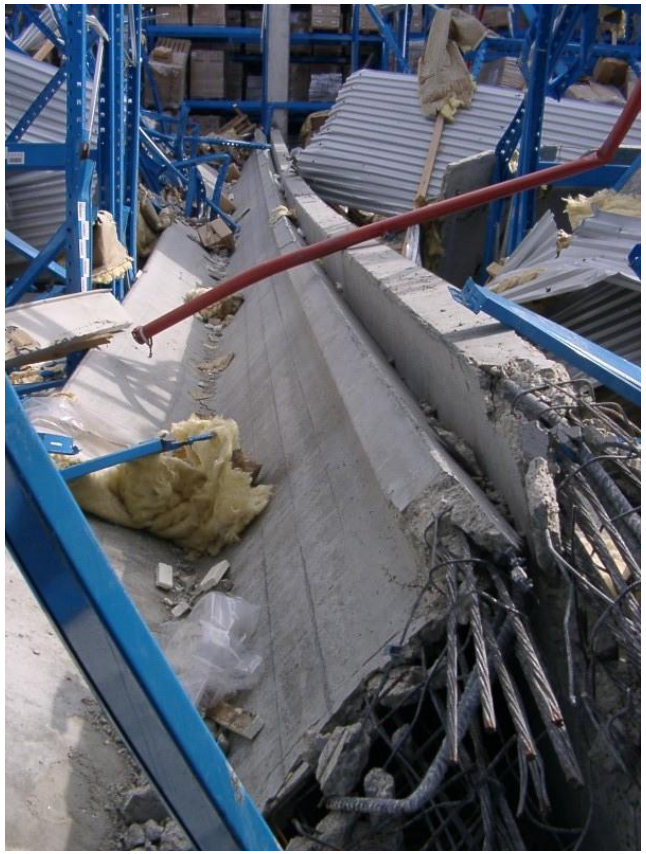

Roofing system

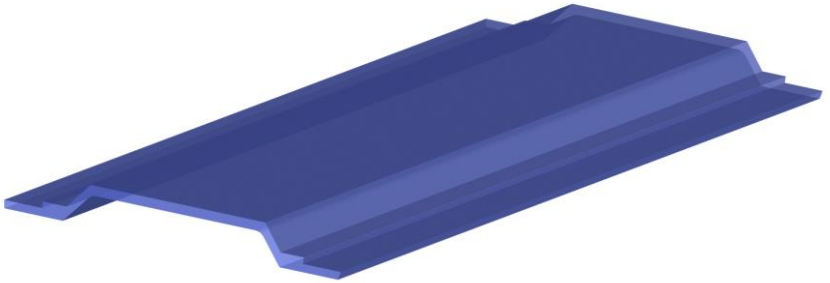

Ω roof element (10 m long)

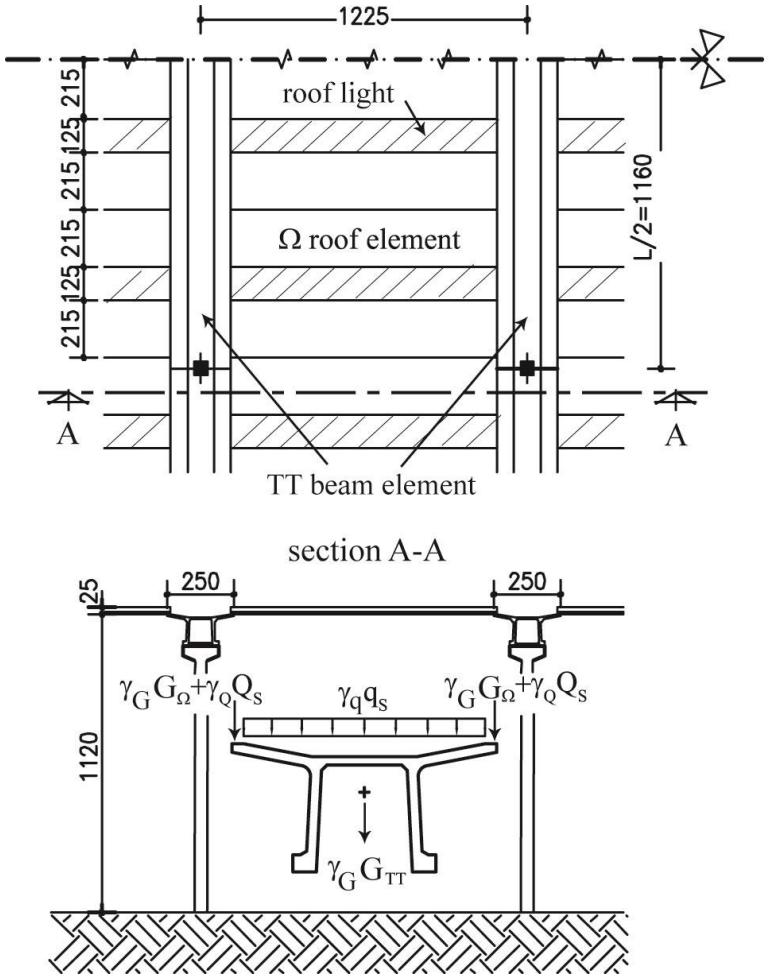

Safety factor	SLS	SLU	G_{TT} [kN/m]	G_Ω [kN/m]	Q_S [kN/m]	q_S [kN/m^2]
γ_G	1	1.4	12.30	9.84	6.67	1.33
γ_Q	1	1.5				
γ_q	1	1.5				

Longitudinal and transversal reinforce of TT beam element and Ω roof element

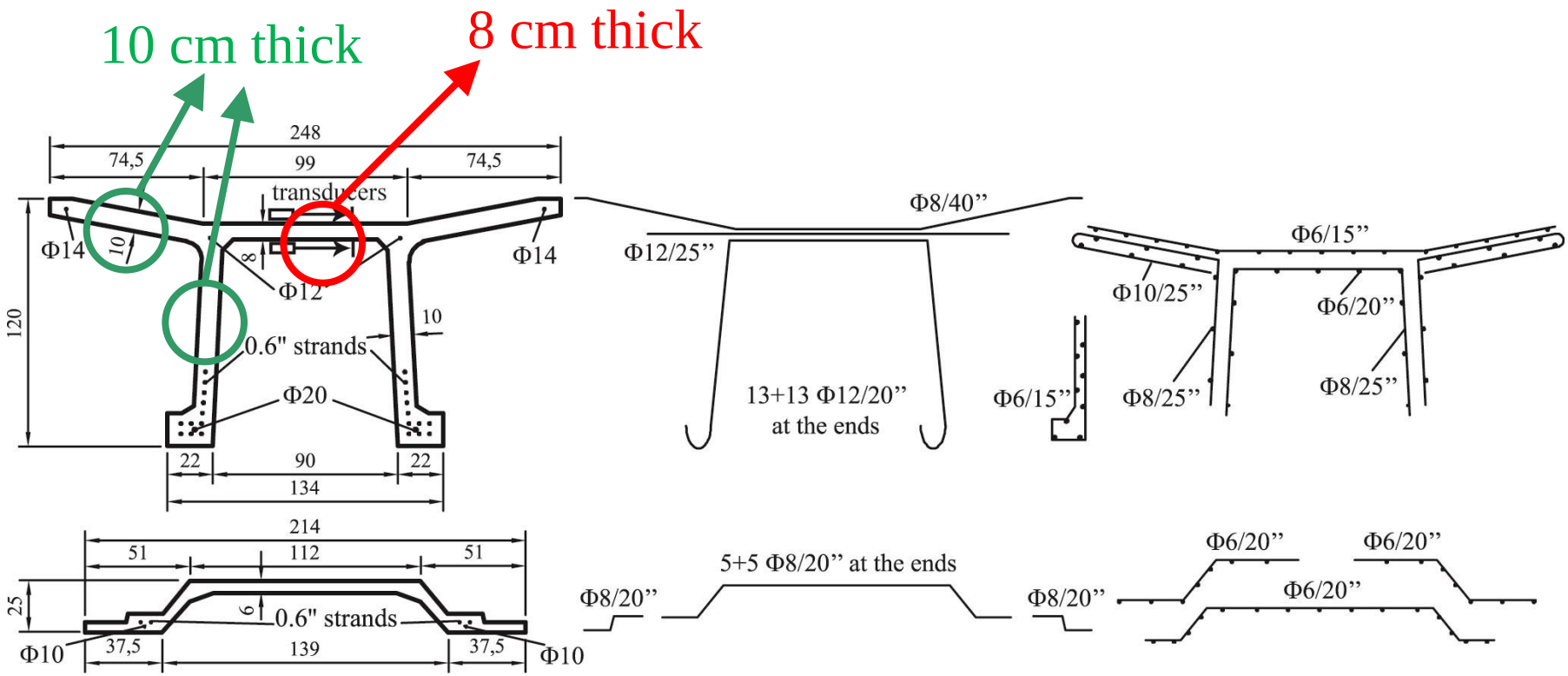

TT beam element

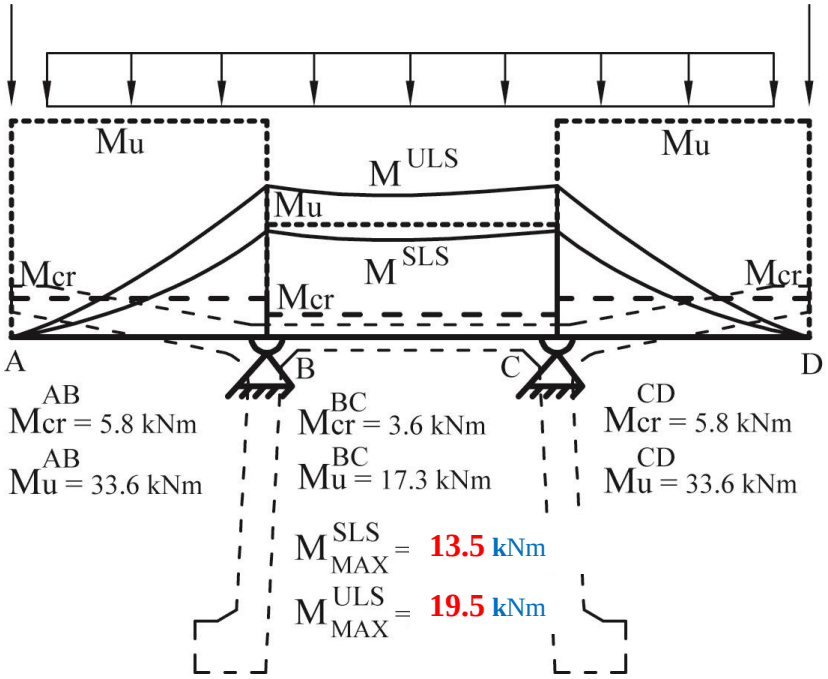

Transversal equilibrium bending moments (characteristic values)

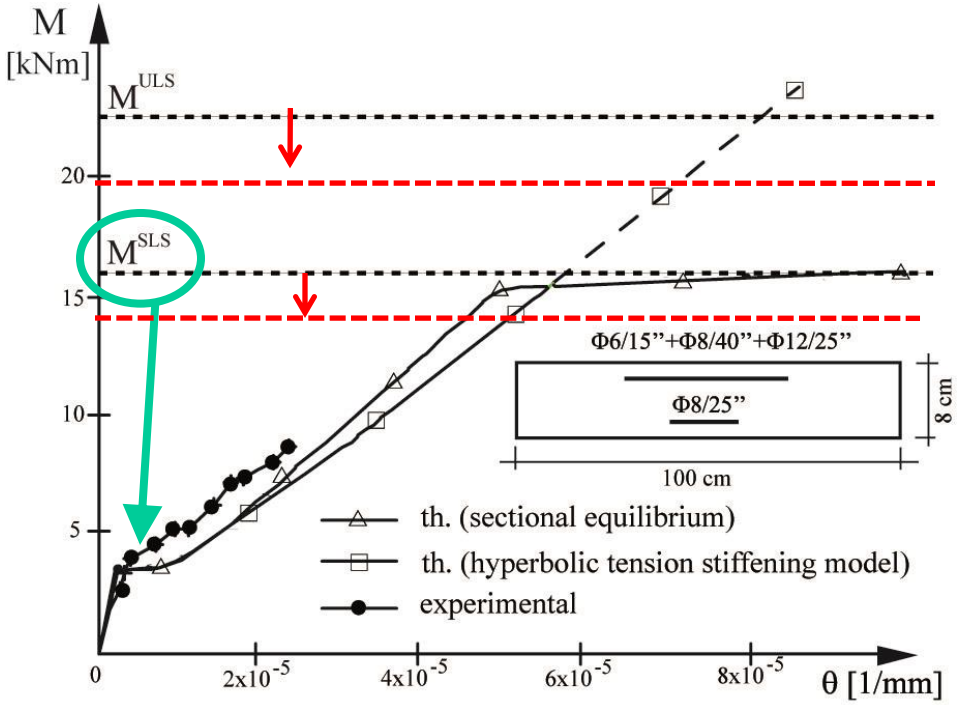

Experimental vs. predicted moment-curvature relationship (upper TT beam element plate)

Situation after structure breakdown

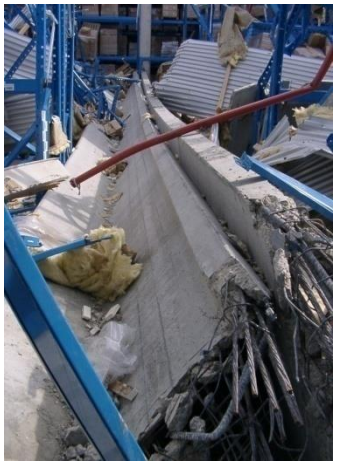

TT beam element: torsional behaviour

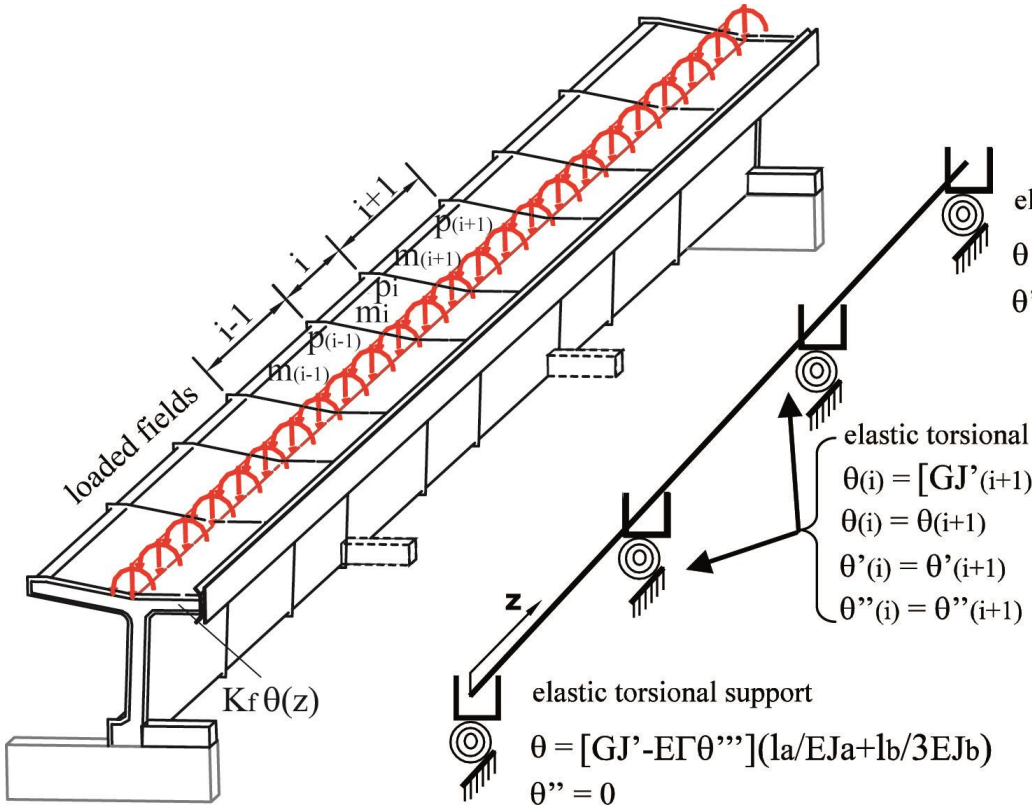

$$\Gamma = \sum_{i=1,3} 1/36 a^3 b^3$$

$$\frac{d^4\vartheta(z)}{dz^4} - \frac{GJ_T(\vartheta')}{E\hat{\Gamma}}\frac{d^2\vartheta(z)}{dz^2} + \frac{K_f(J_f(\vartheta))}{E\hat{\Gamma}}\vartheta(z) = \frac{m_t}{E\hat{\Gamma}}$$

$$\lambda_{1,2,3,4} = \pm\sqrt{\frac{\frac{GJ_T}{E\hat{\Gamma}} \pm \sqrt{\left(\frac{GJ_T}{E\hat{\Gamma}}\right)^2 - 4\frac{K_f}{E\hat{\Gamma}}}}{2}}$$

$$\vartheta_{(i)}(z) = A_{(i)} \cdot e^{\lambda_{1(i)} z} + B_{(i)} \cdot e^{\lambda_{2(i)} z} + C_{(i)} \cdot e^{\lambda_{3(i)} z} + D_{(i)} \cdot e^{\lambda_{4(i)} z} + \frac{m_{t(i)}}{K_{f(i)}}$$

Ω roof element

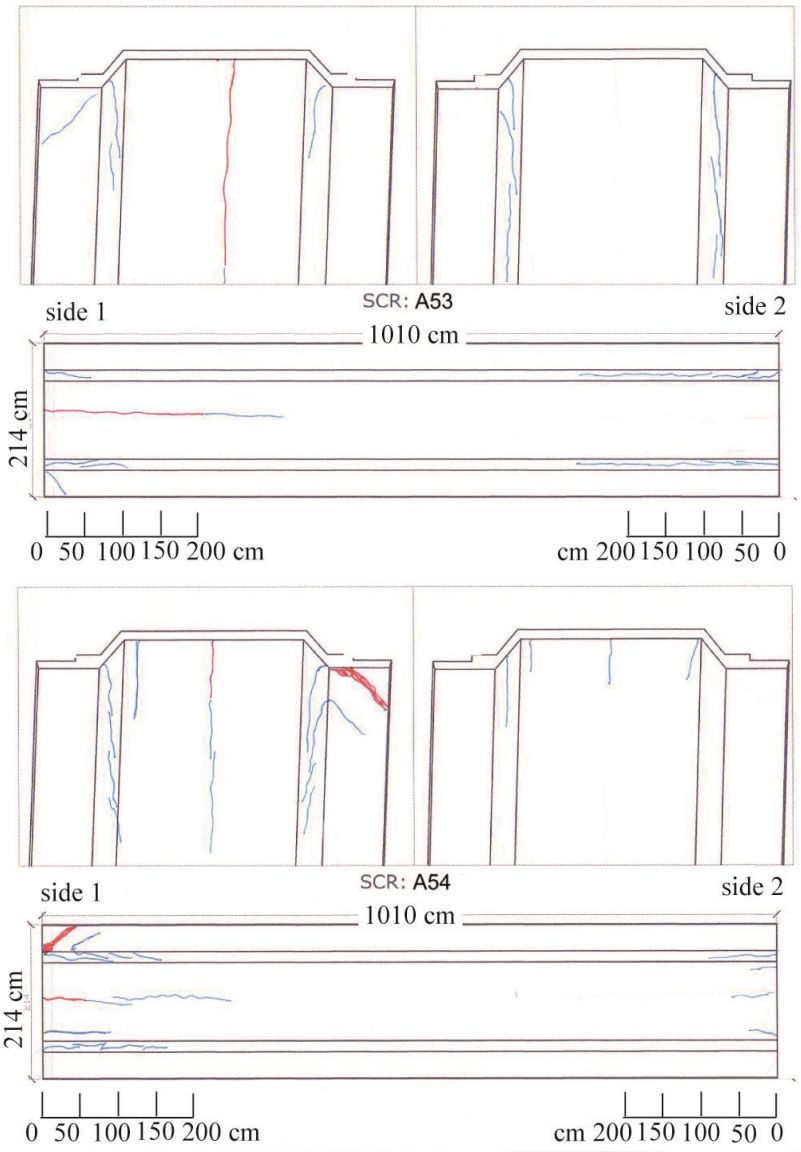

Transversal deformability problems interested also the Ω roof elements placed on TT beams:

- not negligible deflection
- significant crack pattern

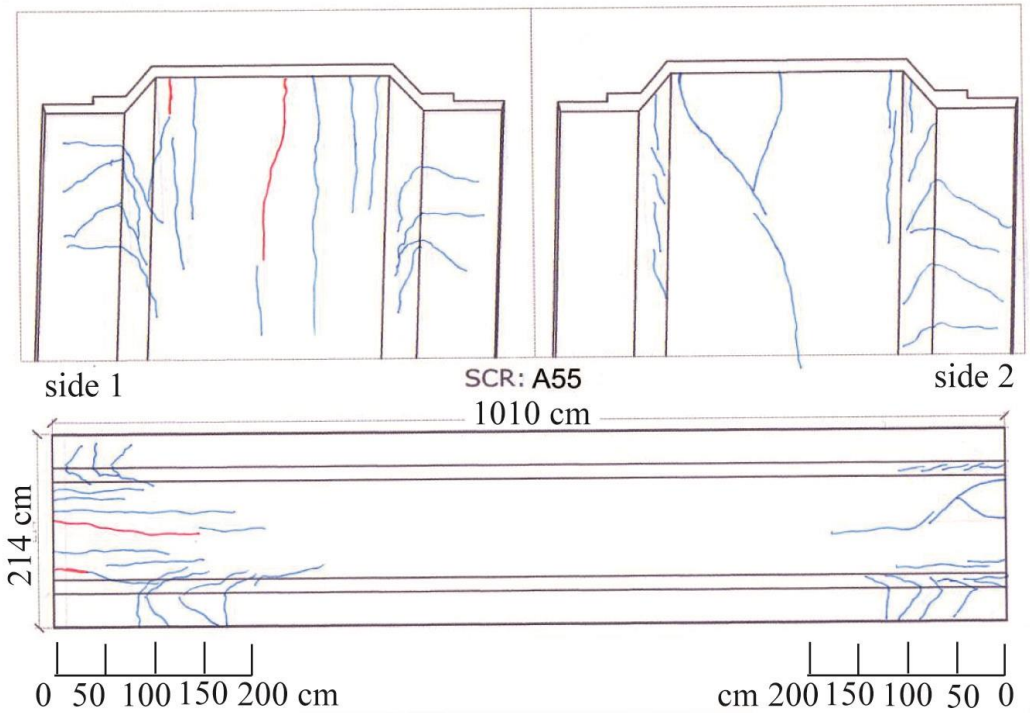

crack pattern of in-situ Ω roof elements

Ω roof element: laboratory tests

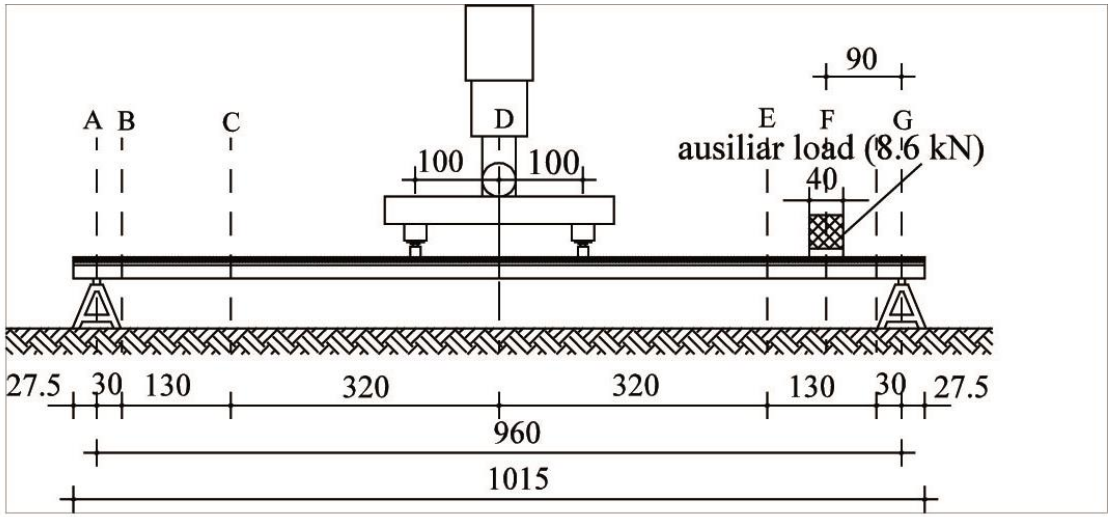

Long.bending moment vs. vertical displacements of full size SCR roof elements

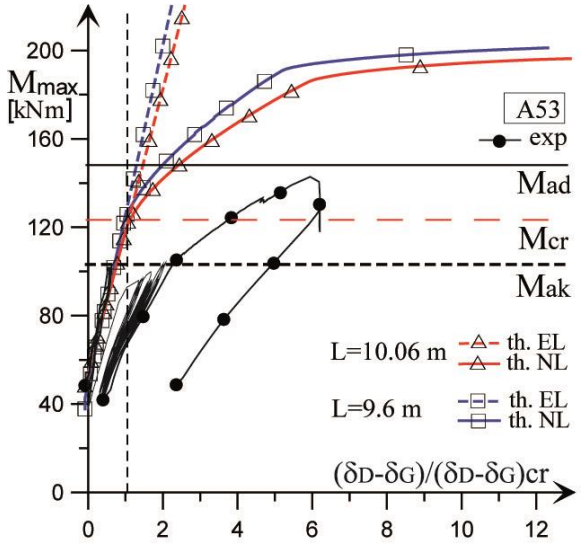

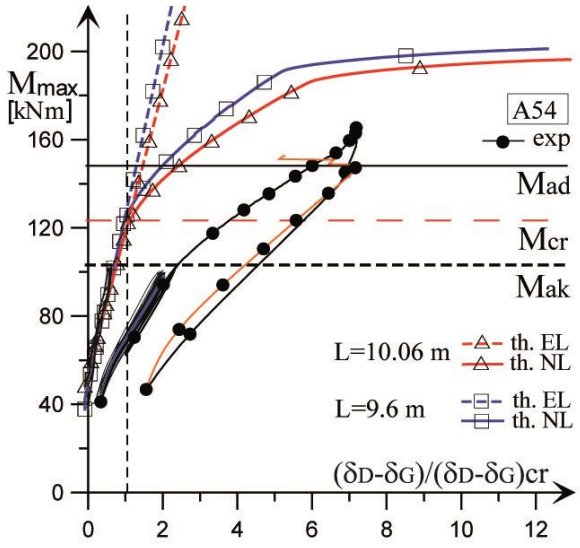

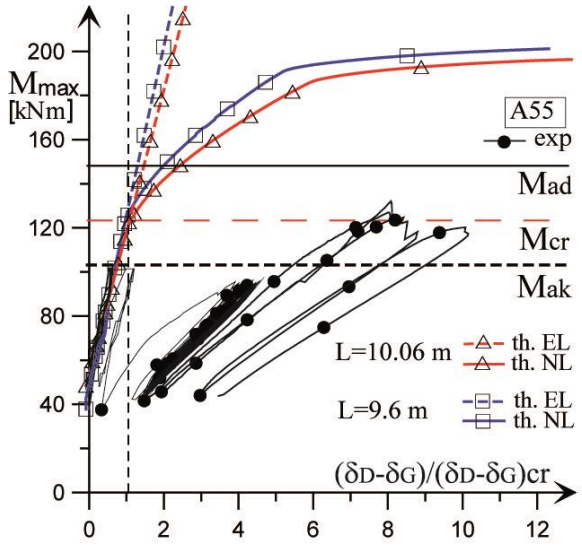

Ω roof element: laboratory tests

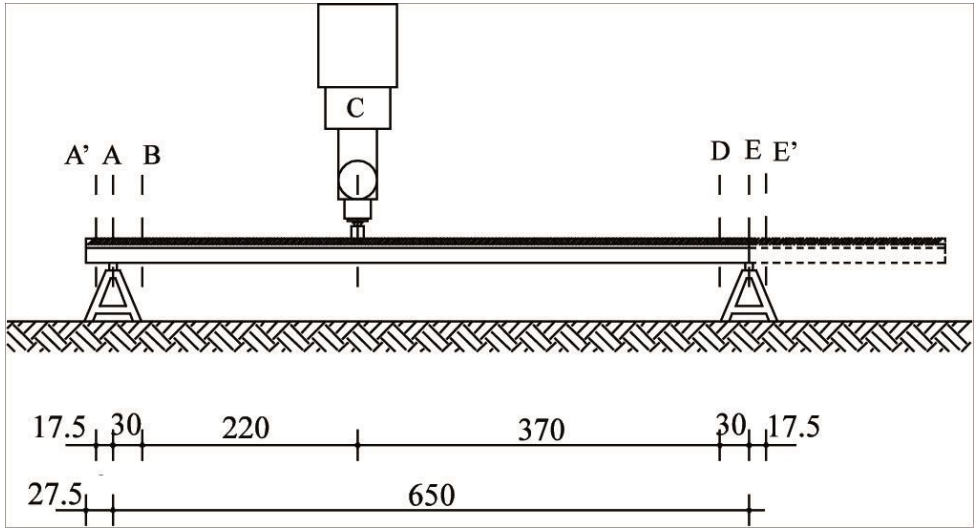

Long. bending moment vs. vertical displacements of full size SCR roof elements

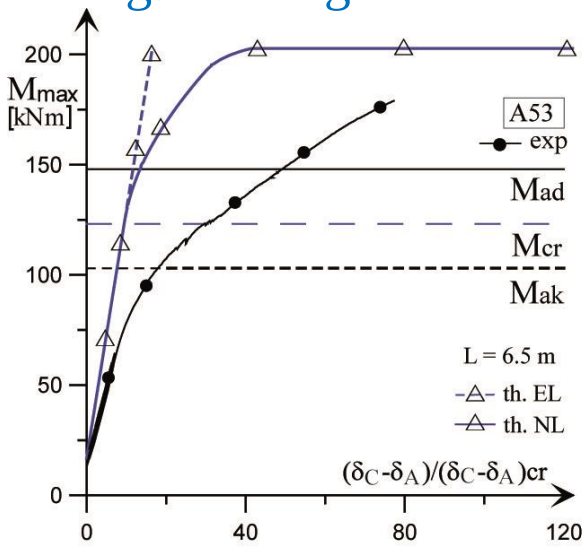

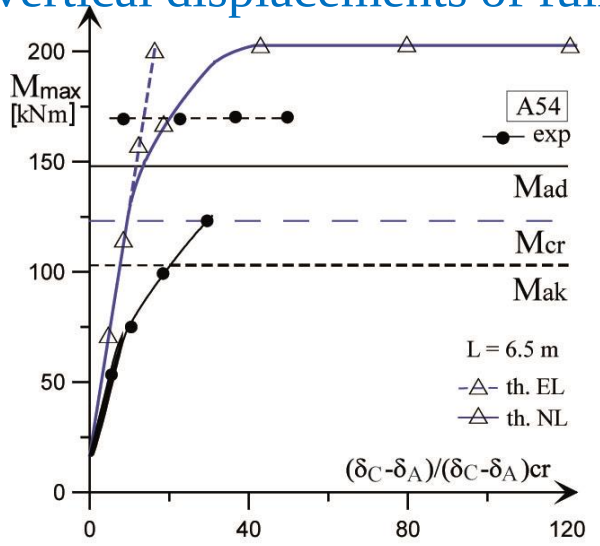

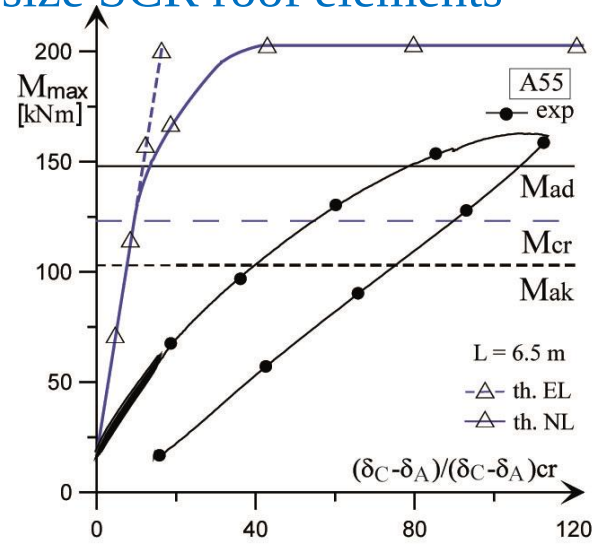

Outline

- ✓ FRC as transverse reinforcement:
  - σ-w constitutive law
  - classification and “structural specimen”
  - fibre alignement
  - second order effects
- ✓ FRC for local bending
  - self stresses due to shrinkage and thermal effects
  - which structural ductility
  - stress diffusion and size effects
- ✓ Advanced materials for light composite structures
  - opportunities
  - complex resistant mechanisms
  - open question and unexplored potentialities

FRC to substitute transverse reinforcement

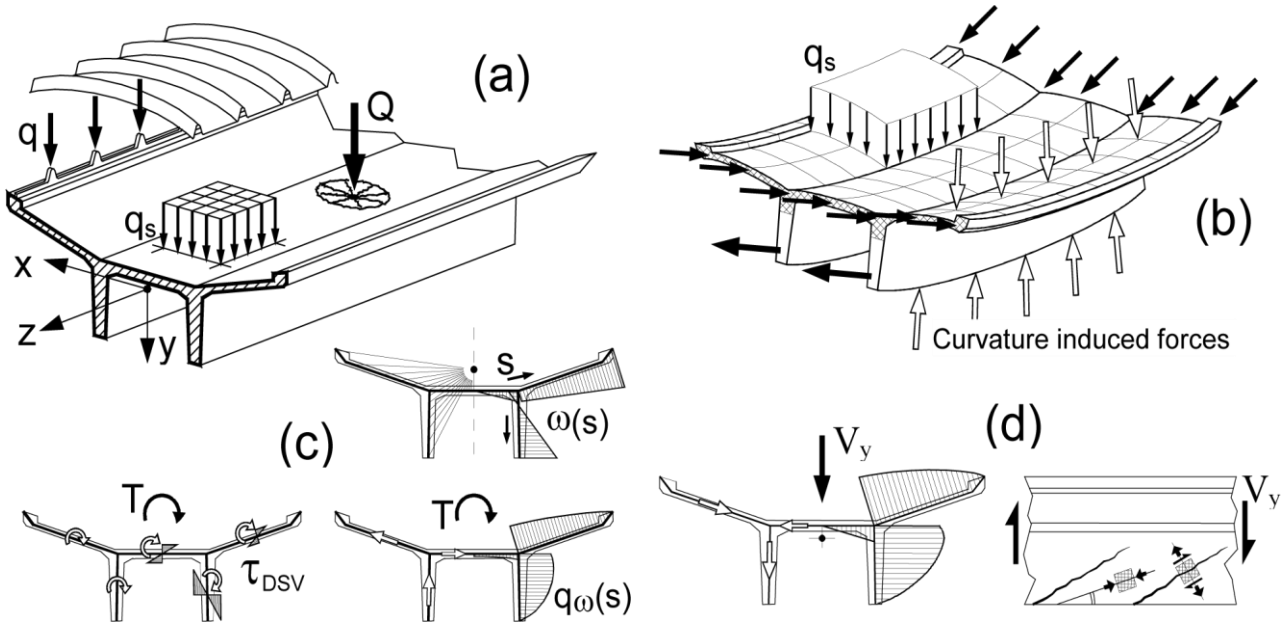

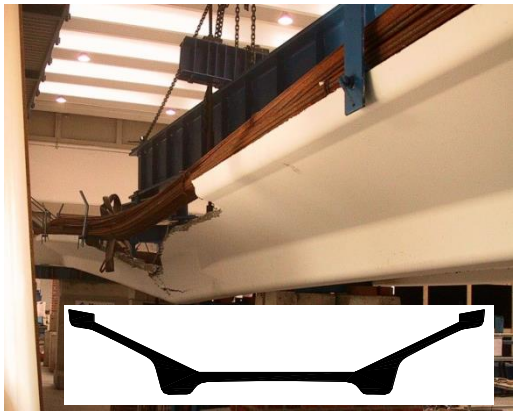

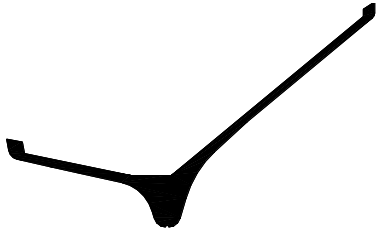

Classification for FRC market

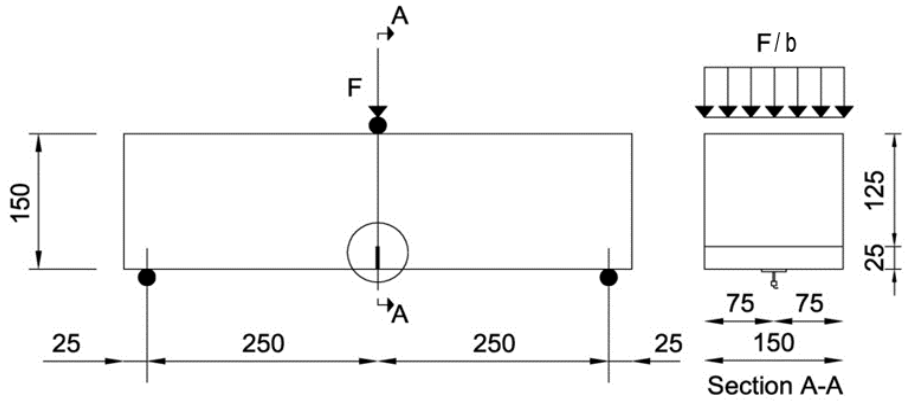

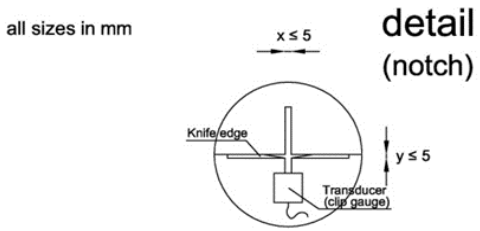

Reference test

EN 14651

h_{sp} = 125 mm

b = 150 mm

$$f_{R,j} = \frac{3F_j l}{2bh_{sp}^2}$$

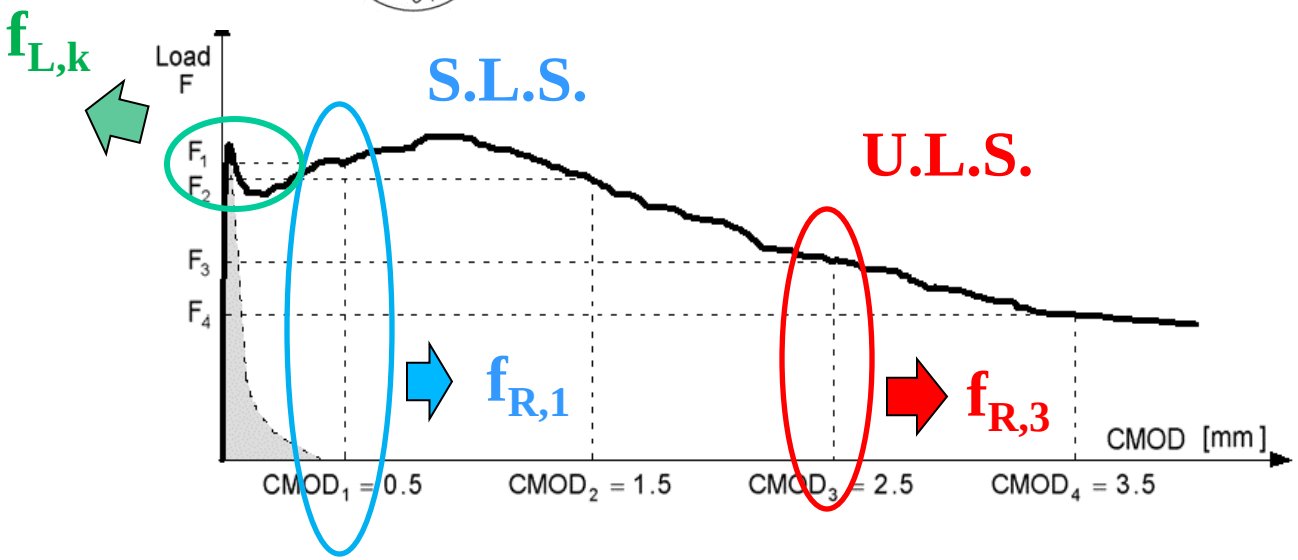

Performance based design

cement 425:	472 kg	fine sand	0/4 850kg
fly ash:	45 kg	coarse sand	4/8 886 kg
water	200 l (w/b =0.39)		
superplast.	1.3%	**hooked-end fibres 65/35**	**50 kg**

slump flow diameter: 690 mm

T50	2 sec
V-funnel time (0 min)	3.5 sec
V-funnel time (5 min)	4 sec
L-box (standard)	h2/h1 = 1

Classification

f_{R1k} ***1.0; 1.5; 2.0; 2.5; 3.0; 4.0; 5.0; 6.0; 7.0; 8.0 [MPa]***

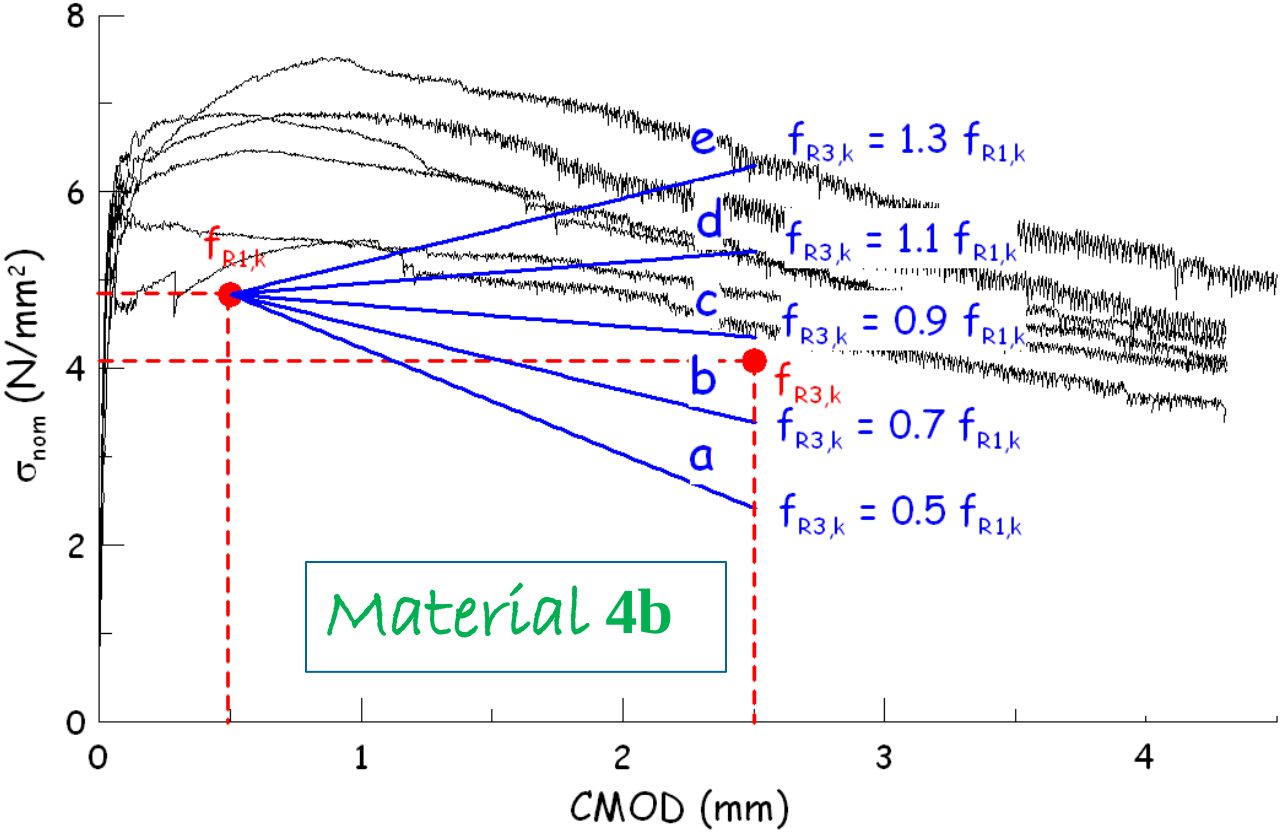

$$f_{eq,k} = f_{eq,av} - ks$$

$n = 6$: $k = 1{,}87$

	strength [Mpa]	st. dev [Mpa]
$f_{L,av}$	5,43	0,47
f_{Lk}	**4,55**	
$f_{R1,av}$	6,32	0,79
f_{R1k}	**4,84**	
$f_{R3,av}$	5,32	0,66
f_{R3k}	**4,08**	

Minimum performance for a FRC

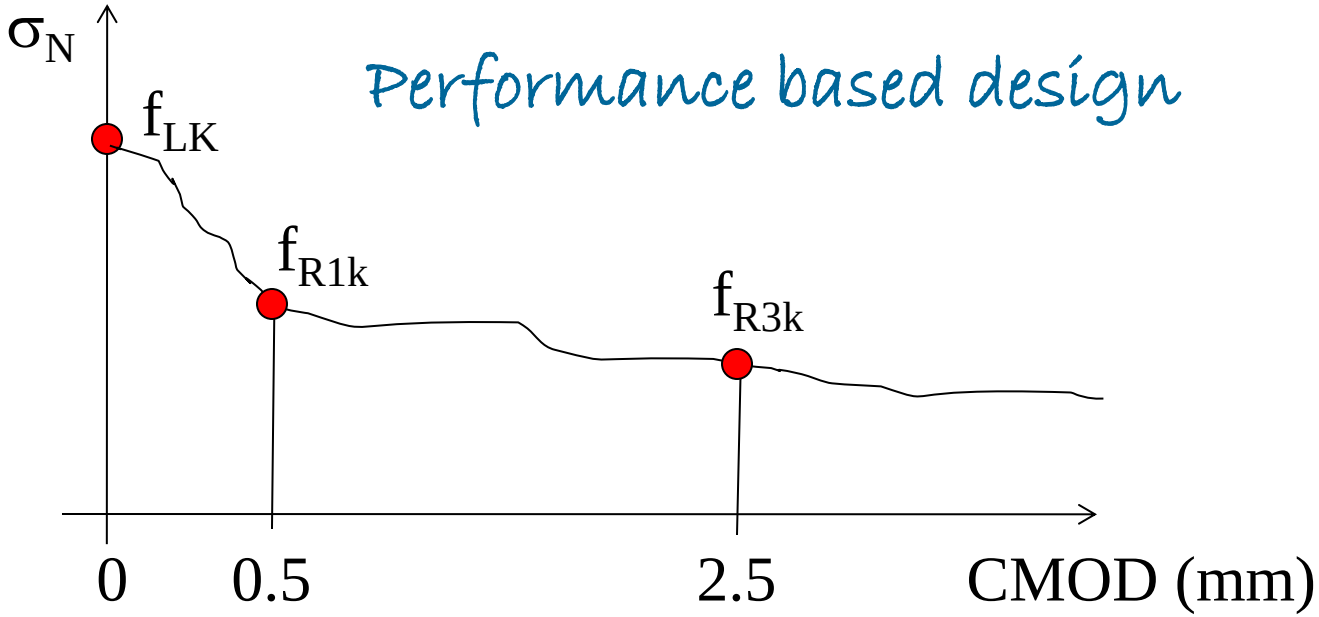

(5) **Fibre reinforcement can substitute (also partially) conventional reinforcement at ultimate limit state** if the following relationships are fulfilled:

$$f_{R1k}/f_{Lk} > 0.4; \qquad f_{R3k}/f_{R1k} > 0.5$$

Bending tests on roof elements

by di Prisco, Failla,Plizzari, 2003

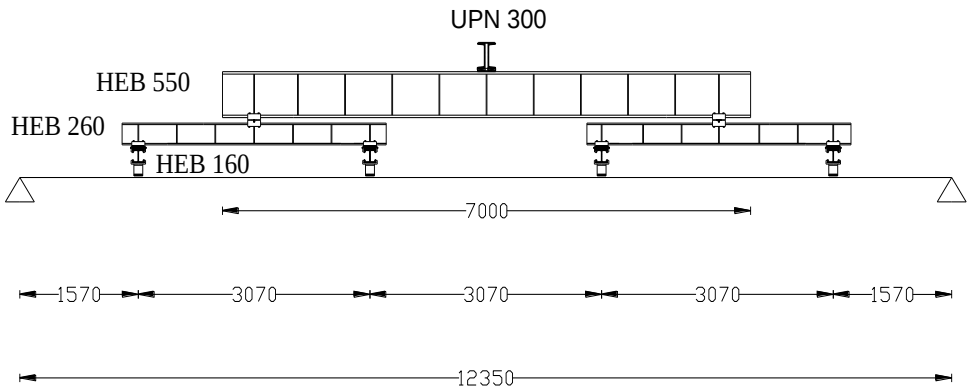

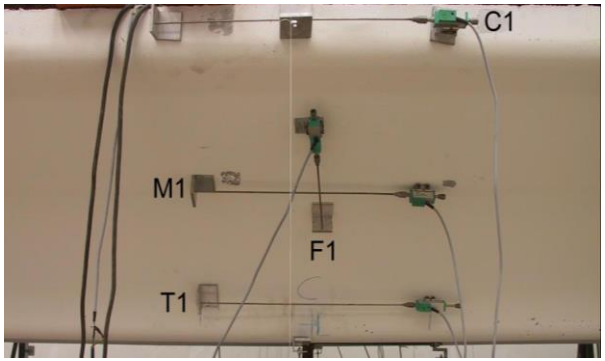

$l_{cs,wing}$

$l_{cs,slab}$

COMPARISON - SECTION C

Load - Total displacement

R/C

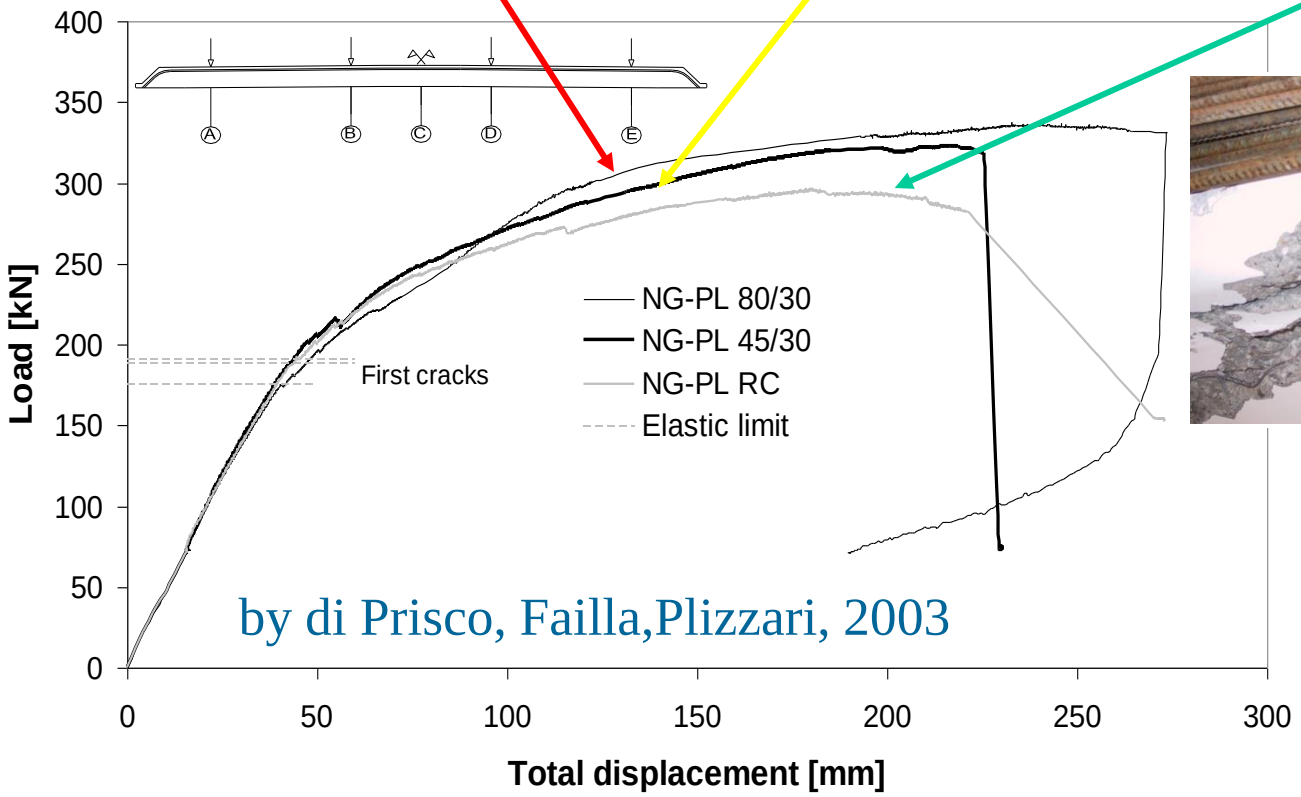

✓the bridge ... of the characteristic structural length

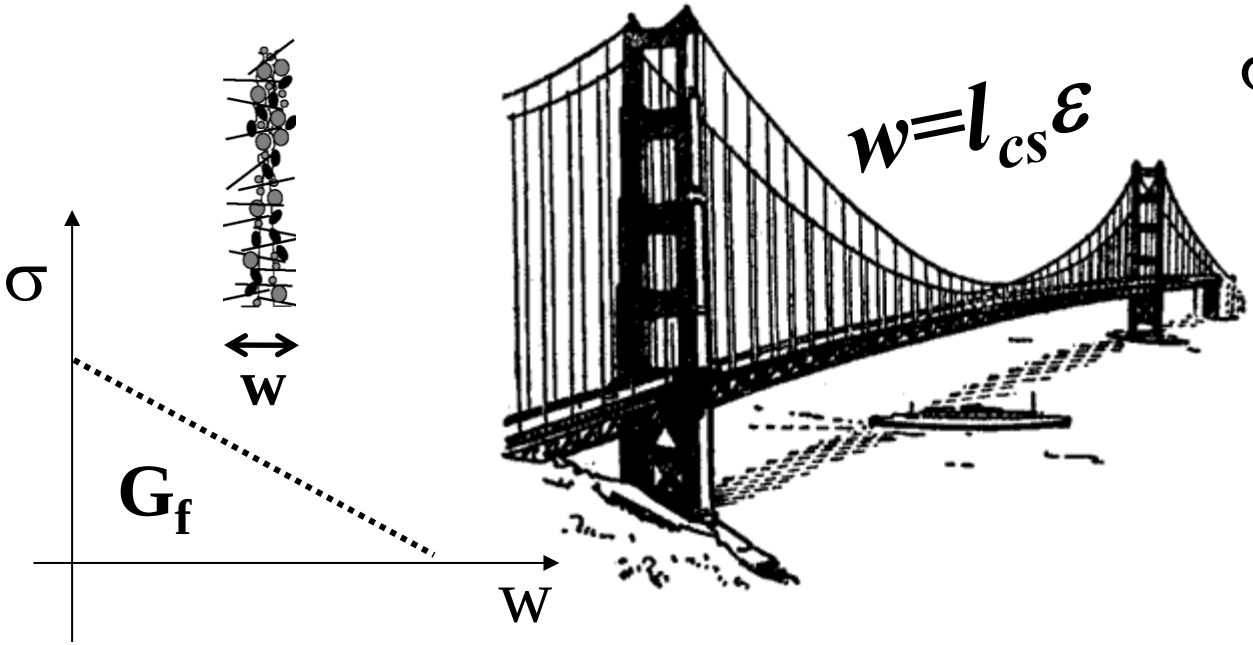

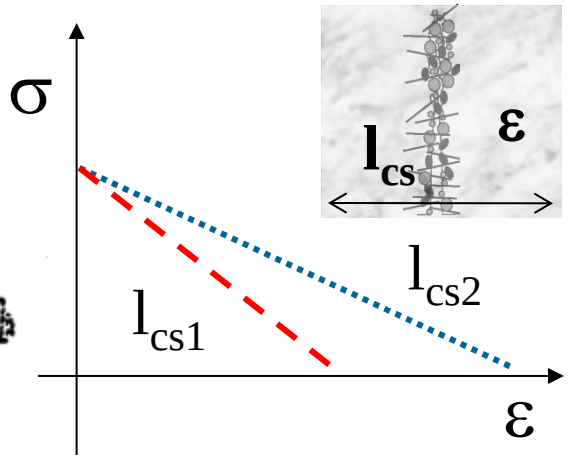

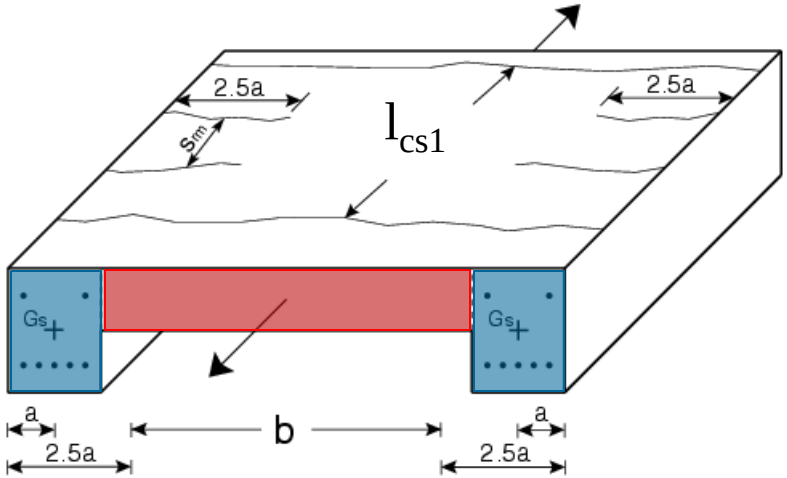

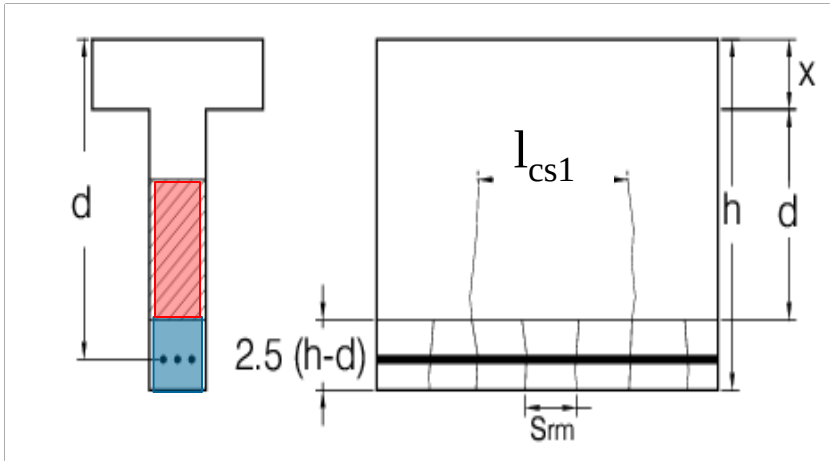

The characteristic structural length

Plane section approach

$$l_{cs} = \min\{s_{rm}, y\}$$

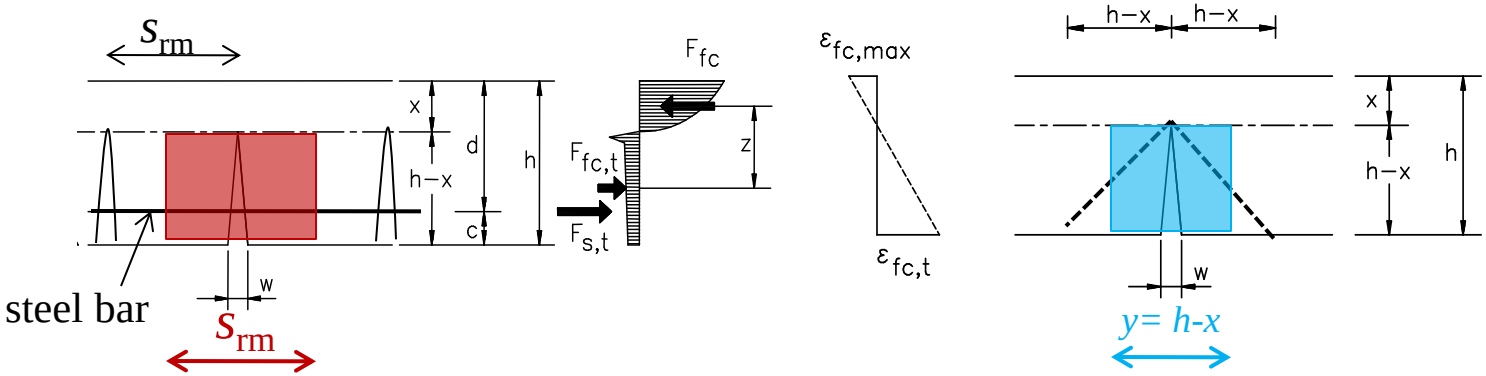

N.B. In sections without traditional reinforcement under bending or under combined tensile – flexural and compressive – flexural forces with resulting force external to the section, **y = h is assumed**. The same assumption can be taken for slabs.

F.E. approach: l_{cs} = *localization limiter*

elastic check by FE

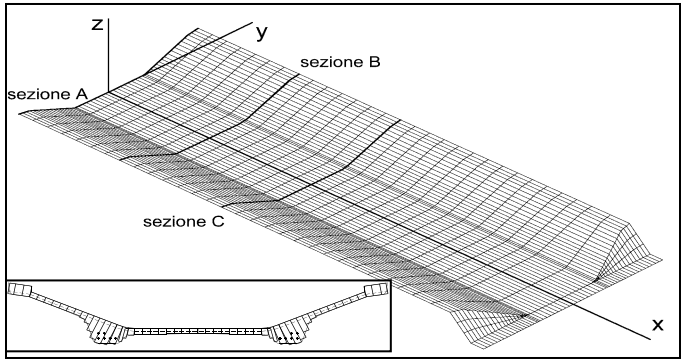

eccentric load

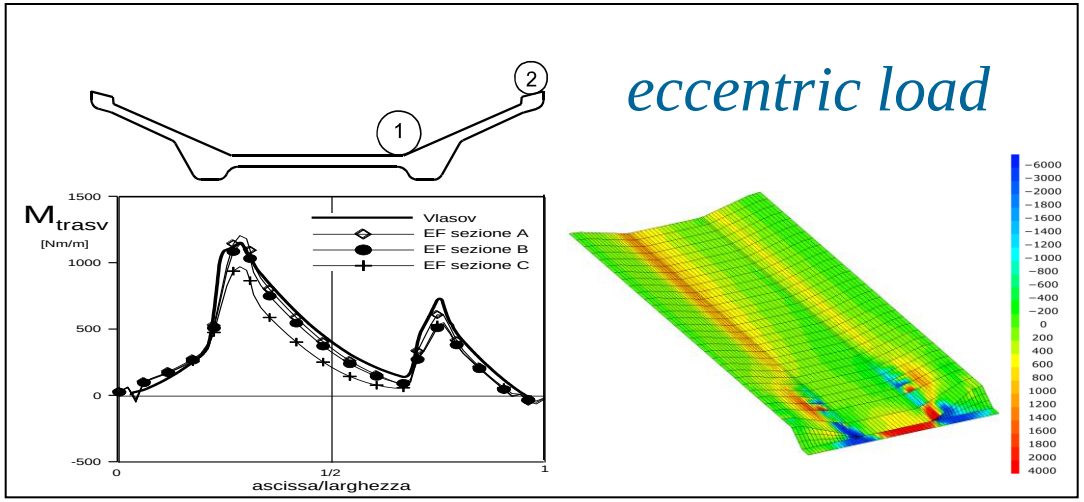

at failure

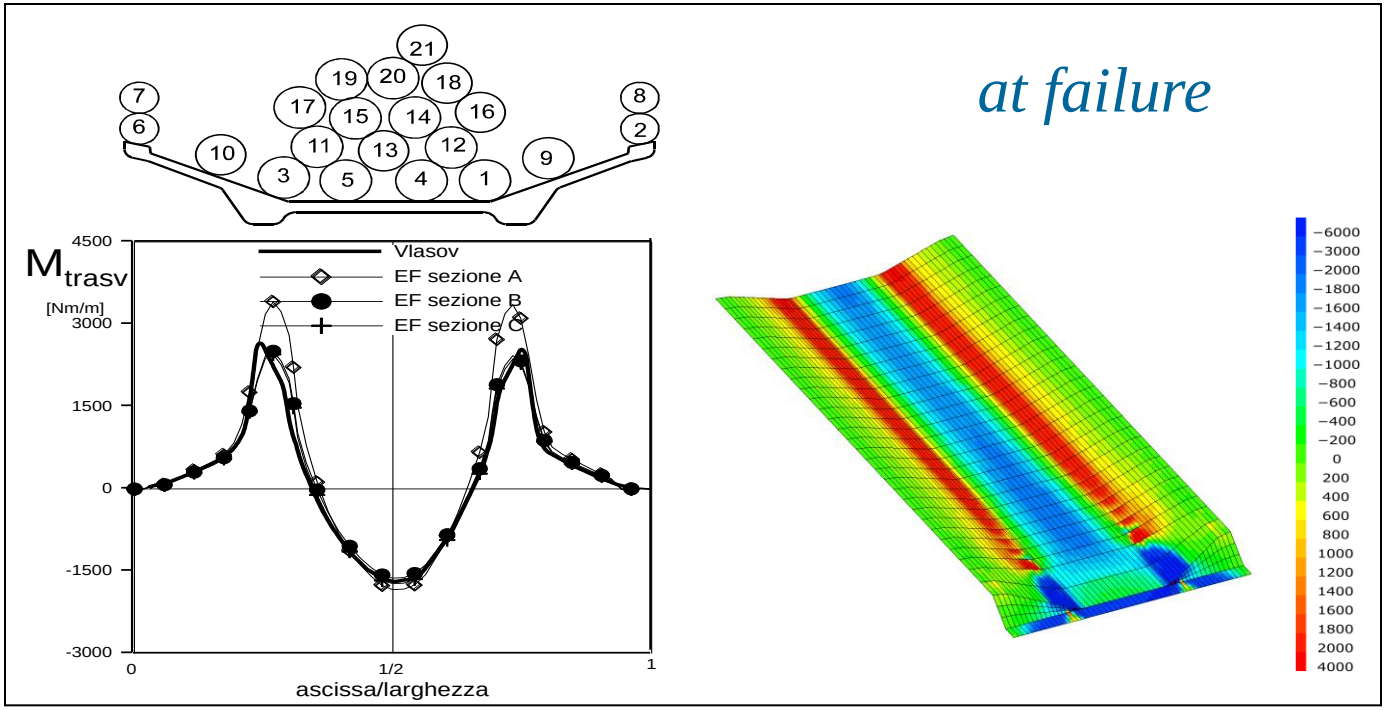

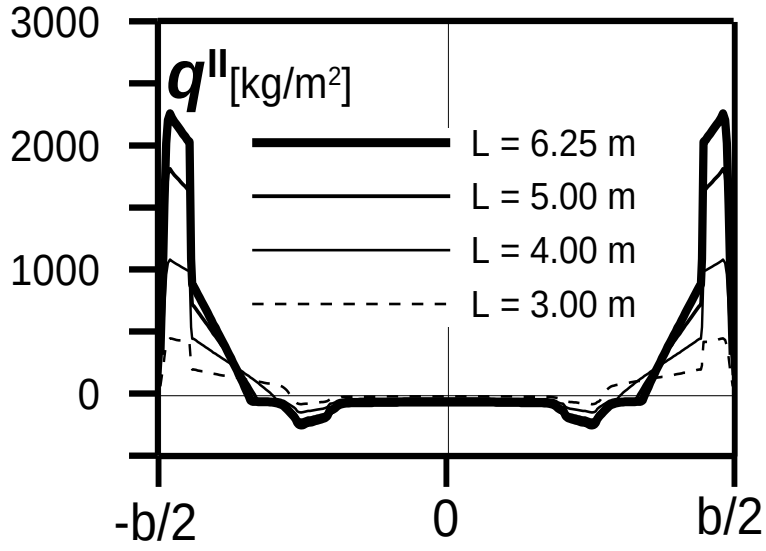
3000
2000
1000
0
q^{II}[kg/m²]
L = 6.25 m
L = 5.00 m
L = 4.00 m
L = 3.00 m
-b/2
0
b/2

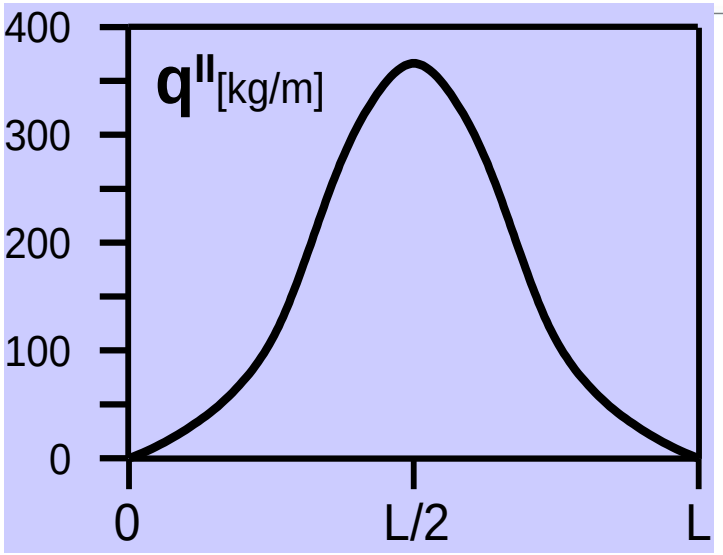
400
300
200
100
0
q^{II}[kg/m]
0
L/2
L

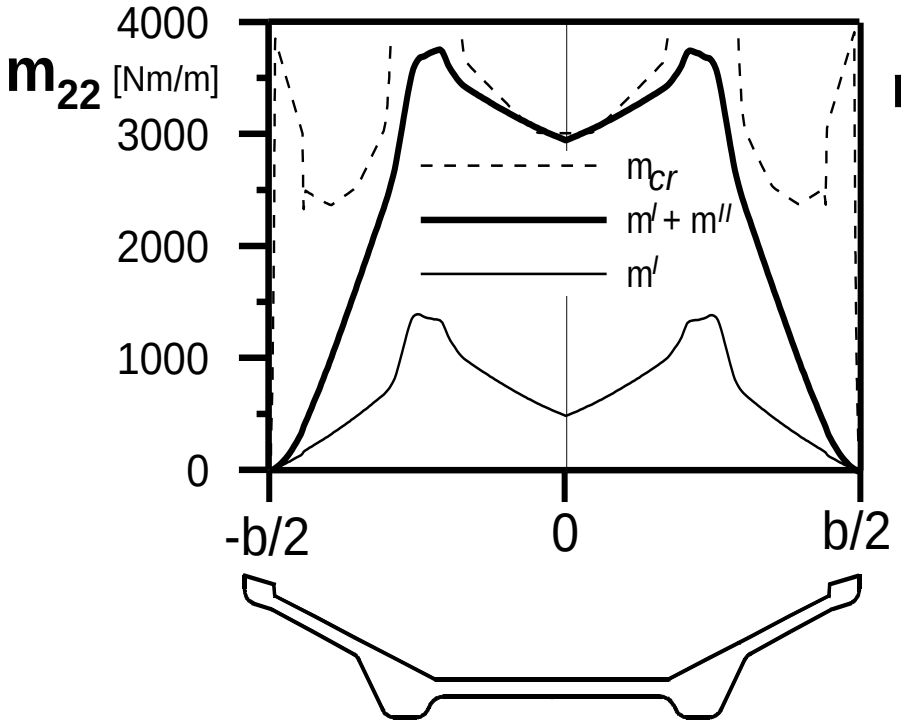
m_{22} [Nm/m]
4000
3000
2000
1000
0
m_{cr}
$m^{I} + m^{II}$
m^{I}
-b/2
0
b/2

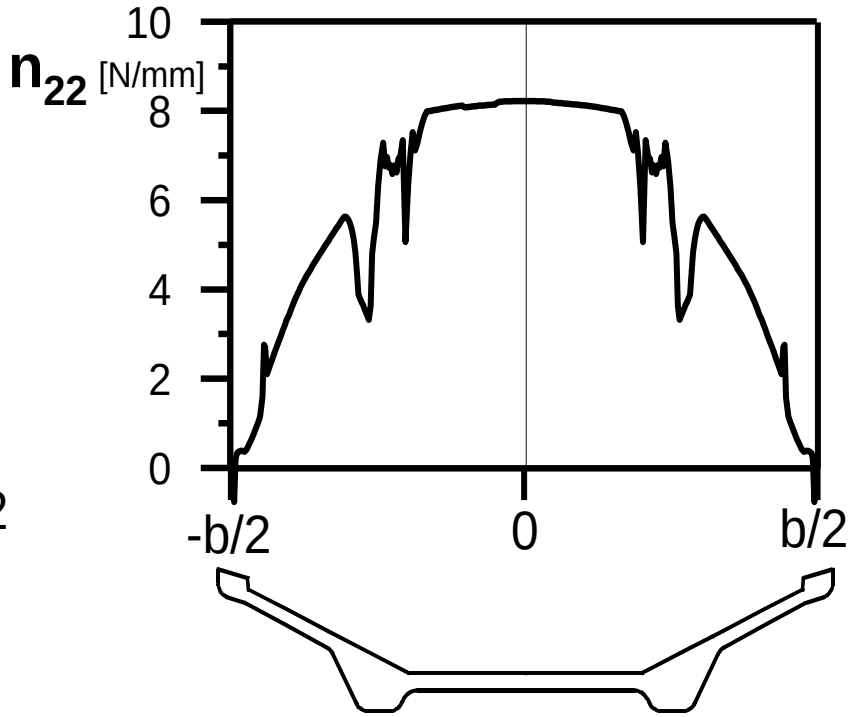
n_{22} [N/mm]
10
8
6
4
2
0
-b/2
0
b/2

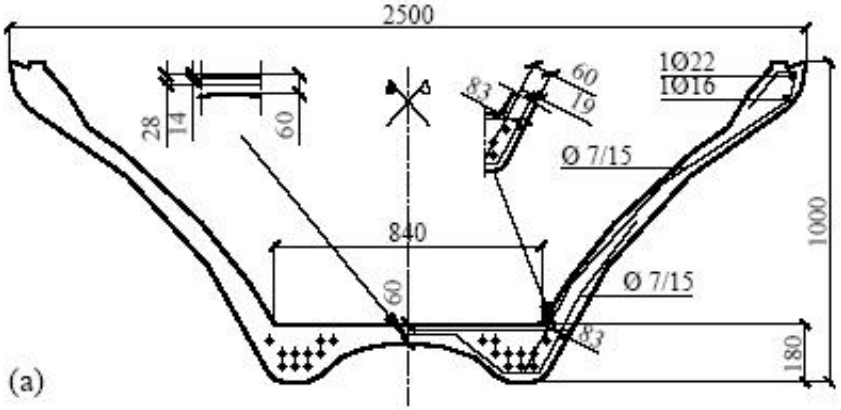

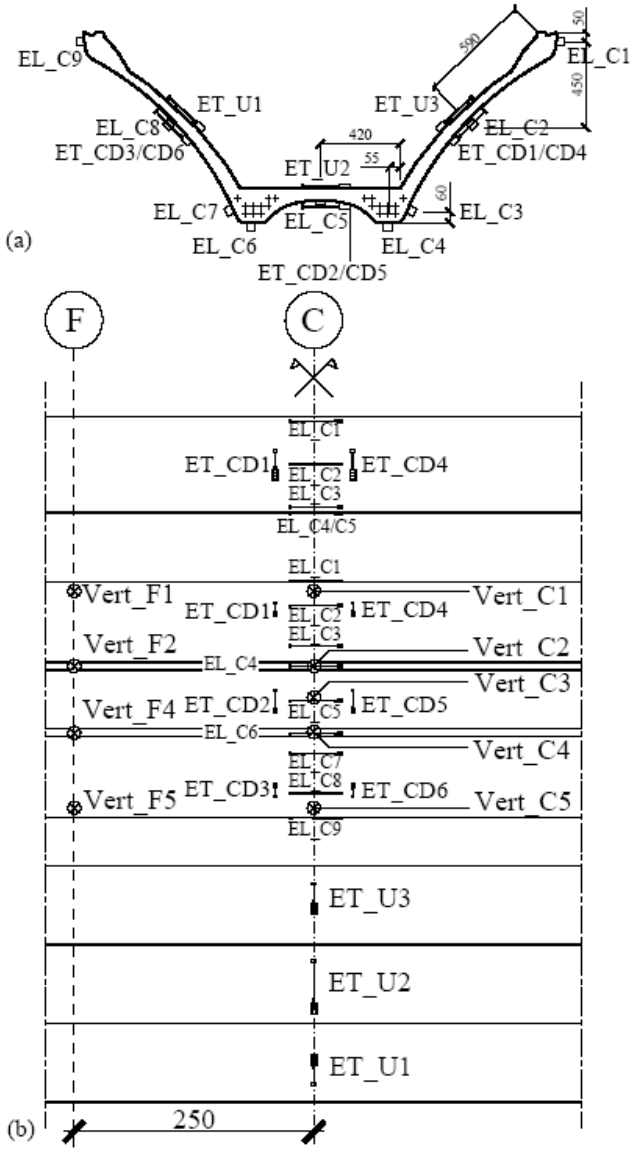

Figure 2. Instrumental equipment in the central segment: (a) cross section view; (b) longitudinal projections.

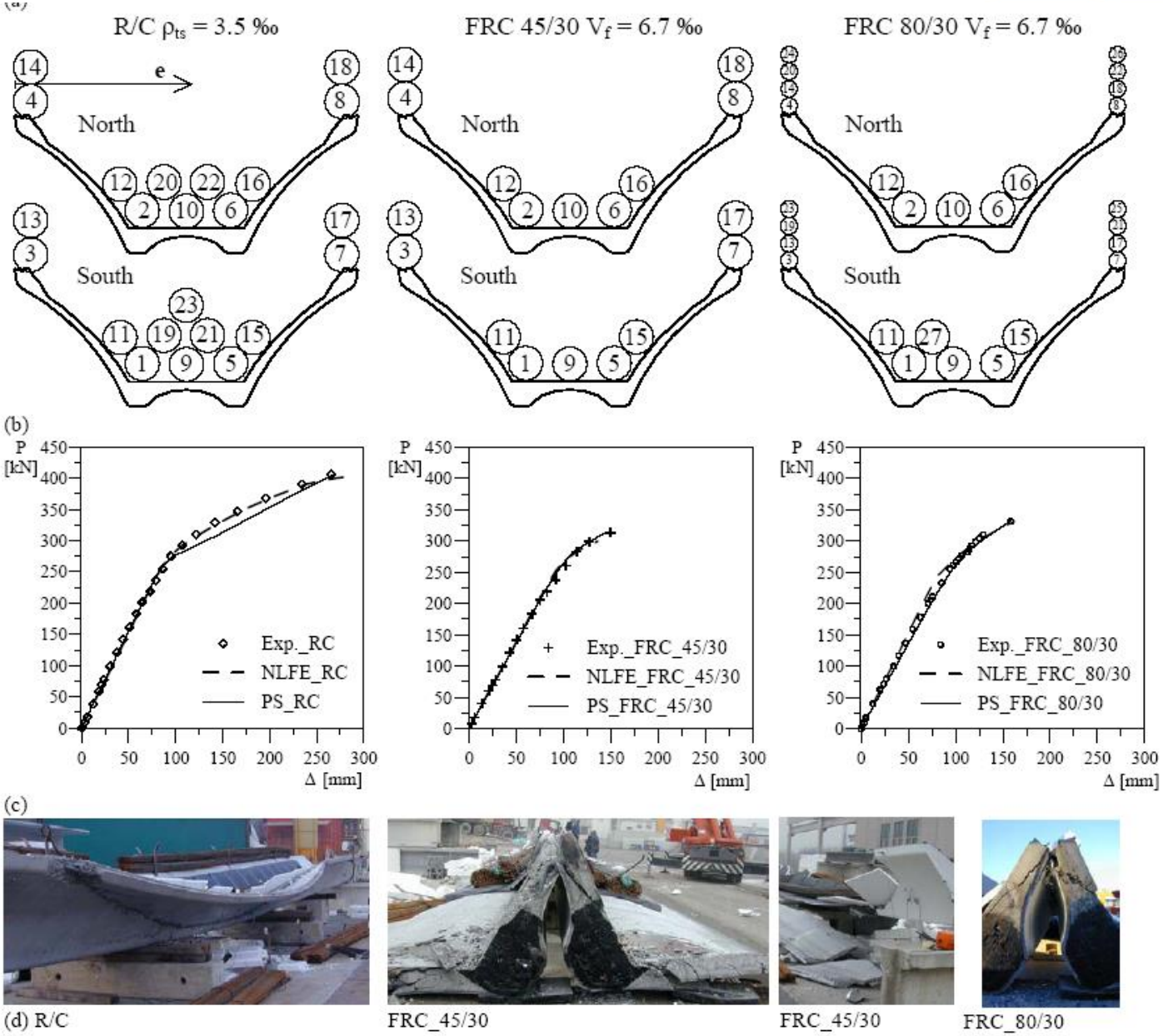

Figure 3. Structural tests: (a) typical loading situation view; (b) steel bundle location, (c) total load vs. midspan deflection measured with bottom LVDTs; (d) collapse views.

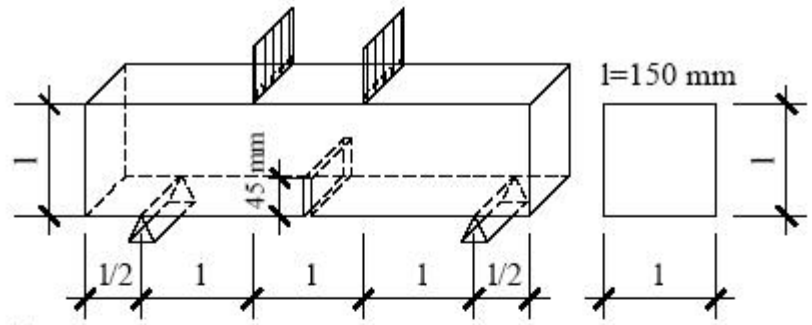

(a)

(b)

Figure 4. UNI test: (a) geometry and test set-up; (b) specimen image during testing.

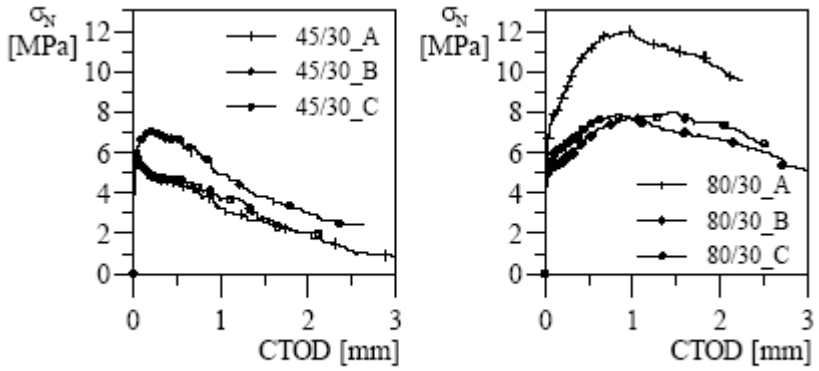

(a) (b)

Figure 5. Load vs. CTOD for UNI tests: (a) 45/30; (b) 80/30

Table 1. Experimental mechanical characteristics of materials.

	R_{cm}	$f_{If,m}$	$f_{eq0\text{-}0.6m}$	$f_{eq0.6\text{-}3m}$	f_{yk}	f_{ptk}
	MPa	MPa	MPa	MPa	MPa	MPa
R/C	82.58	-	-	-	500	1860
45/30	75.65	5.22	5.44	2.80	-	1860
80/30	73.20	5.22	7.56	8.12	-	1860

Table 2. Computed mechanical characteristics of materials.

	E_c	ν	f_c	f_{ct}	σ_a	w_a	σ_b	w_b
	MPa		MPa	MPa	MPa	mm	MPa	mm
R/C	39193	0.2	68.54	5.02	-	-	-	-
45/30	38176	0.2	62.79	4.70	2.45	0.3	0.31	1.8
80/30	37801	0.2	60.76	4.70	3.40	0.3	2.55	1.8

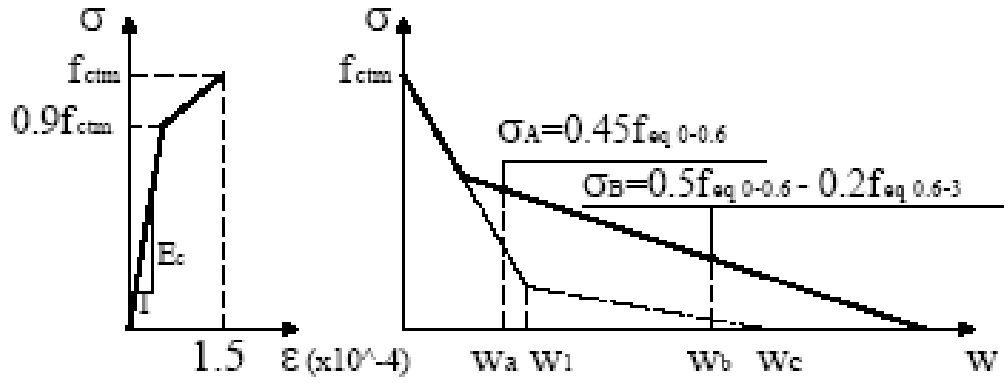
σ
fctm
0.9fctm
Ec
1
1.5
ε (x10^-4)
σA=0.45feq 0-0.6
σB=0.5feq 0-0.6 - 0.2feq 0.6-3
Wa W1
Wb
Wc
W

(a)

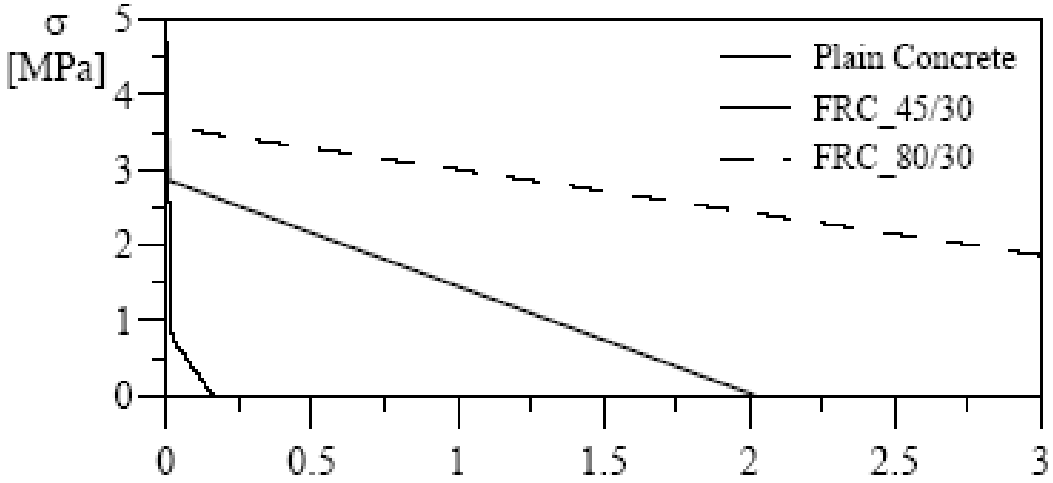
σ
[MPa]
5
4
3
2
1
0
0
0.5
1
1.5
2
2.5
3
Plain Concrete
FRC_45/30
FRC_80/30

Two theoretical approaches

Plane Section

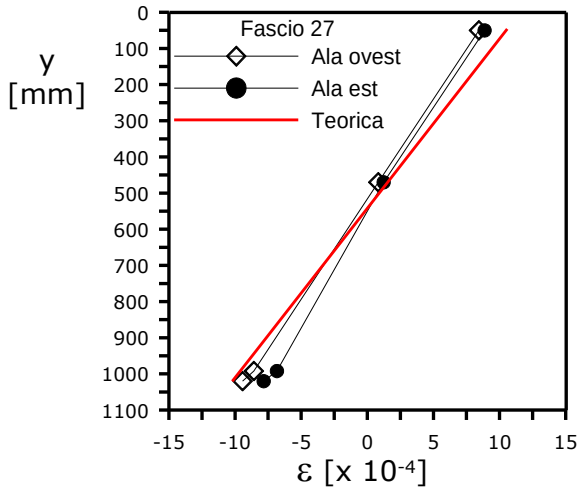

$\varepsilon = w/l_{cs}$

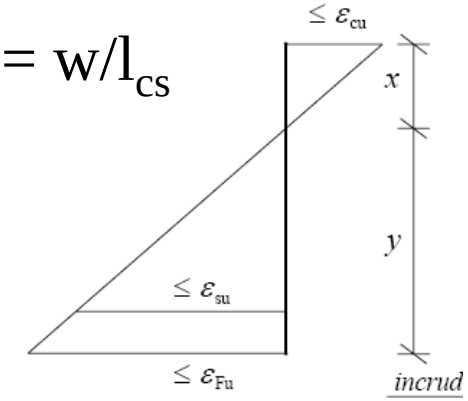

Finite Element & PARC Model

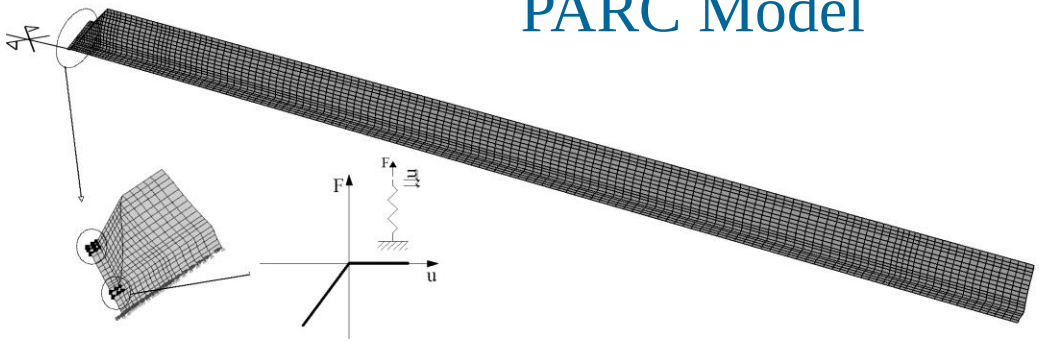

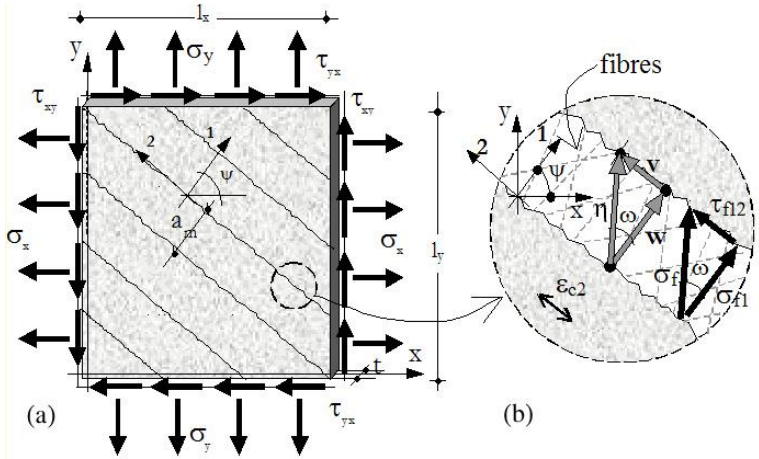

by Belletti,Cerioni, Iori, 2002

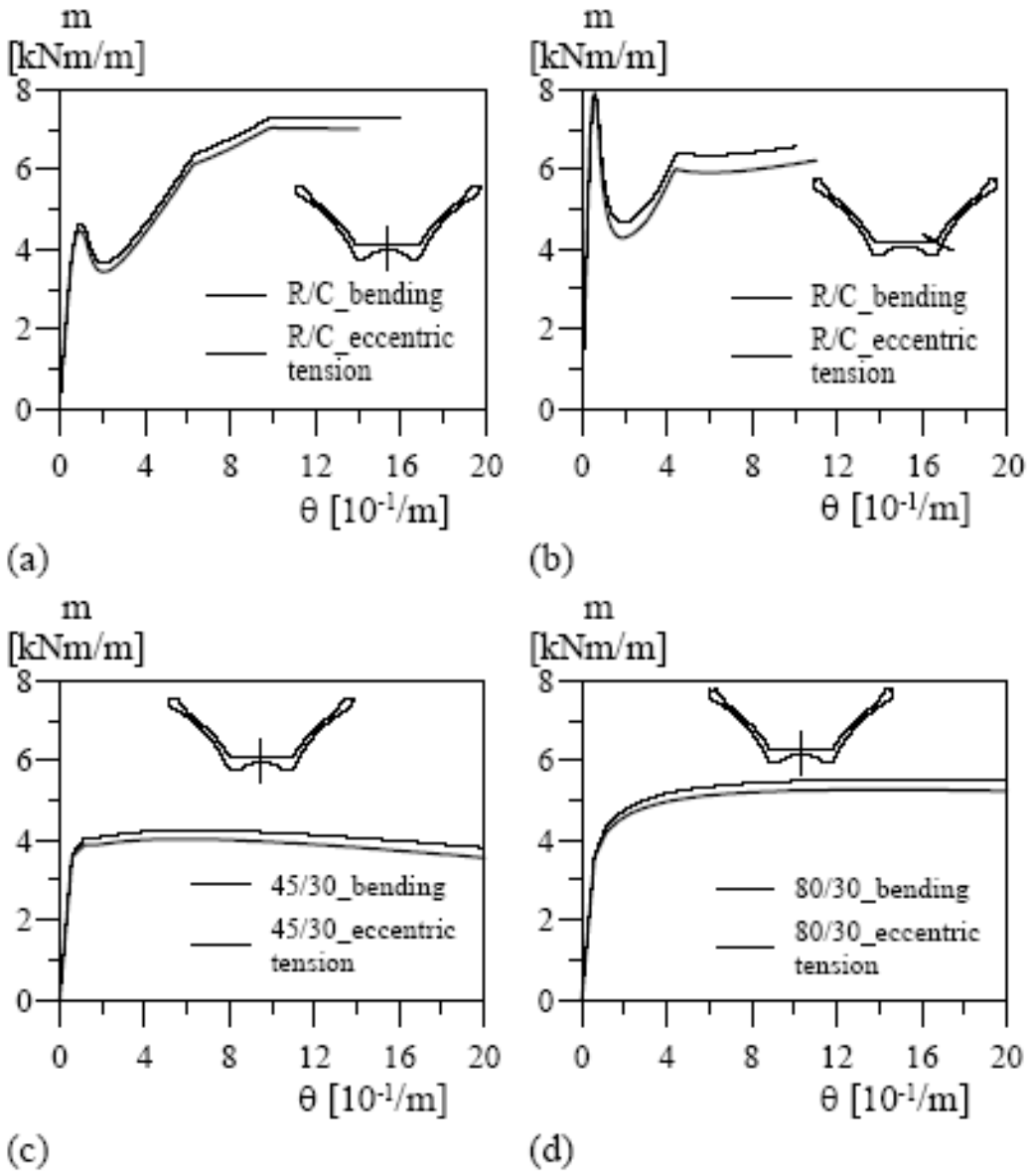
m
[kNm/m]
8
6
4
2
0
0
4
8
12
16
20
θ [10-1/m]
R/C_bending
R/C_eccentric tension
(a)
m
[kNm/m]
R/C_bending
R/C_eccentric tension
(b)
m
[kNm/m]
45/30_bending
45/30_eccentric tension
(c)
m
[kNm/m]
80/30_bending
80/30_eccentric tension
(d)

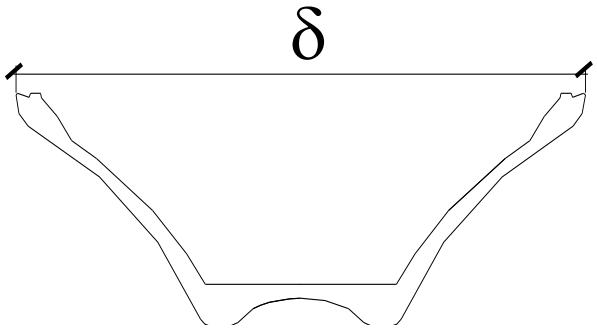
δ

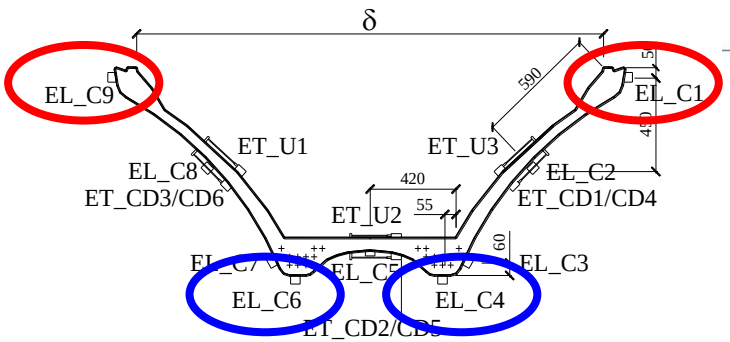
δ
EL_C9
EL_C1
590
15
450
ET_U1
ET_U3
EL_C8
ET_CD3/CD6
EL_C2
ET_CD1/CD4
420
55
ET_U2
60
EL_C7
EL_C5
EL_C3
EL_C6
EL_C4
ET_CD2/CD5

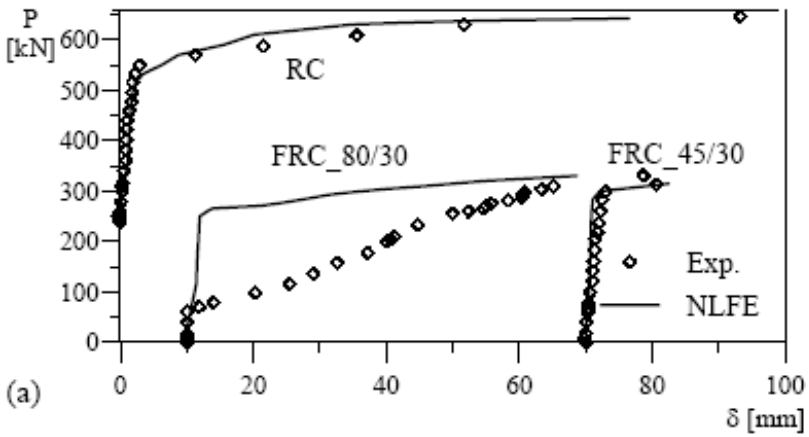
P
[kN]
RC
FRC_80/30
FRC_45/30
Exp.
NLFE
δ [mm]
(a)

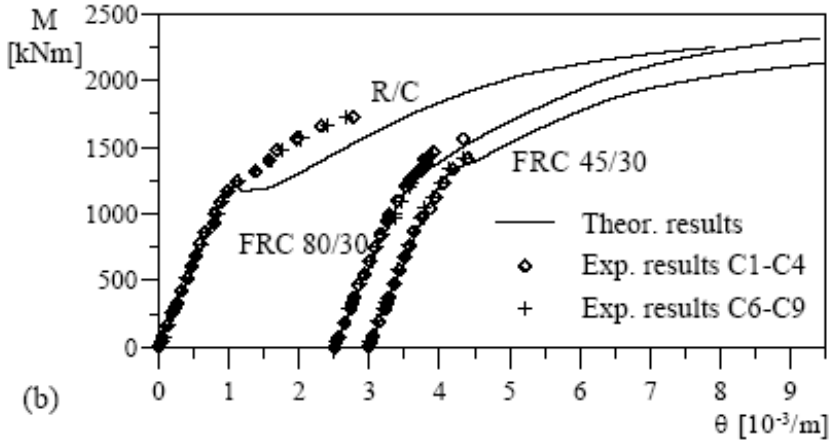
M
[kNm]
R/C
FRC 45/30
FRC 80/30
Theor. results
Exp. results C1-C4
Exp. results C6-C9
θ [10-3/m]
(b)

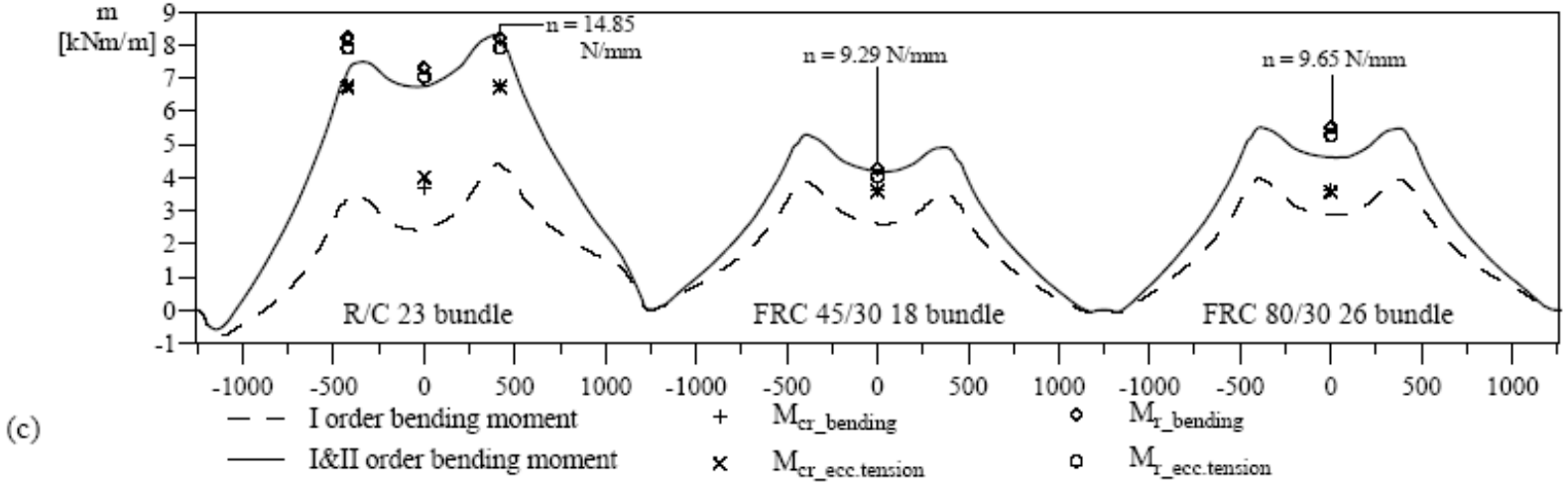
m
[kNm/m]
n = 14.85
N/mm
n = 9.29 N/mm
n = 9.65 N/mm
R/C 23 bundle
FRC 45/30 18 bundle
FRC 80/30 26 bundle
I order bending moment
I&II order bending moment
M cr_bending
M cr_ecc.tension
M r_bending
M r_ecc.tension
(c)

Real-size structures

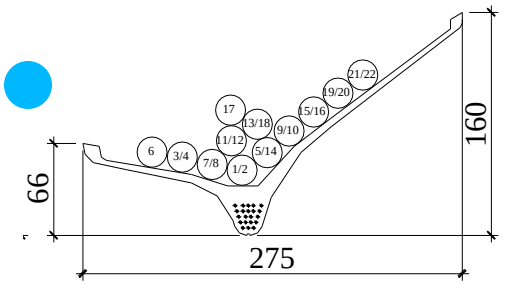

Element	Age [days]	Fibre	R_{cm} [MPa]	Element weight [kg]
P 70 00	17	-	71.20	22840
F 95 45	63	45/30	92.70	18740
F 60 45	45	45/30	62.25	18820
F 110 80	75	80/30	109.90	18480

Real-size structures

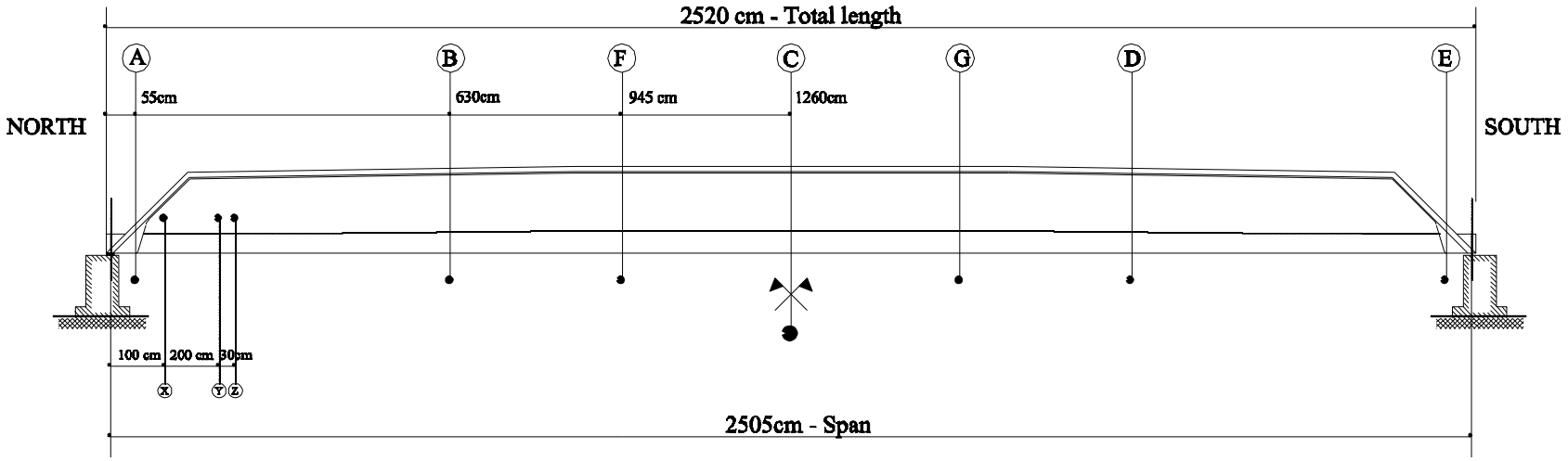

SECTION C

LONGITUDINAL STRAINS

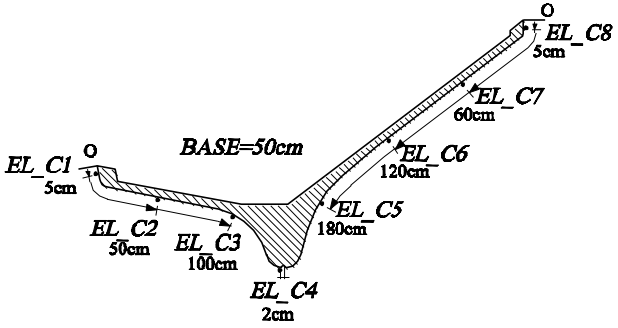

TRANSVERSAL STRAINS

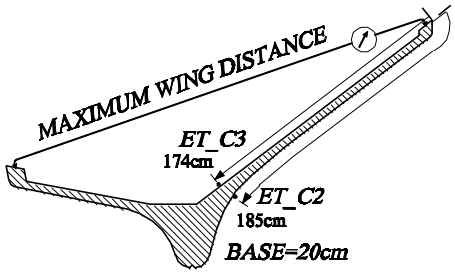

VERTICAL/HORIZONTAL DISPLACEMENTS

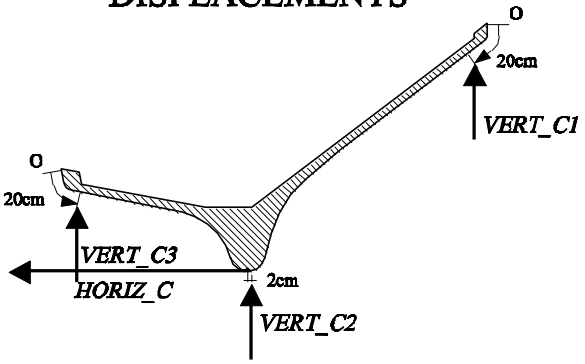

Real-size structures

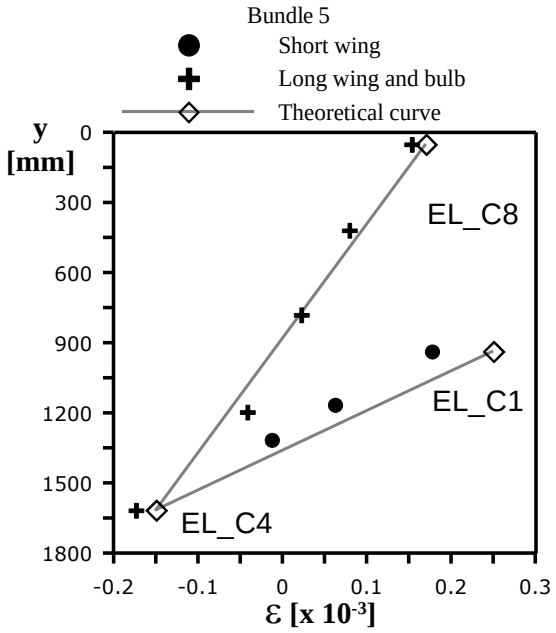

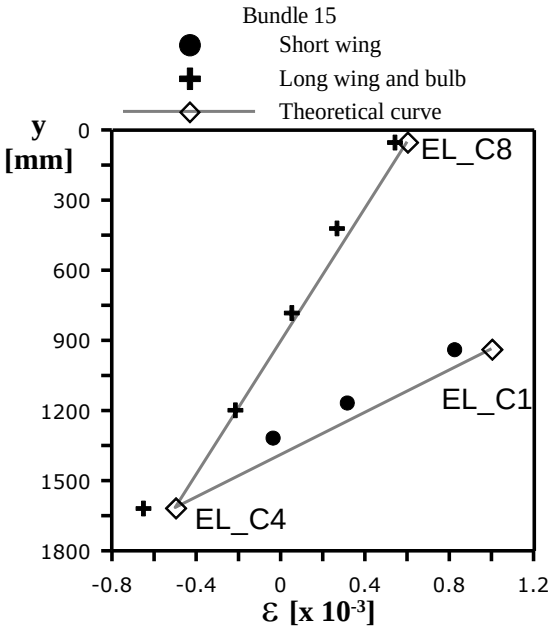

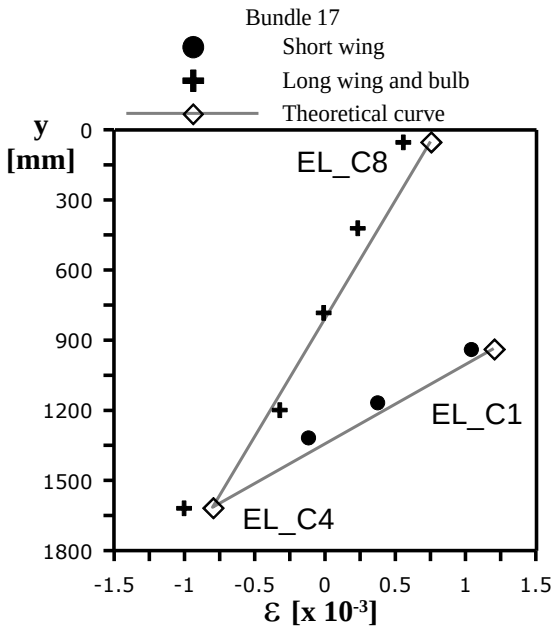

Precast Element	P [kN]	M_{CEB} [kNm]	M_{EC2} [kNm]	M_{EXP} [kNm]
P 70 00	418.80	2565 (+26.8%)	2461 (+20.3%)	2023
F 95 45	351.48	2383 (+40.4%)	2232 (+31.5%)	1697
F 60 45	343.01	2090 (+25.8%)	2042 (+22.9%)	1661
F 110 80	342.40	2530 (+53.4%)	2294 (+39.1%)	1649

-35%

Full-size structures

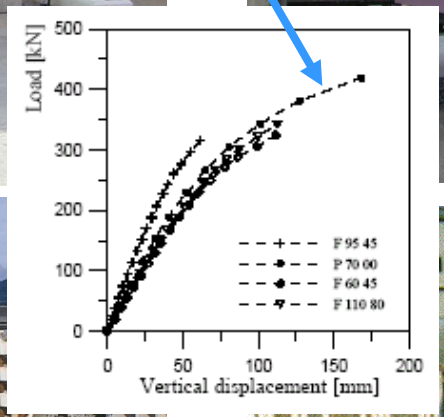

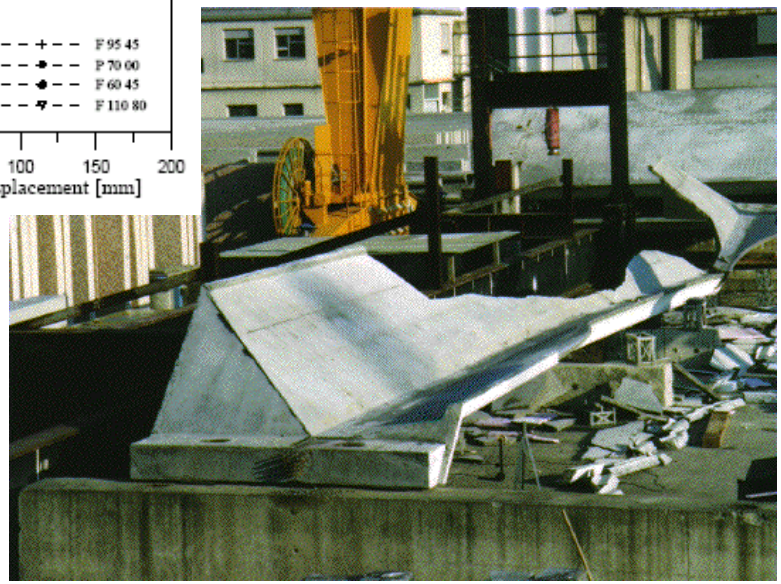

Real-size structures

theoretical prediction

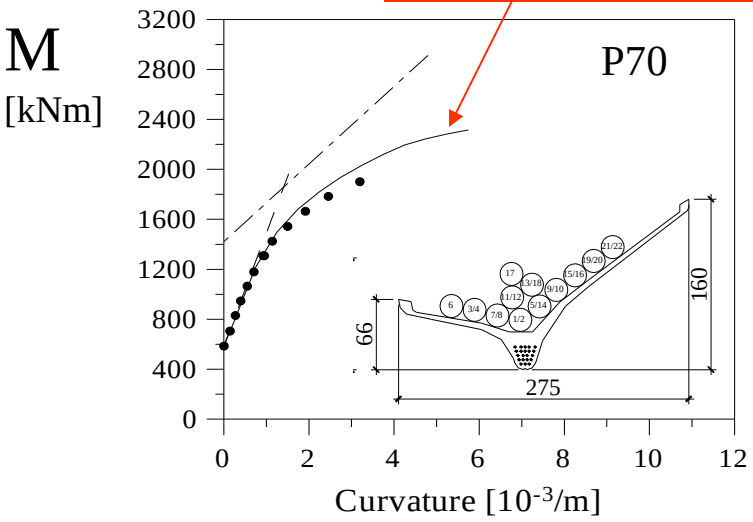

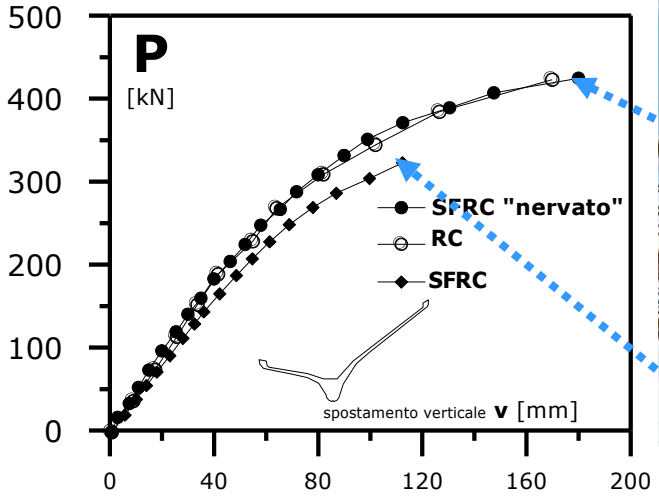

Workability, passing and filling ability


Slump-flow


V-funnel


L-box


U-box


J-ring

Conventional tests on fresh concrete to guarantee a homogeneous fibre distribution

The real question remains: is the mix robust enough?

A “triangular” optimization

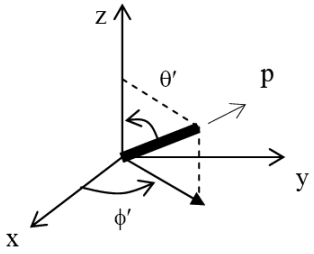

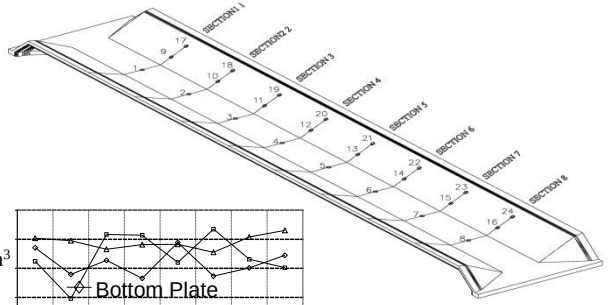

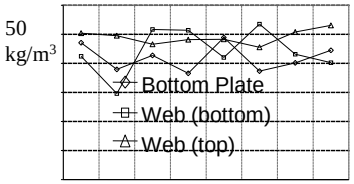

Mechanical properties

Fiber dispersion and orientation

SCSFRC

structural performance

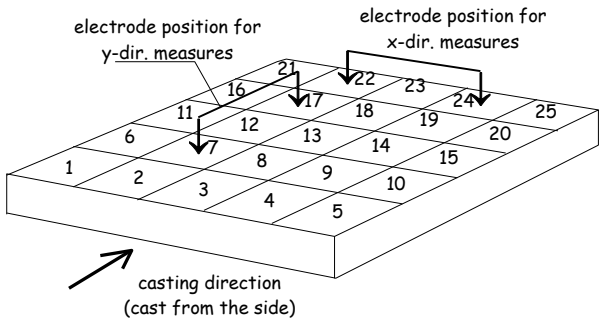

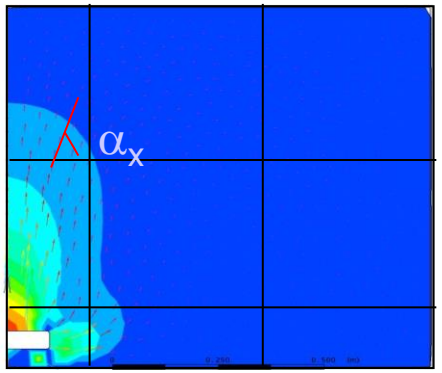

Fractional shear rate vector orientation

Fresh state behaviour

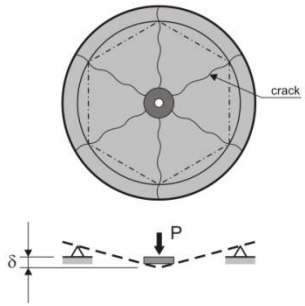

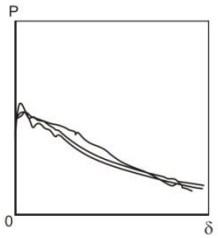

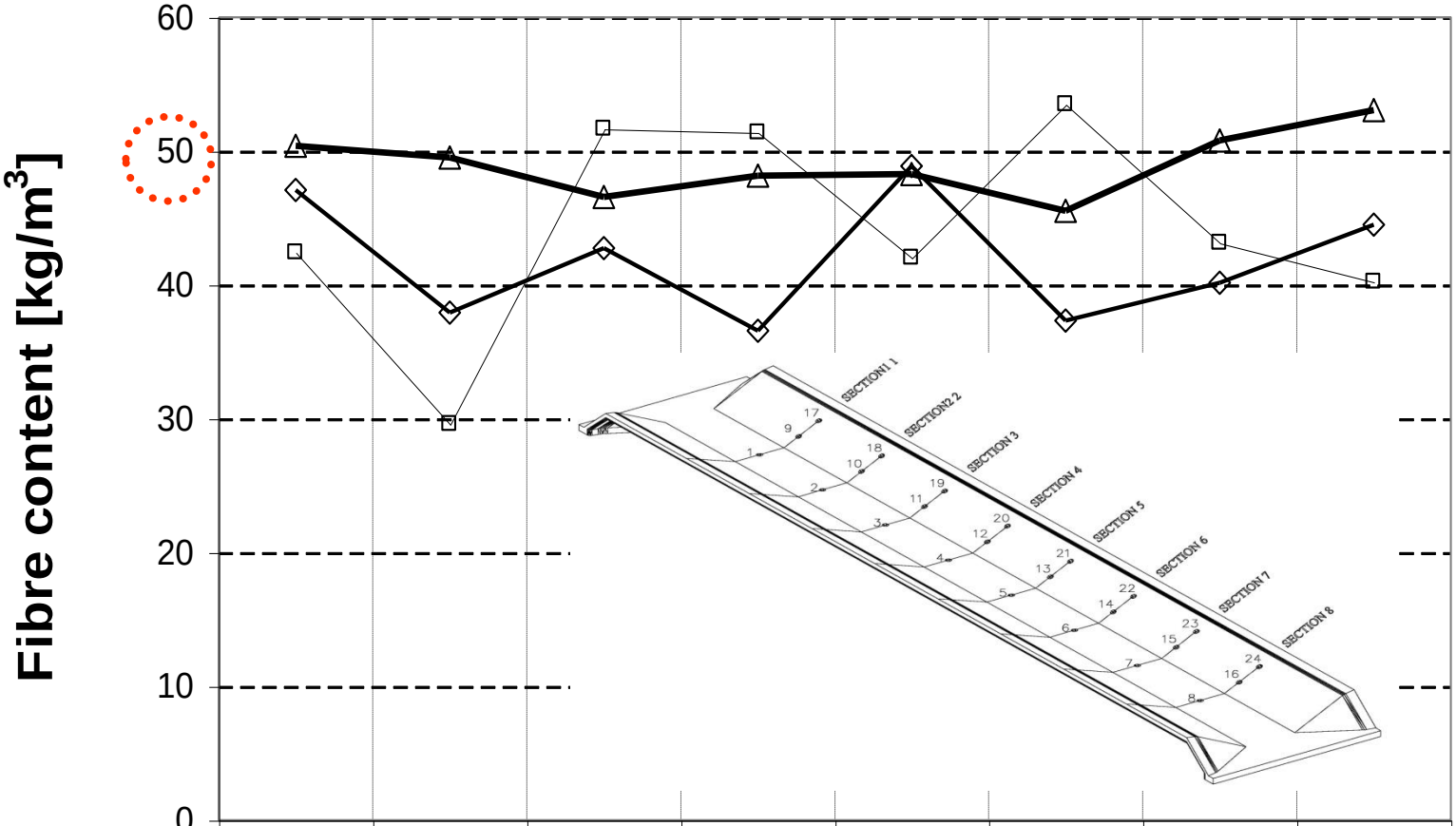

	Section 1	Section 2	Section 3	Section 4	Section 5	Section 6	Section 7	Section 8
Bottom Plate	47,10	37,93	42,77	36,58	48,90	37,33	40,18	44,49
Web (bottom)	42,41	29,61	51,68	51,41	42,02	53,50	43,15	40,26
Web (top)	50,39	49,52	46,58	48,18	48,29	45,53	50,81	53,06

by Ferrara and Meda, 2006

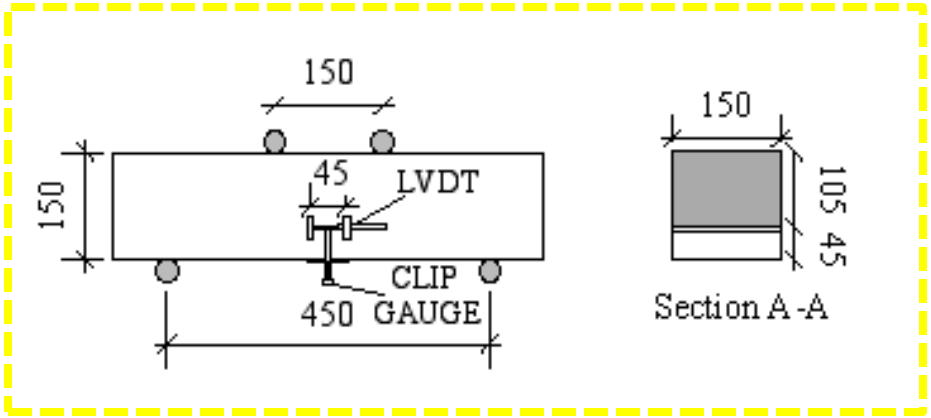

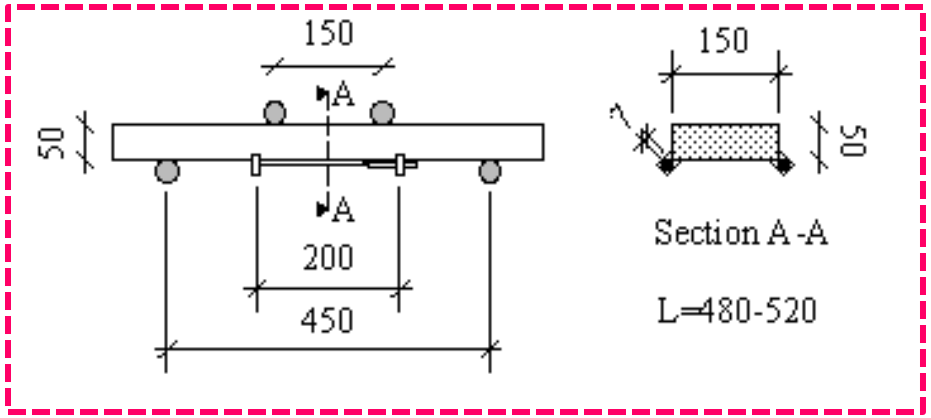

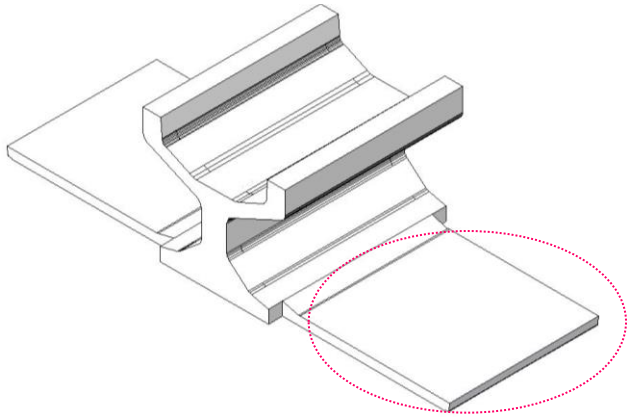

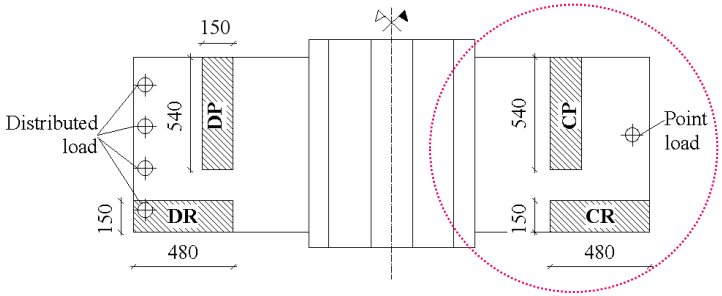

Table 1. Material description

Code	R_{cm} [MPa]	Steel c_f [kg/m^3]	l_f/d_f	l_f [mm]	f_{fu} [MPa]	Polypropylene c_f [kg/m^3]	l_f [mm]	f_{fu} [MPa]
P	61.19	-	-	-	-	-	-	-
S-1	54.43	25+ 25	75 50	60 30	1192 1192	3	12	450
S-2	57.09	50	80	30	2300	3	12	450
S-3	61.09	50	45	30	1250	3	12	450

by Bonalumi et al., 2006

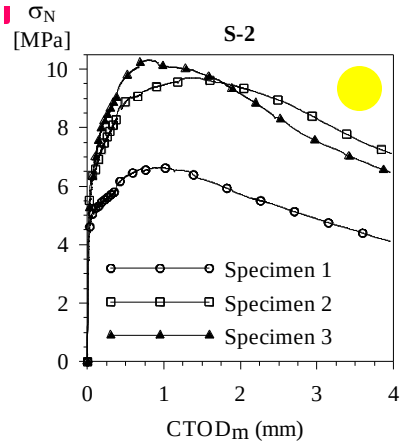

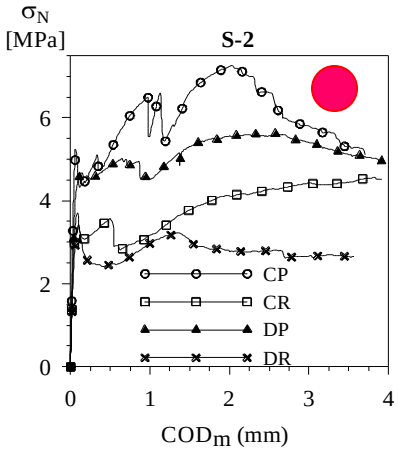

Classification tests *Structural test*

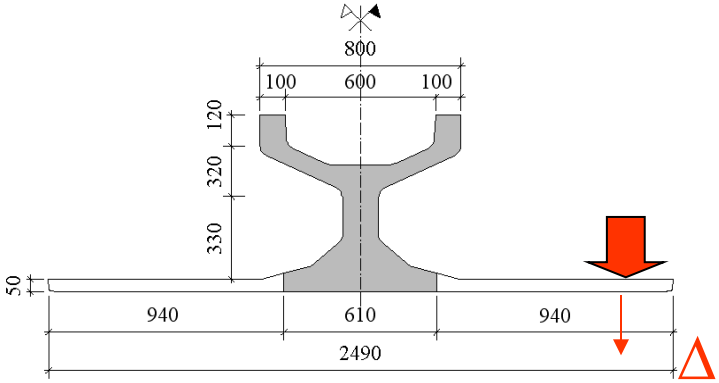
800
100
600
100
120
320
330
50
940
610
940
2490
Δ

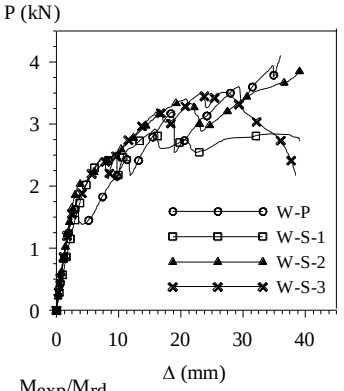
P (kN)
W-P
W-S-1
W-S-2
W-S-3
Δ (mm)

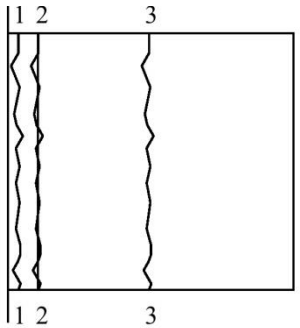
1 2
3
1 2
3

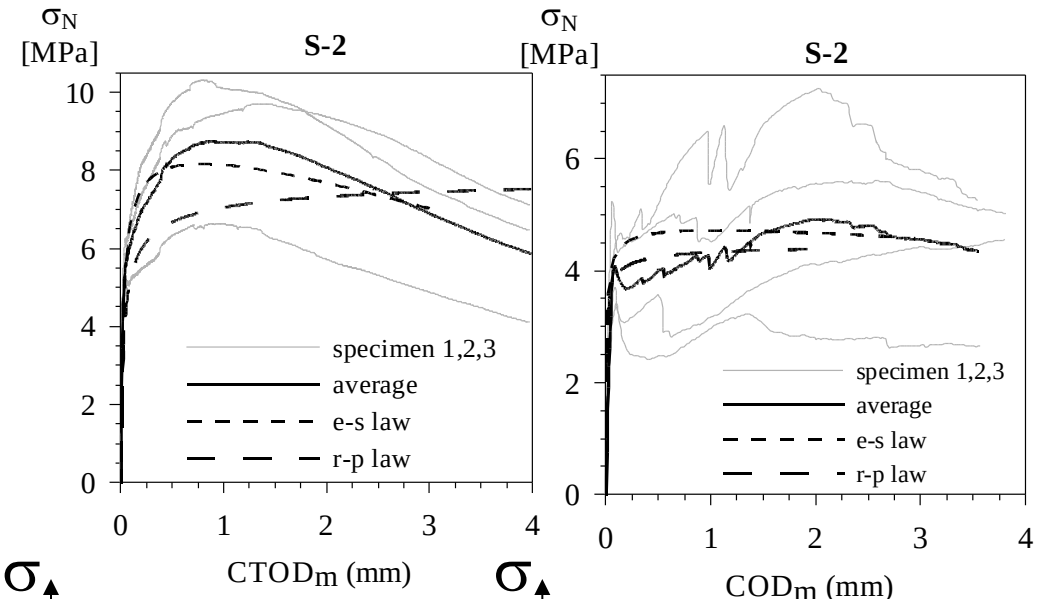
σN [MPa]
S-2
specimen 1,2,3
average
e-s law
r-p law
CTODm (mm)
σN [MPa]
S-2
specimen 1,2,3
average
e-s law
r-p law
CODm (mm)

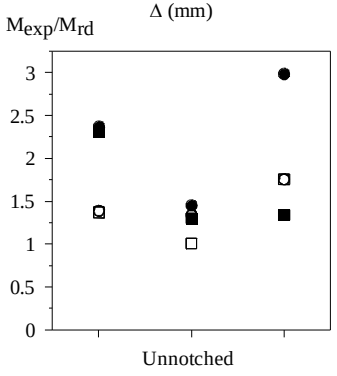
Mexp/Mrd
Unnotched

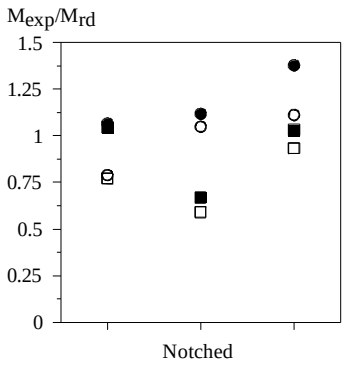
Mexp/Mrd
Notched

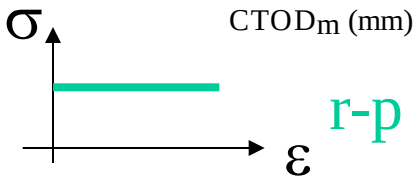
σ
ε
r-p

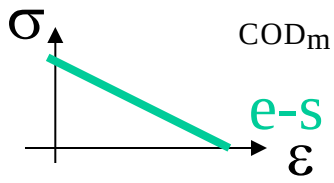
σ
ε
e-s

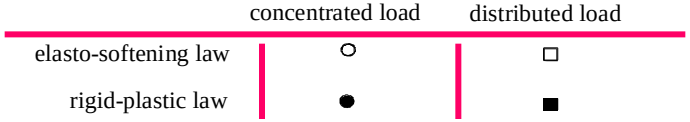
concentrated load
distributed load
elasto-softening law
rigid-plastic law

A non destructive test to identify fibre distribution

by Ferrara et al. 2010

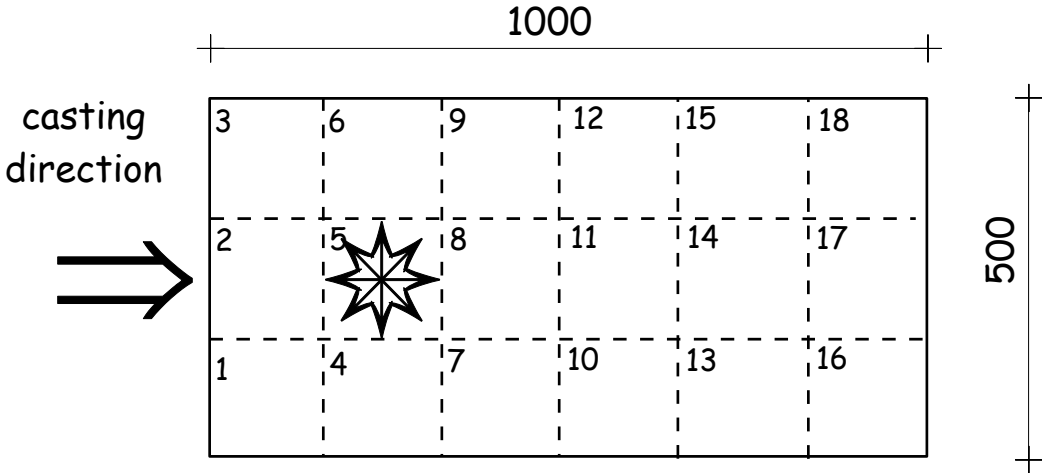

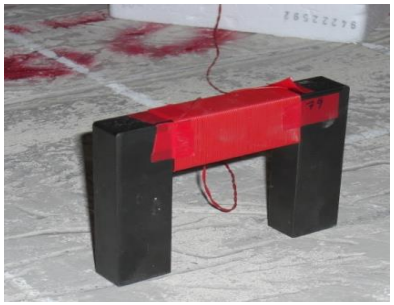

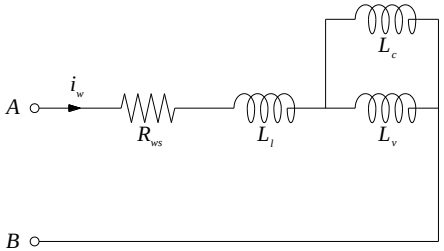

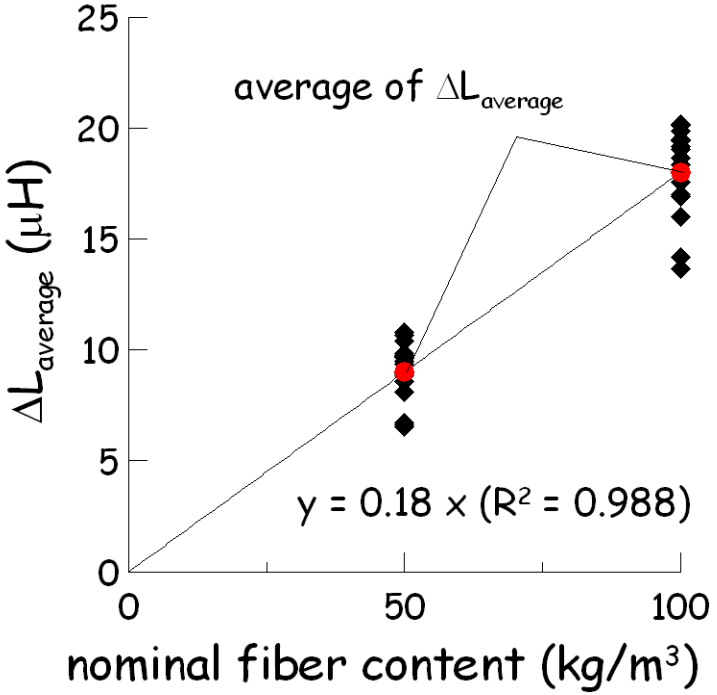

100 kg/m³

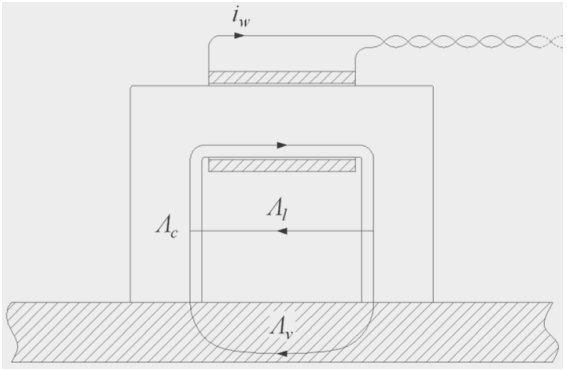

3 ND = 110.5	6 ND = 110.5	9 ND = 106.6 D = 109.9	12 ND = 103.6 D = 106.7	15 ND = 97.5	18 ND = 88.7
2 ND = 101.8 D = 119.1	5 ND = 108.7 D = 109.5	8 ND = 103.5 D = 107.8	11 ND = 100 D = 101.9	14 ND = 93.7 D = 98.2	17 ND = 79.4 D = 85
1 ND = 100.8	4 ND = 111.7	7 ND = 105.7 D = 105.6	10 ND = 99.5 D = 99.4	13 ND = 94.2	16 ND = 75.9

A destructive test to characterize FRC anisotropy

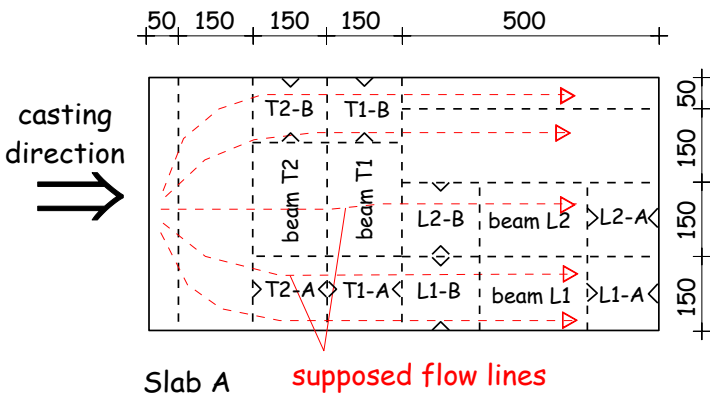

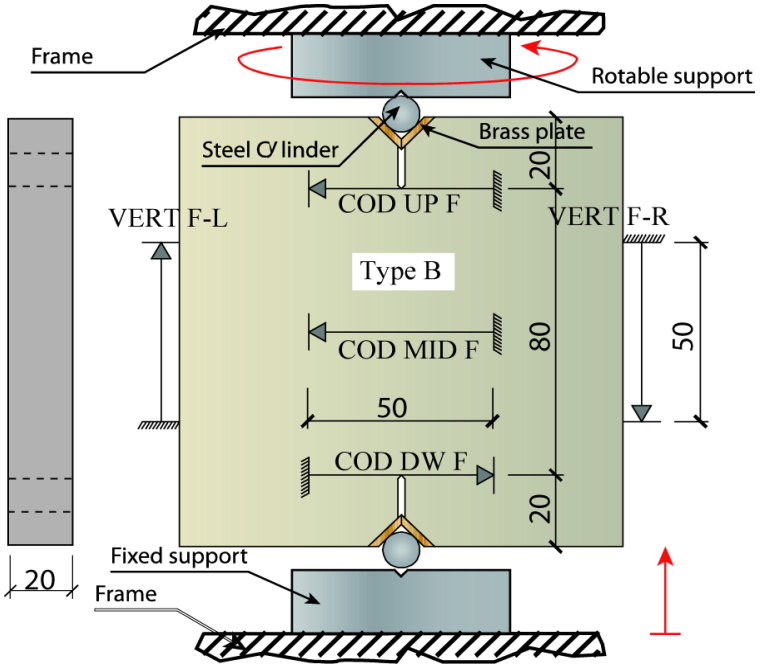

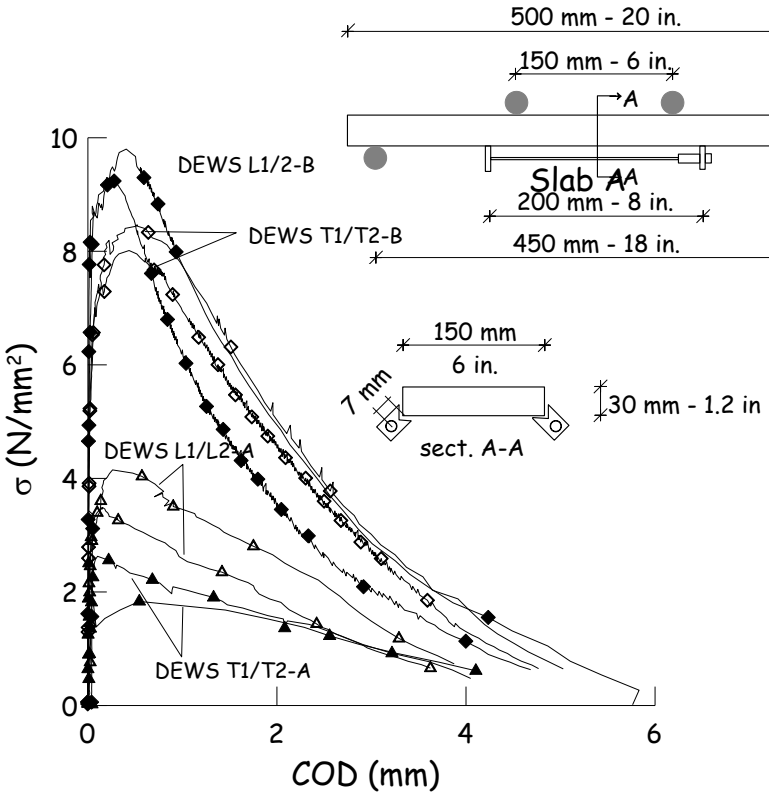

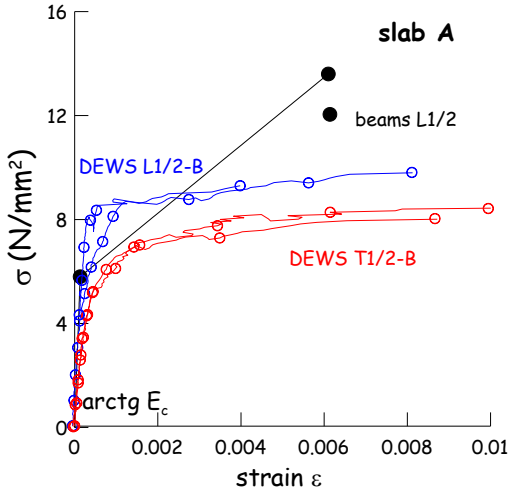

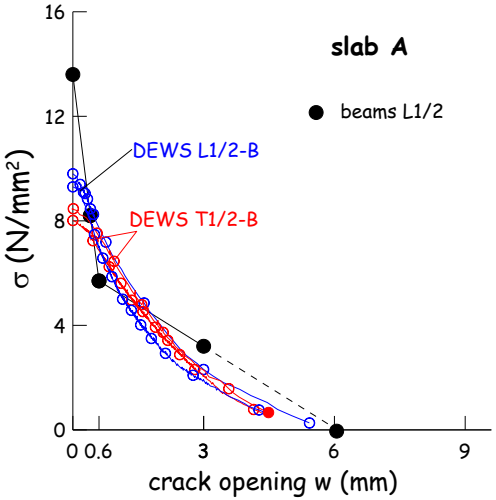

FRC is not homogeneous and not isotropic!

The inhomogeneity and anisotropic effects due to casting procedure can be taken into account by a special coefficient K that is at this time just empirical.

5.6.7 Orientation factor

$$f_{Ftsd,mod} = \cdot f_{Ftsd}/K \qquad f_{Ftud,mod} = \cdot f_{Ftud}/K$$

Isotropic fibre distribution is assumed	$K = 1.0$
For favourable effects	$K < 1.0$
For unfavourable effects	$K > 1.0$

✓ the limit state definition

$$w_u = min\,(l_{cs} \cdot \varepsilon_{Fu}\,,\, 2.5\ mm)$$

ductility

2% for variable strain distribution along the cross section
1% for constant tensile strain distribution along the cross section.

Fibre geometry

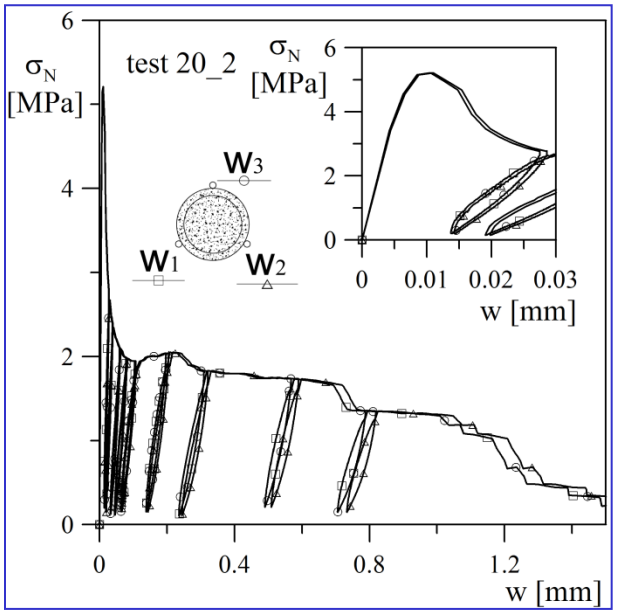

***valid for all the fibres** in the market*
For long steel fibres (crimped or hooked) could be on the safe side!

f_c = 75 Mpa; Fibre content = 50 kg/m^3; Fibre length = 30mm; Aspect ratio = 45; Low carbon

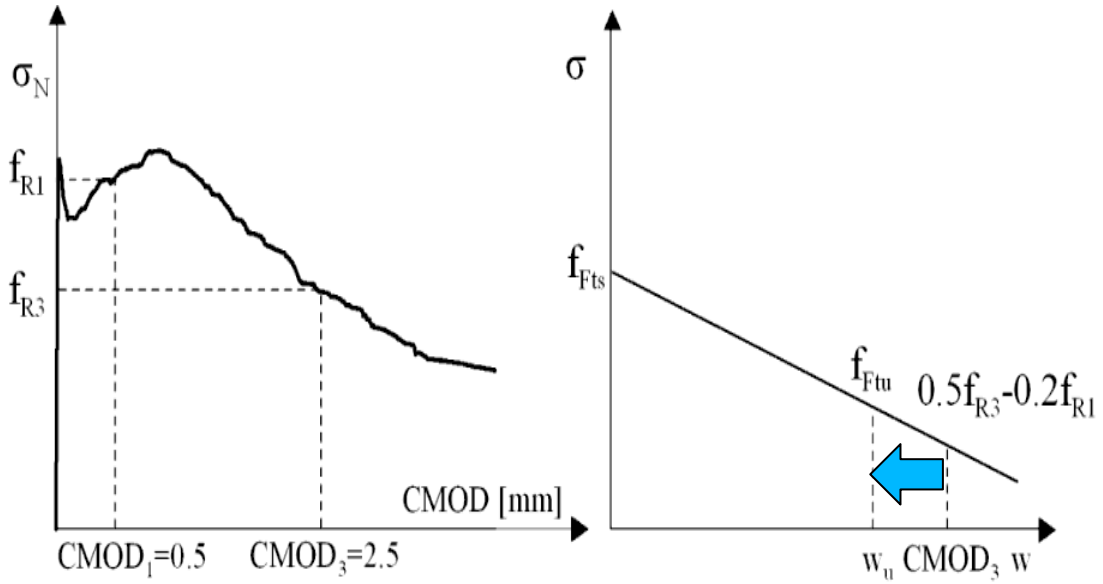

$$\theta_u = w_u/h$$

$$\delta_u = \delta_u(\theta_u, L_i)$$

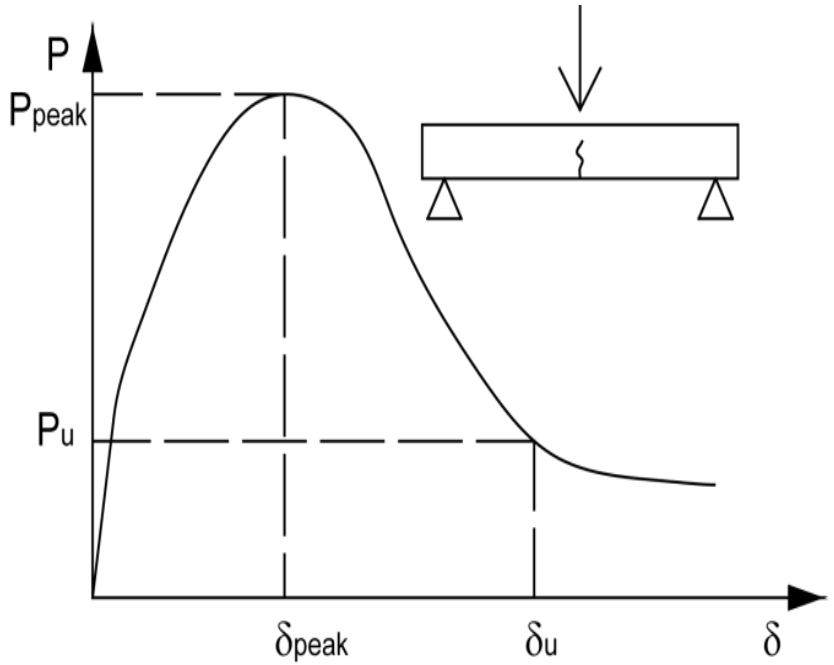

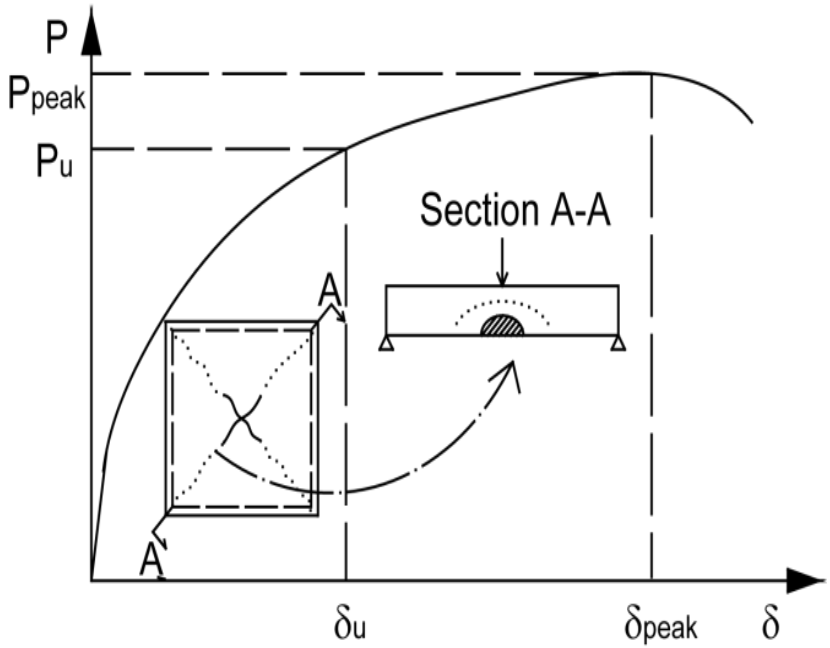

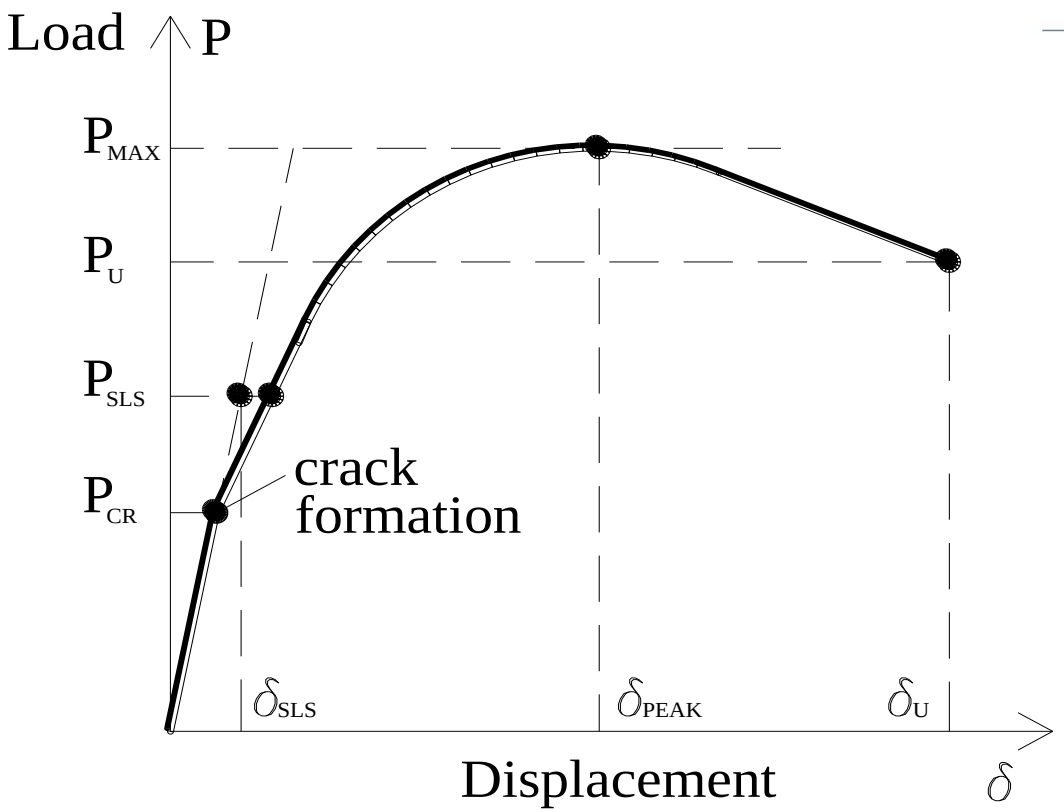

$$\delta_u \geq 20\ \delta_{SLS}$$

$$\delta_{peak} \geq 5\ \delta_{SLS}$$

Shrinkage, thermal coations, settlements …

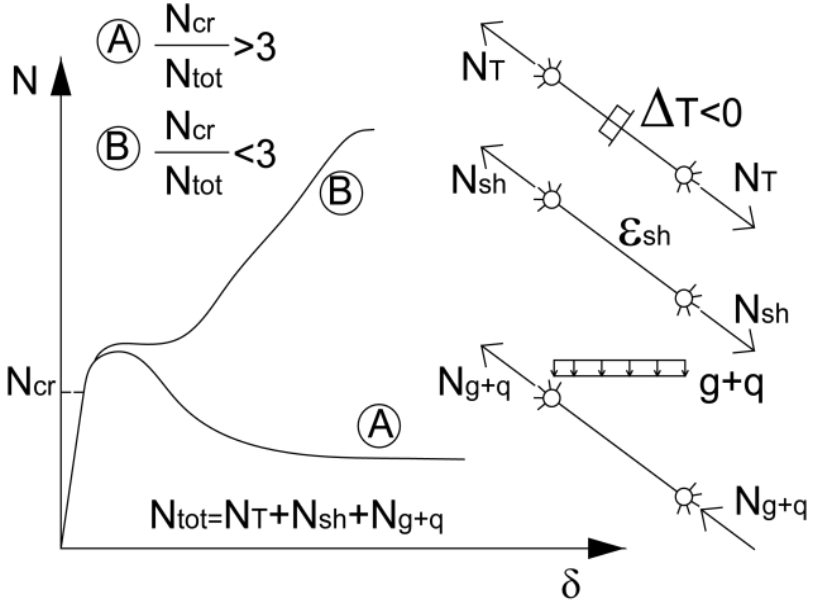

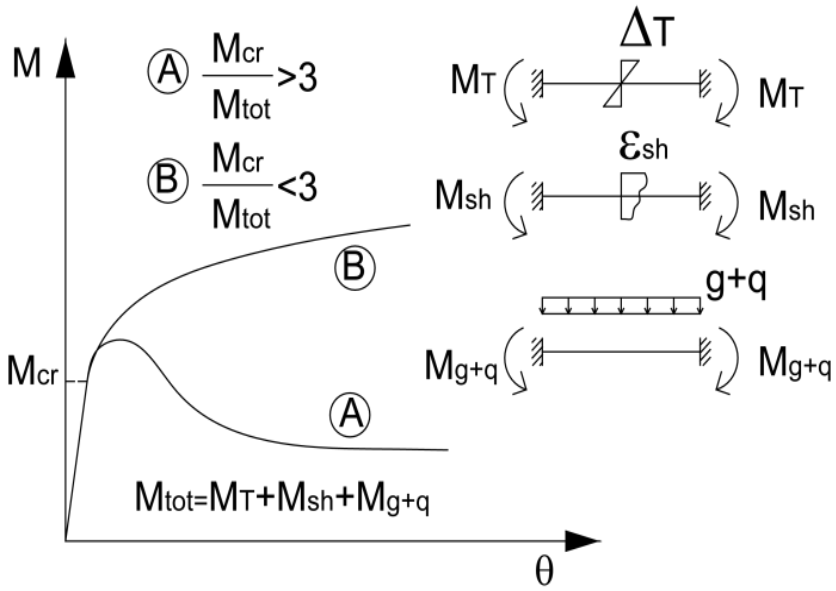

FRC for local bending

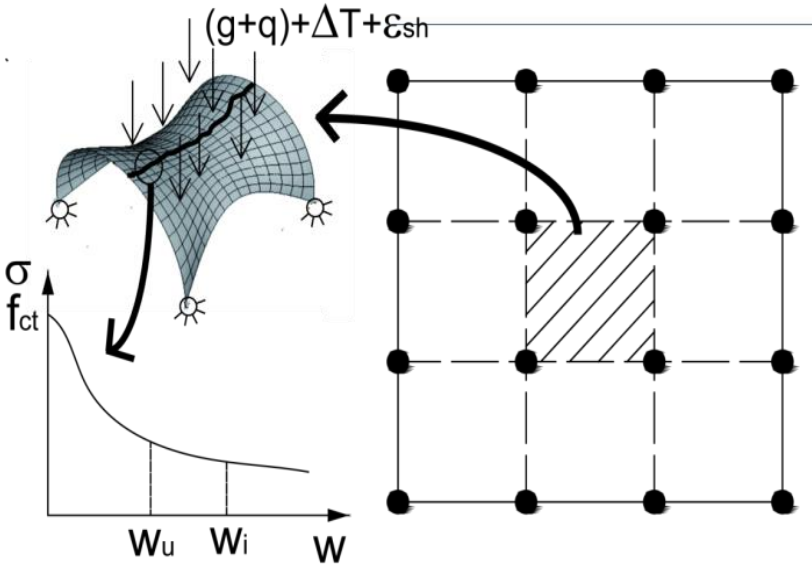

Size effect

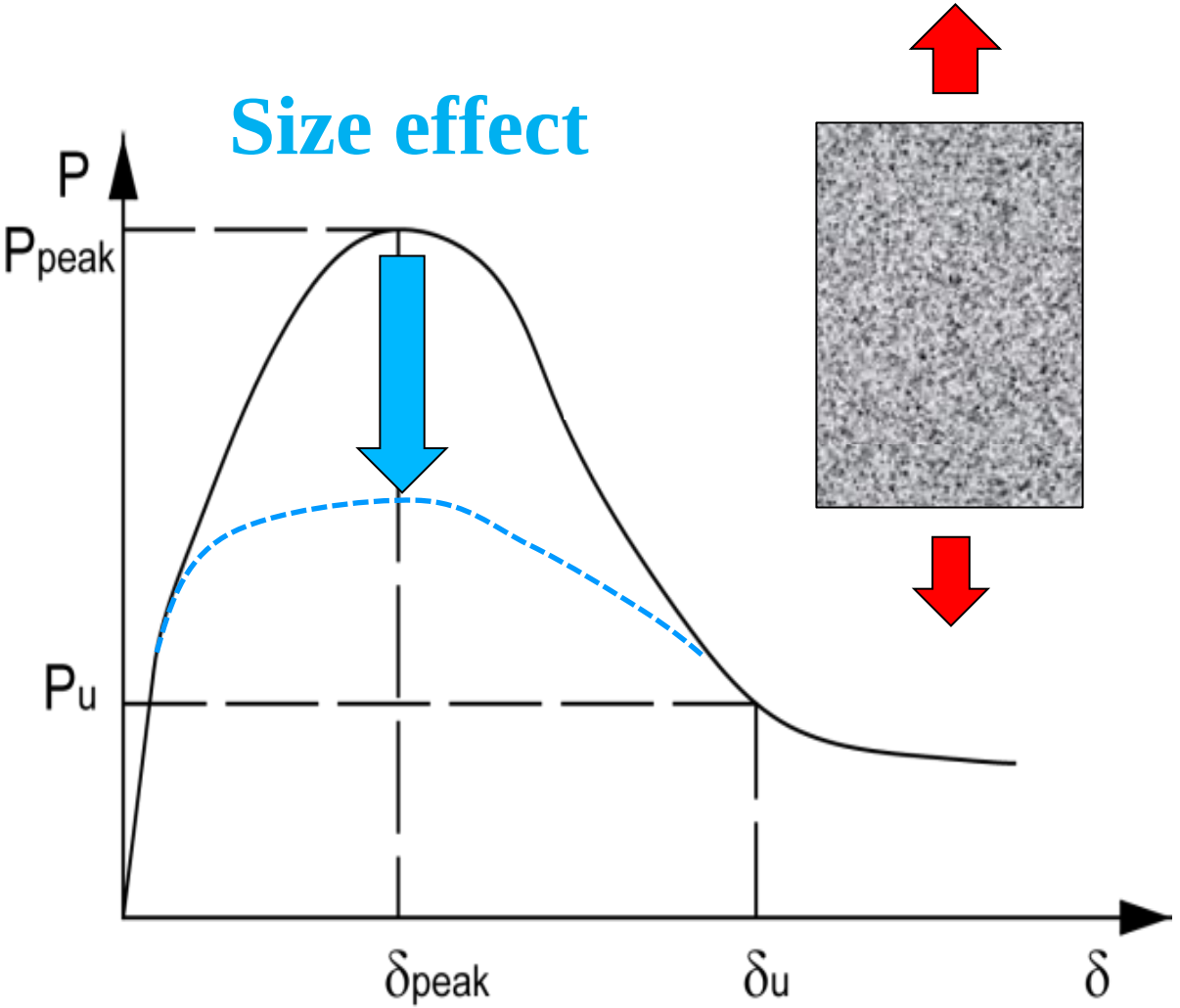

Size effect in tension

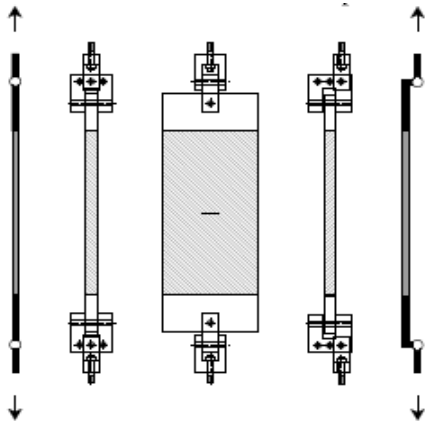

Specimen Type	Height [mm]	Width [mm]	Thick. [mm]	Notch [mm]
P	150	84	60	16.8
M	375	210	60	42
G	938	525	60	105

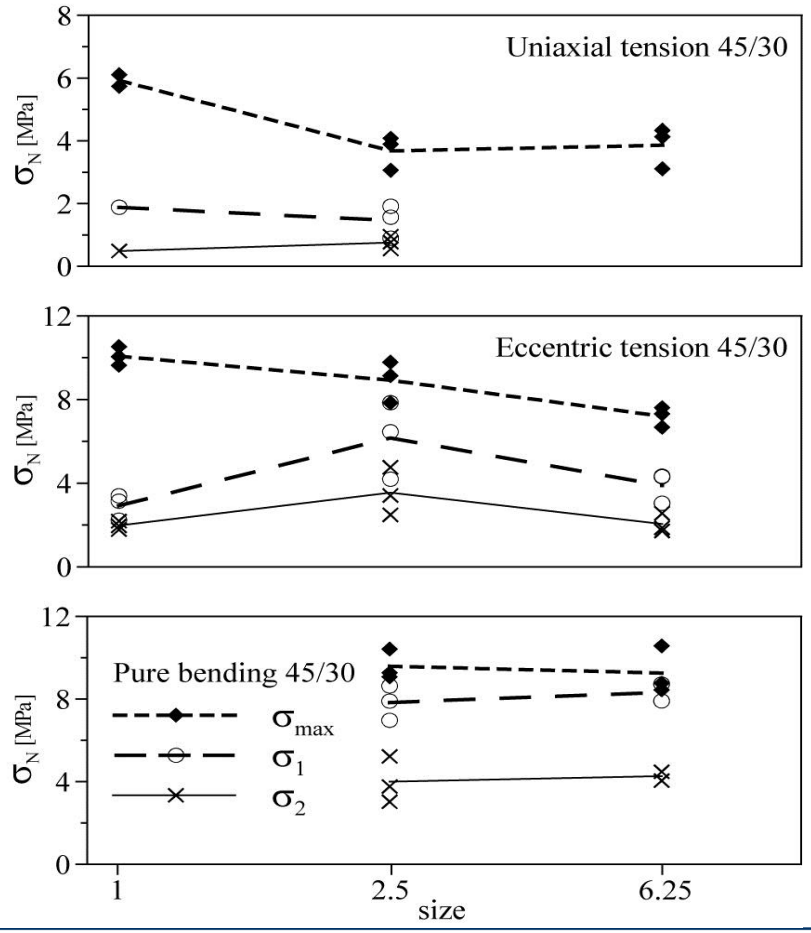

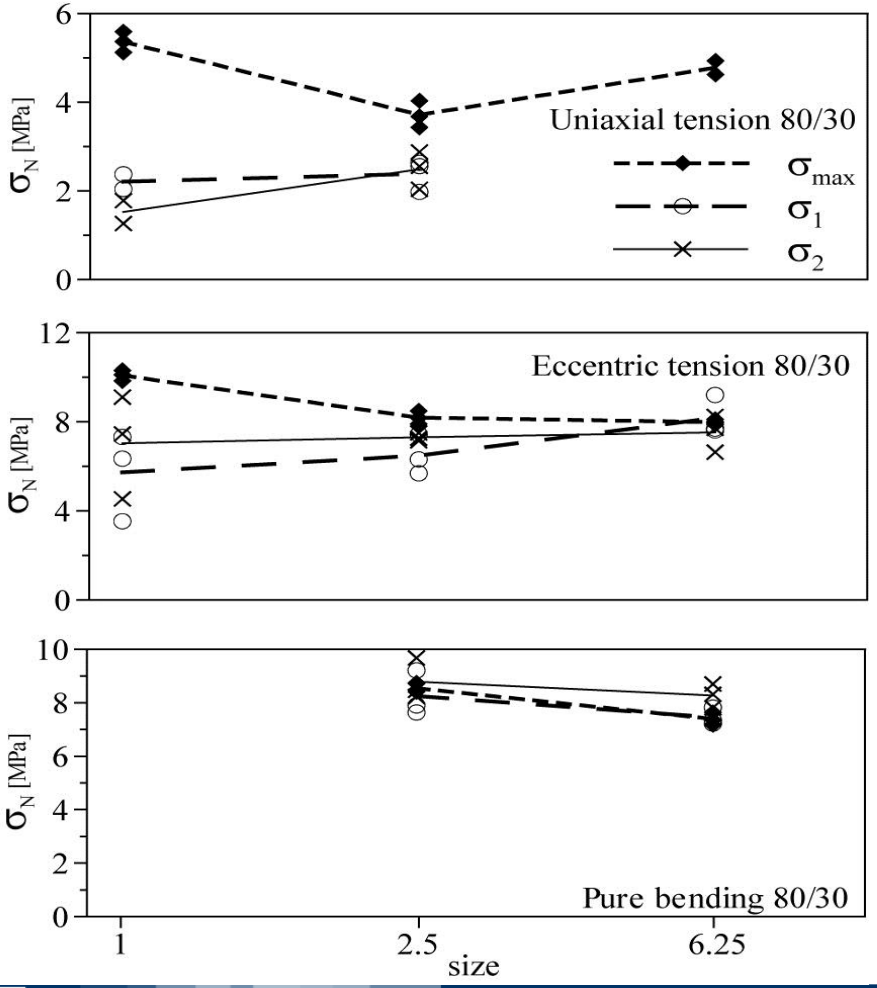

Bottle shaped strut

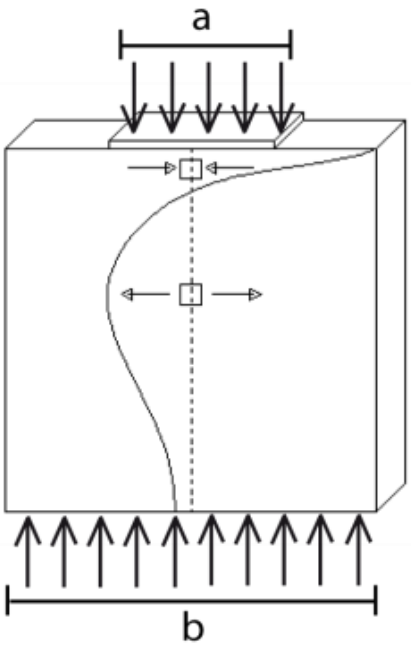

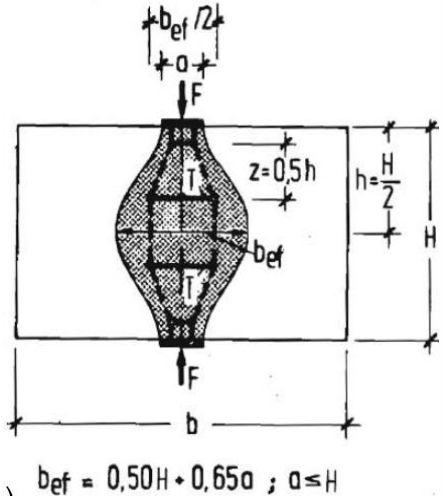

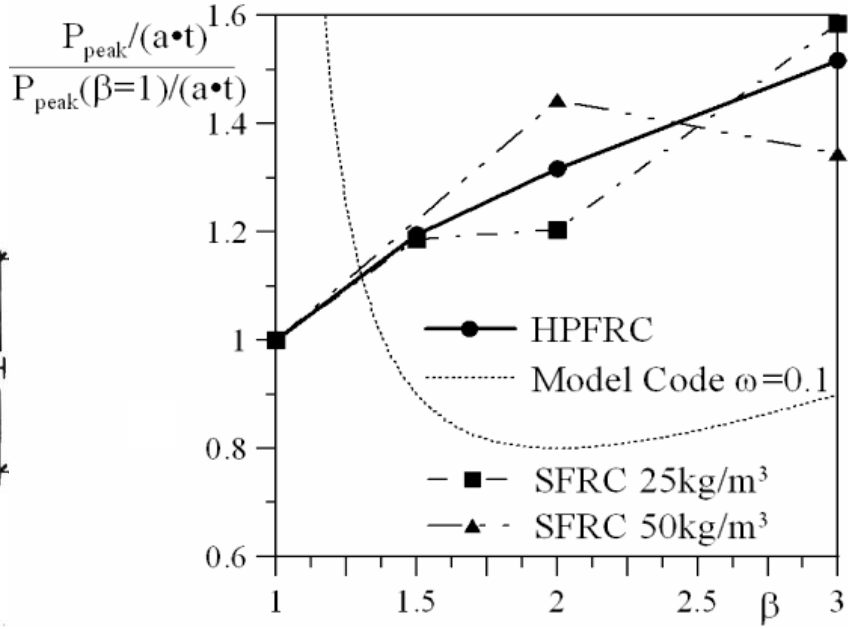

b/a	$\sigma_{c,max}/f_c$				
	NSC	HSC	UHSC	UHPC-1-HT	UHPC-2-HT
2.3	0.89	0.6	0.41	0.87	0.96
4.7	1.18	0.59	0.38	1.04	1.44
6.9	1.75	0.73	0.56	1.28	1.66
10.7	2.48	1.15	0.81	1.73	2.22

by T. Leutbecher, E. Fehling, 2012

Size effect

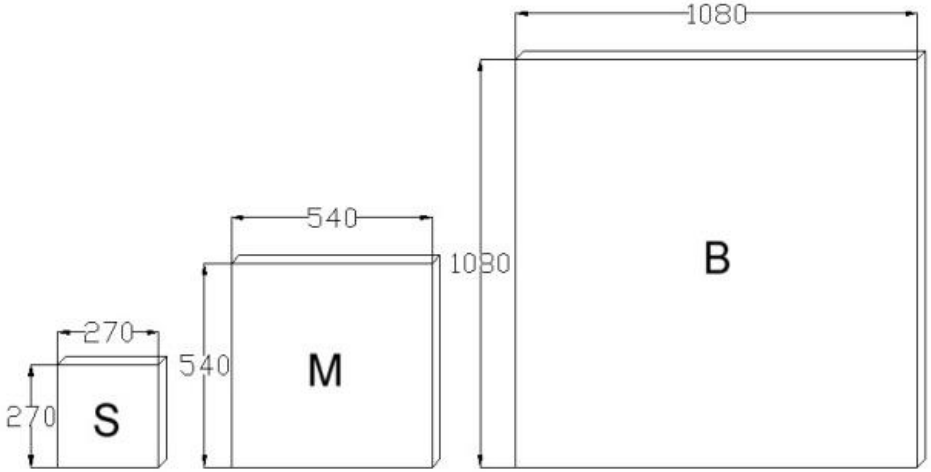
1080
540
270
1080
540
270
S
M
B

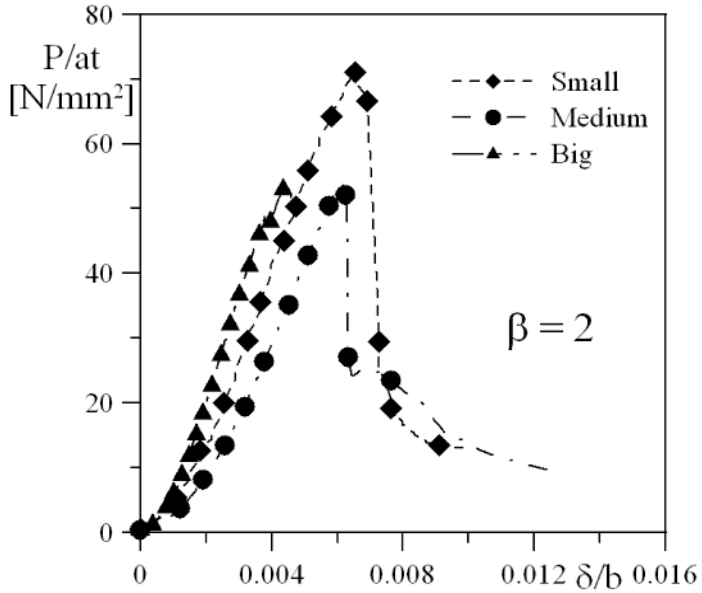
80
P/at
[N/mm²]
60
40
20
0
Small
Medium
Big
β = 2
0
0.004
0.008
0.012 δ/b 0.016

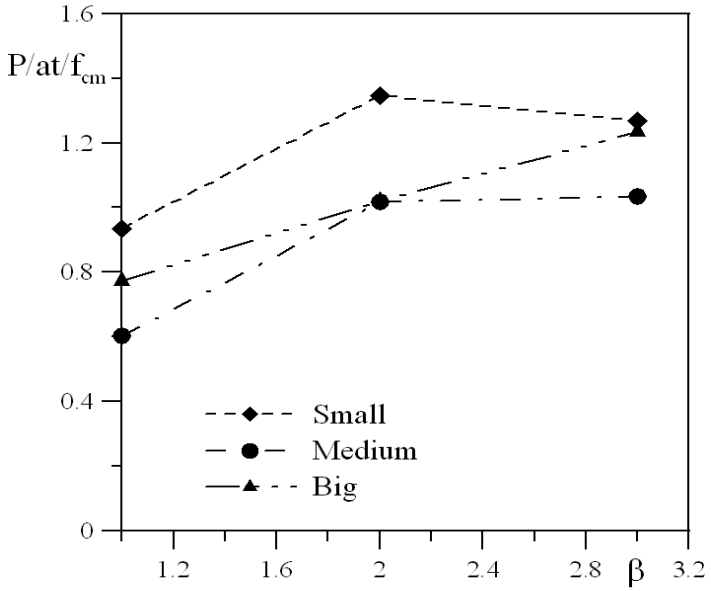
1.6
P/at/f_cm
1.2
0.8
0.4
0
Small
Medium
Big
1.2
1.6
2
2.4
2.8
β
3.2

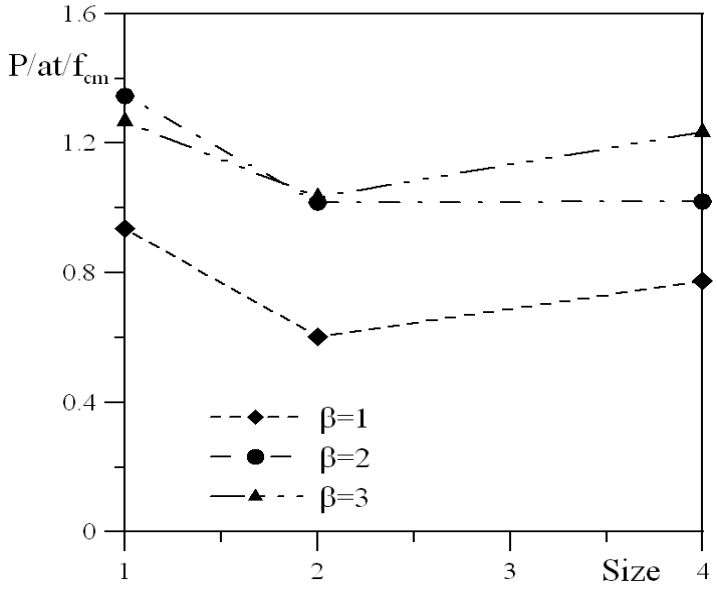
1.6
P/at/f_cm
1.2
0.8
0.4
0
β=1
β=2
β=3
1
2
3
Size
4

Residual stress after thermal damage

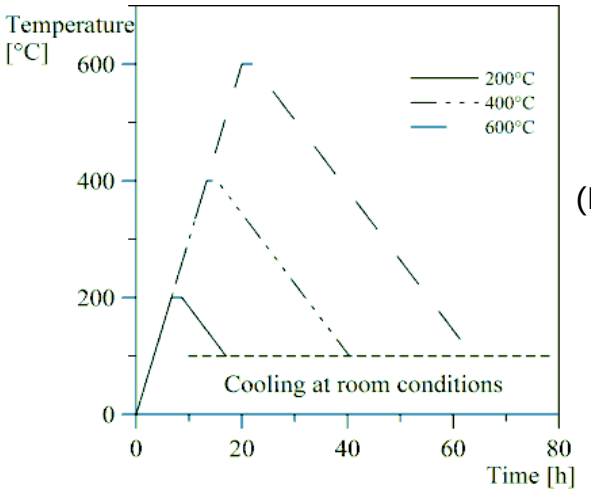

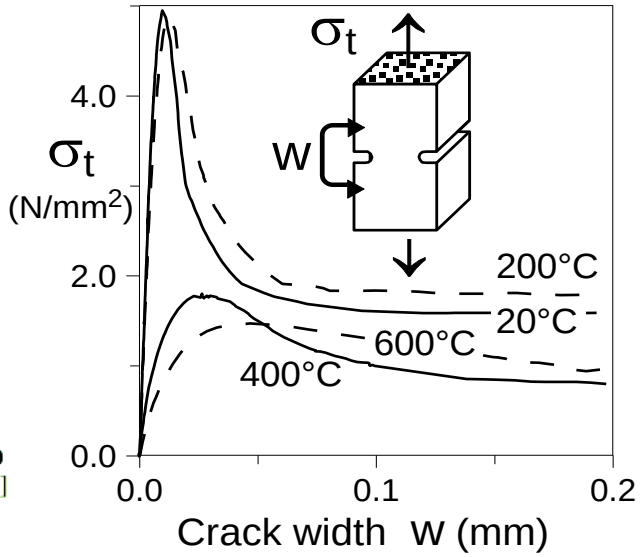

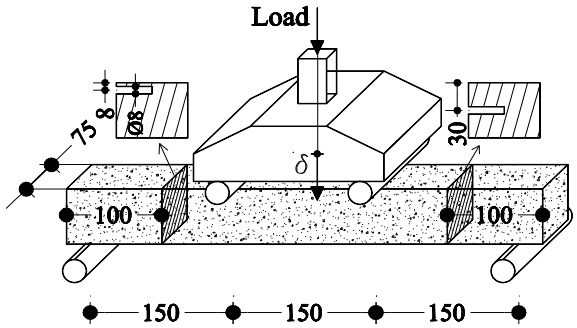

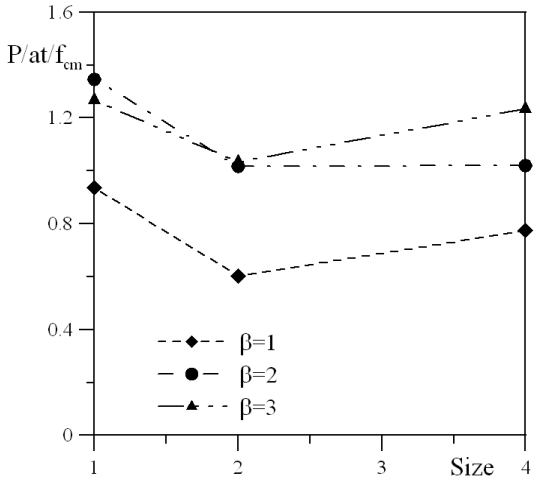

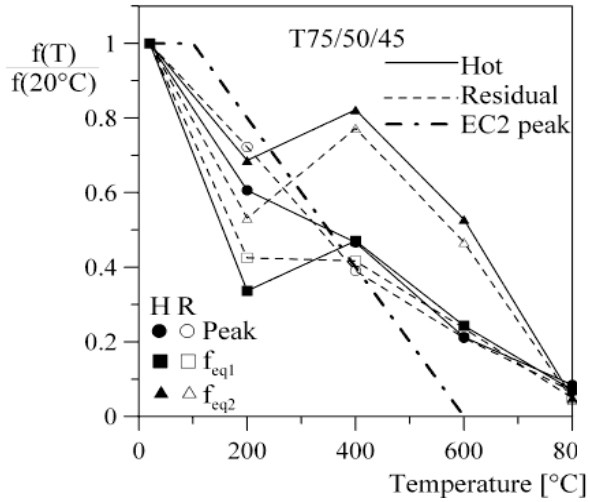

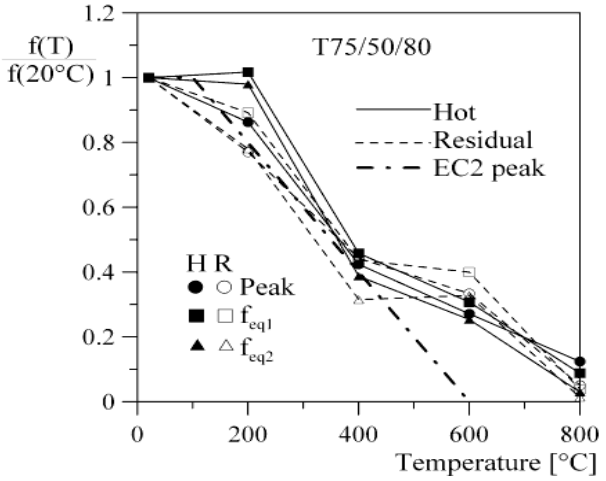

TRC: the use of non metallic AR glass fabrics

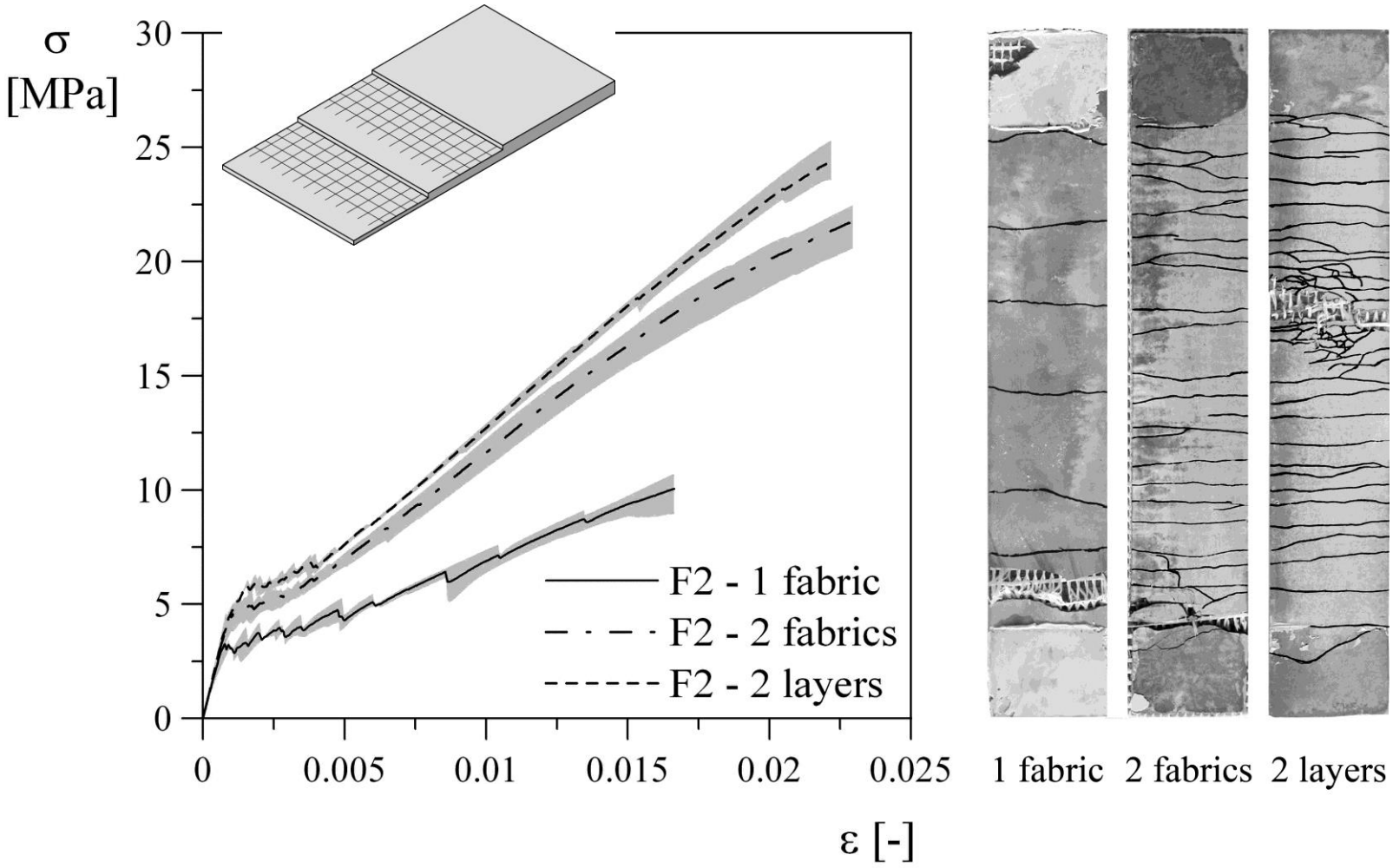

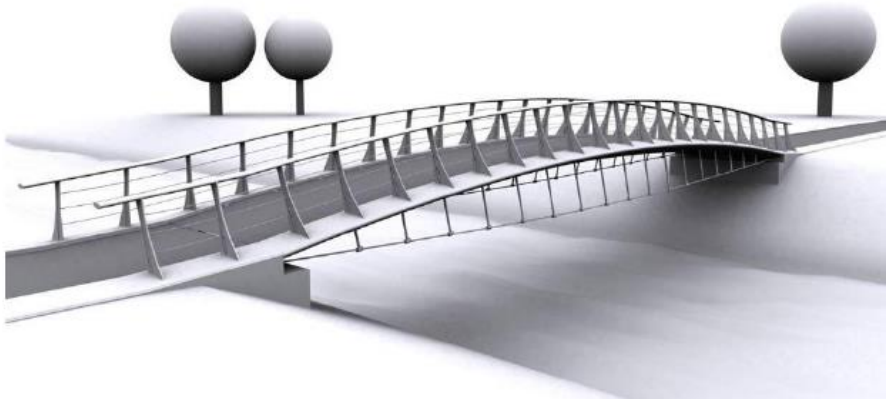

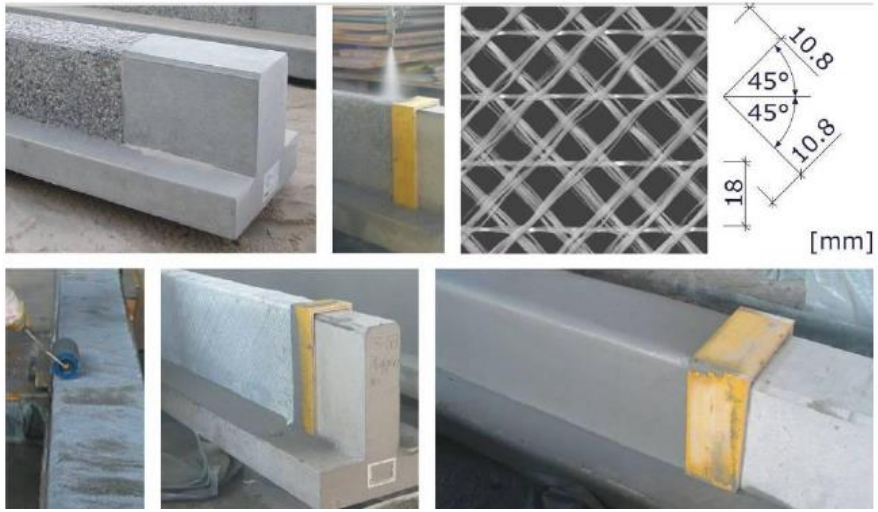

by Manfred Curbach and Silke Sheerer, 2011

UHPFRC: fire resistant advanced material

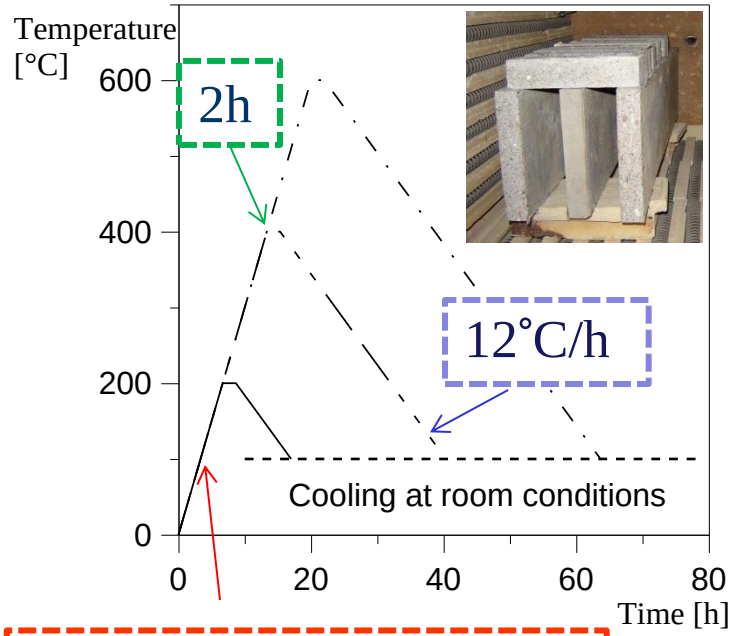

30°C/h in the heating process

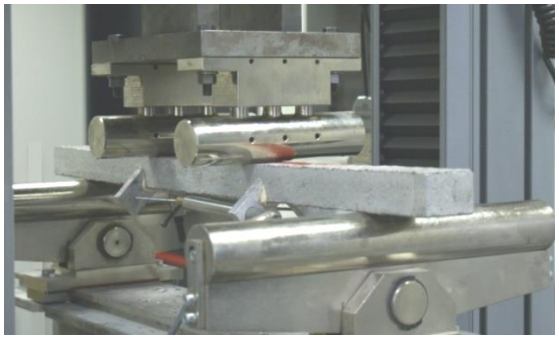

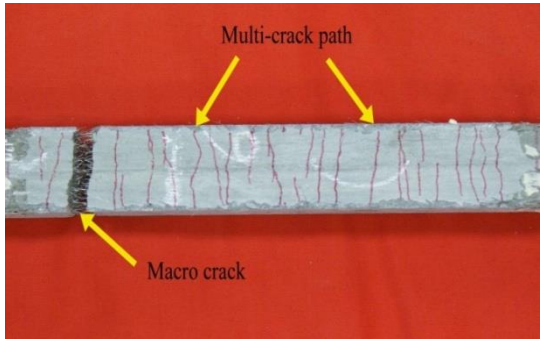

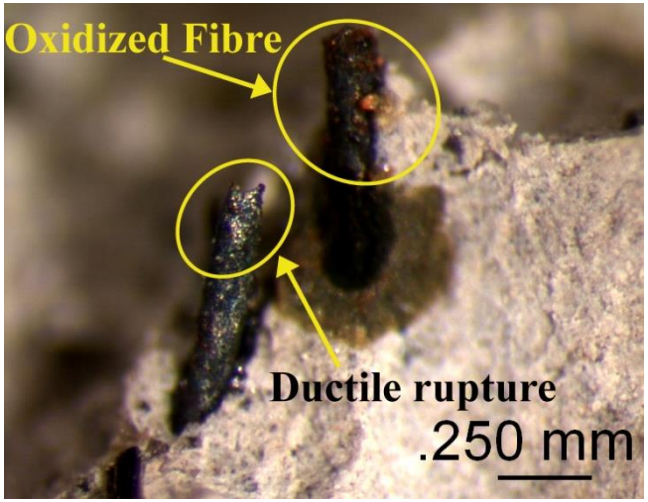

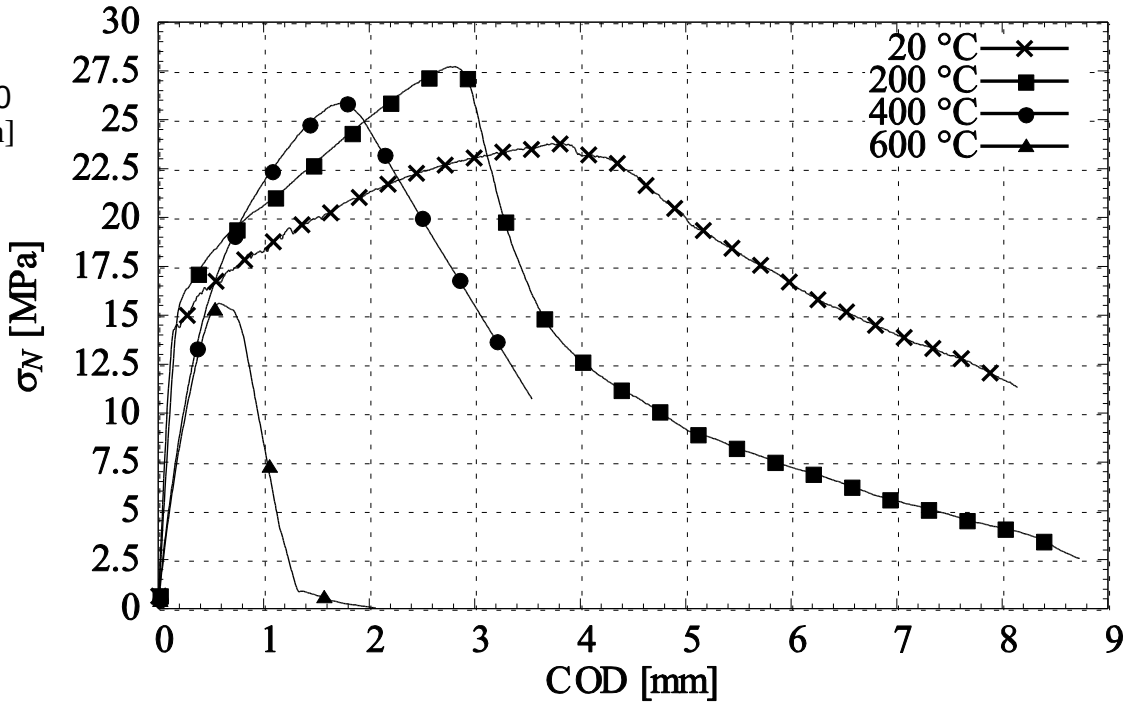

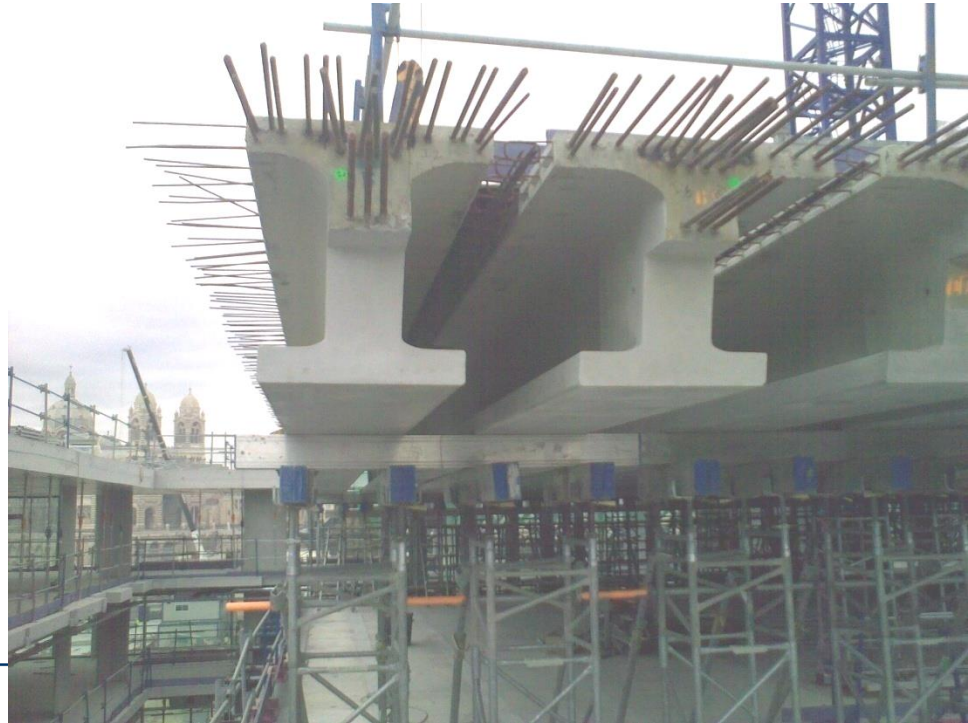

Thin layers for composite structure

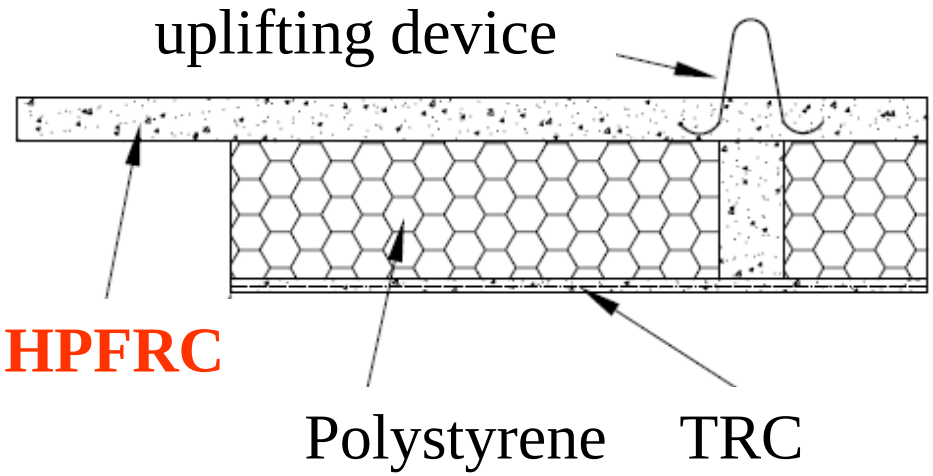

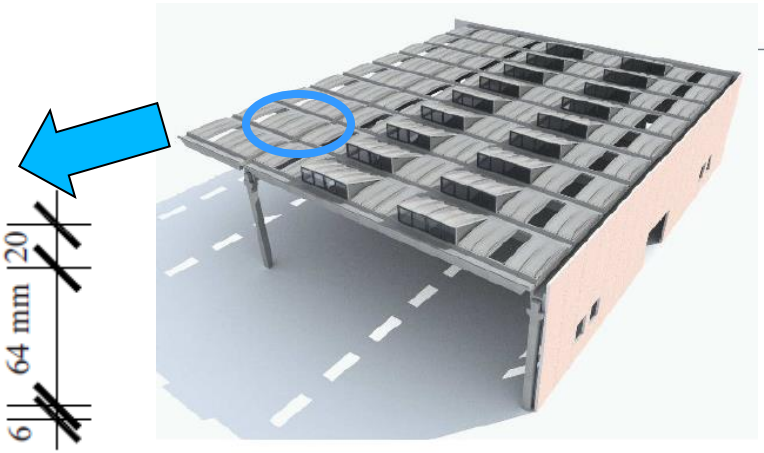

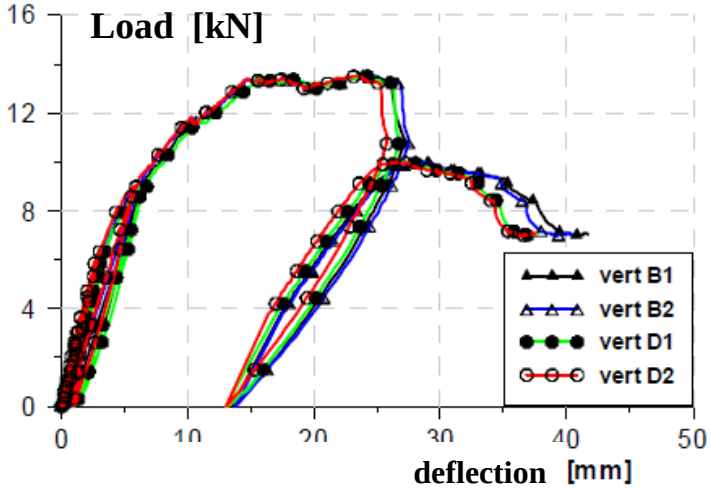

by F. Müller, C. Kohlmeyer, J. Schnell, 2012

No.	Failure mode		
A	tension failure of the reinforcement	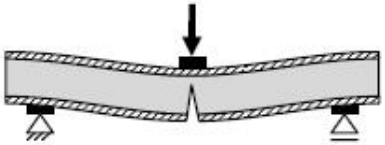	
B	compression failure of the core at the point of load application	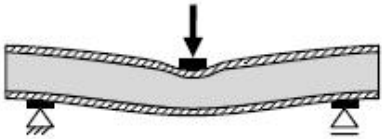	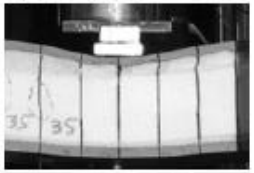
C	local bending failure of the upper facing	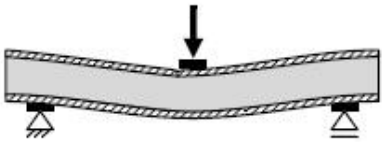	
D	local shear failure of the upper facing	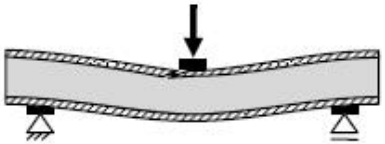	
E	shear failure of the core and delamination of core and facings	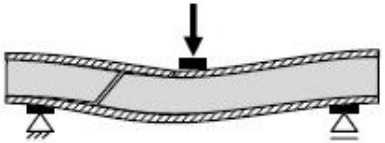	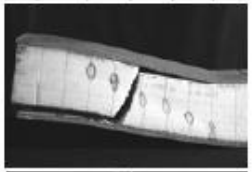
F	longitudinal shear failure of the bond between the core and the upper facing (at one or both ends)	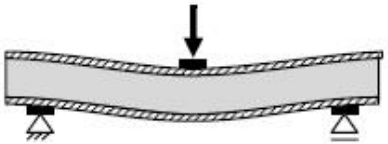	
G	compression failure of the core at the supports (at one or both ends)	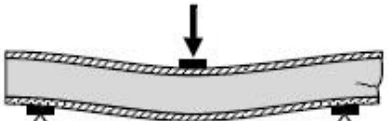	

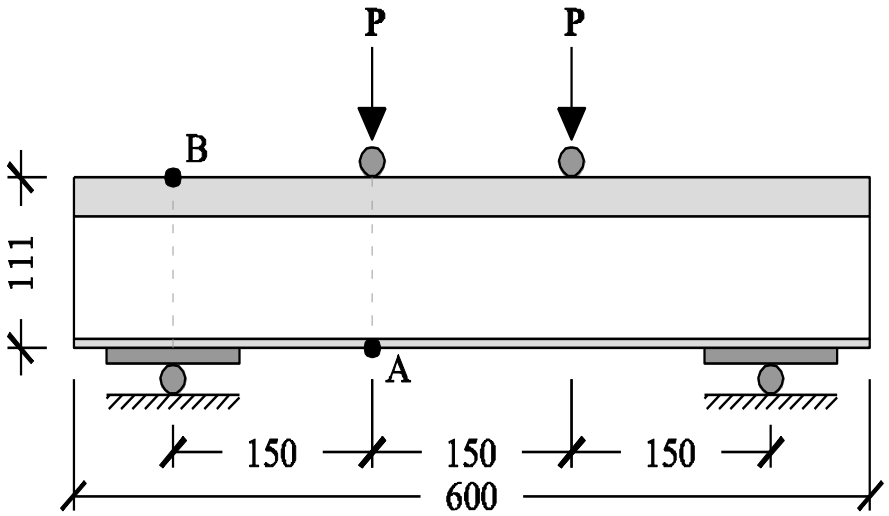
P
P
B
A
111
150
150
150
600

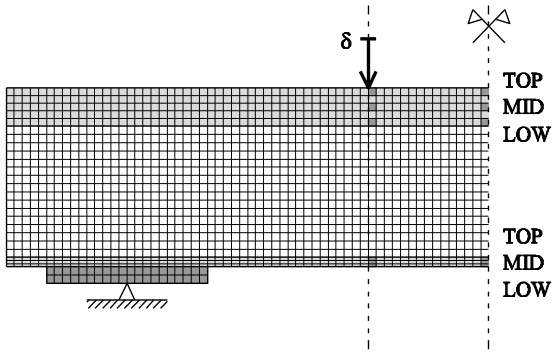
δ
TOP
MID
LOW
TOP
MID
LOW

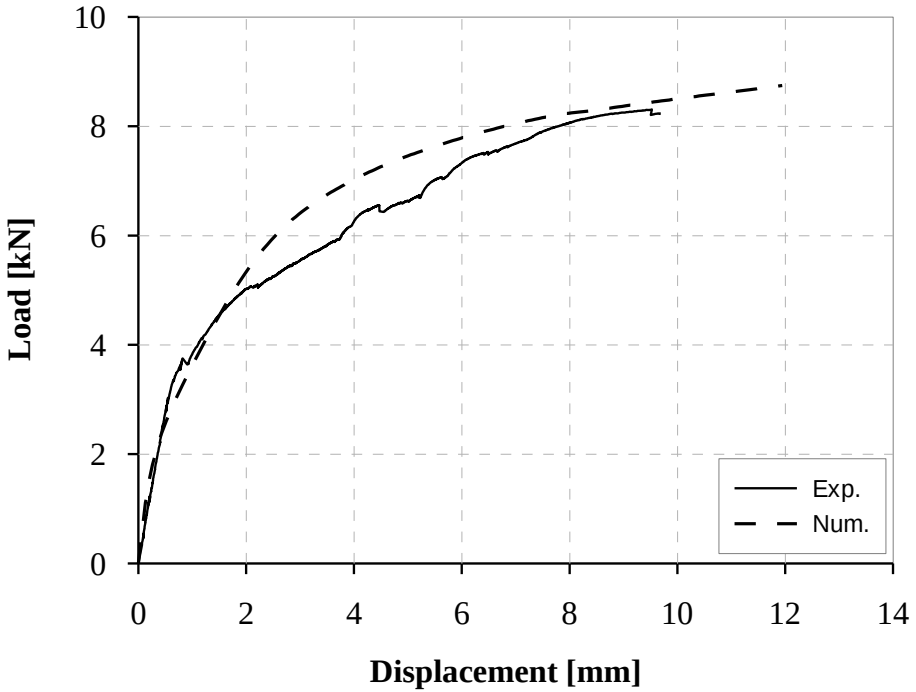
Load [kN]
Displacement [mm]
Exp.
Num.
0
2
4
6
8
10
12
14

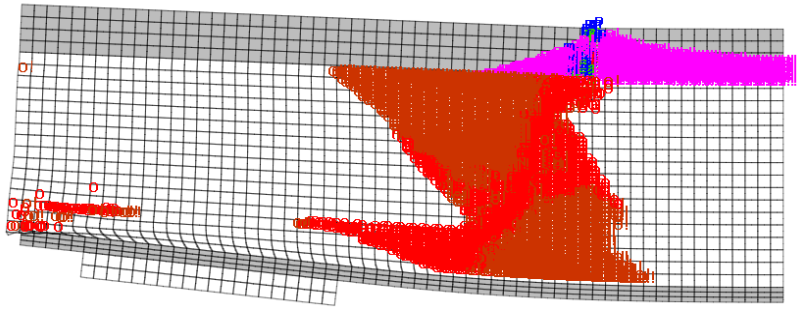

Buckling of TRM layer

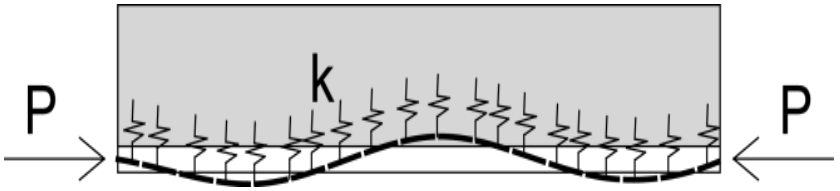

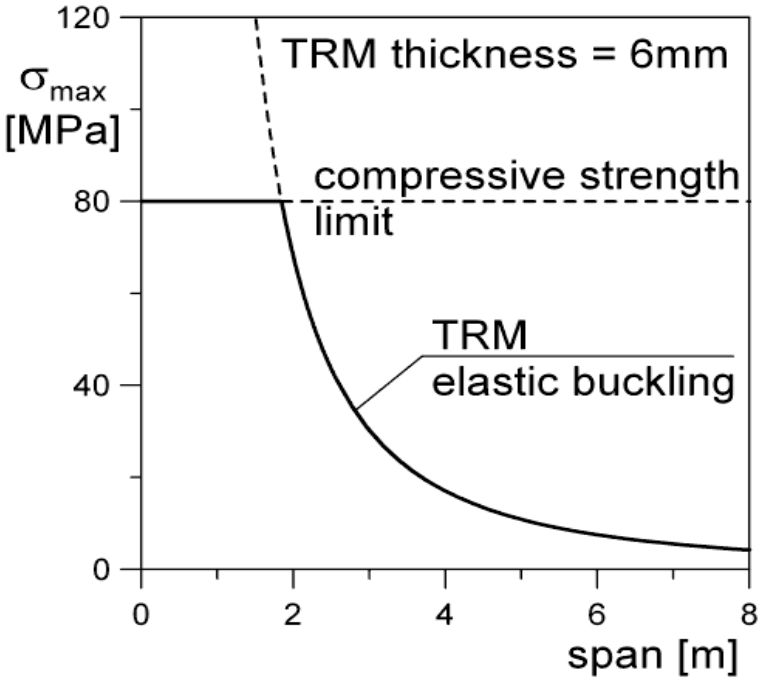

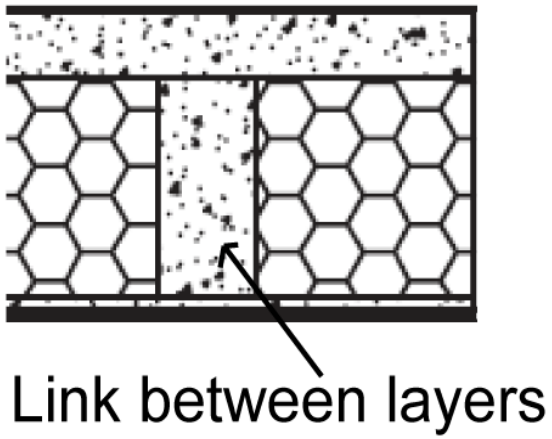

Size effect in unaixial tension

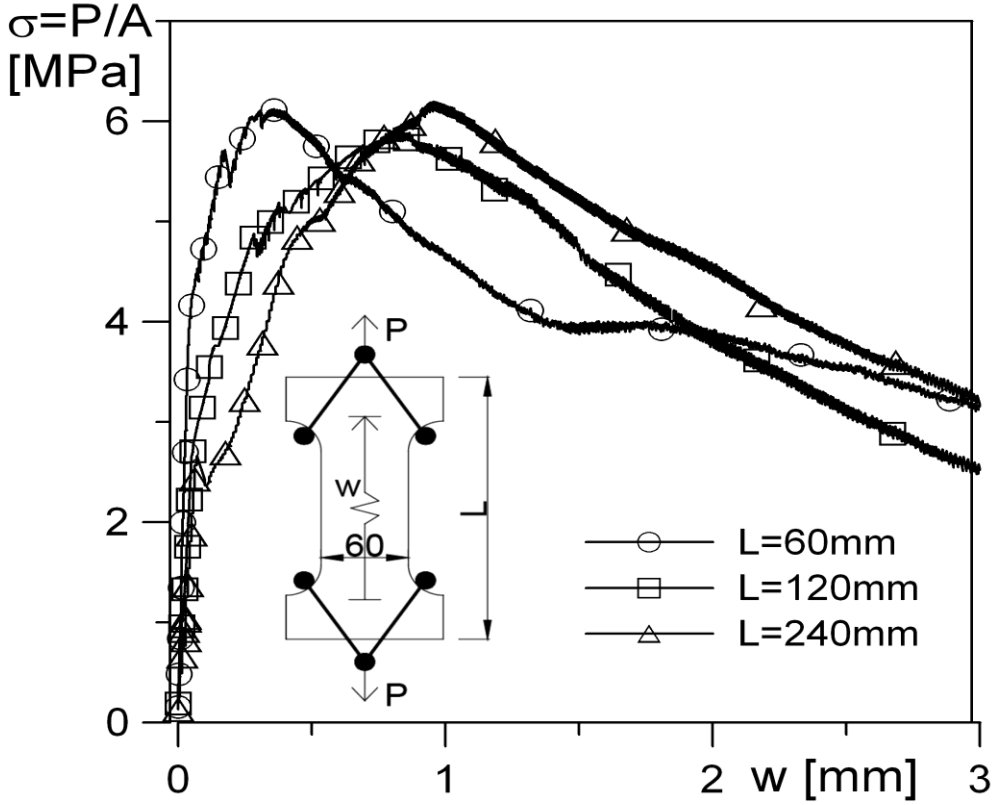

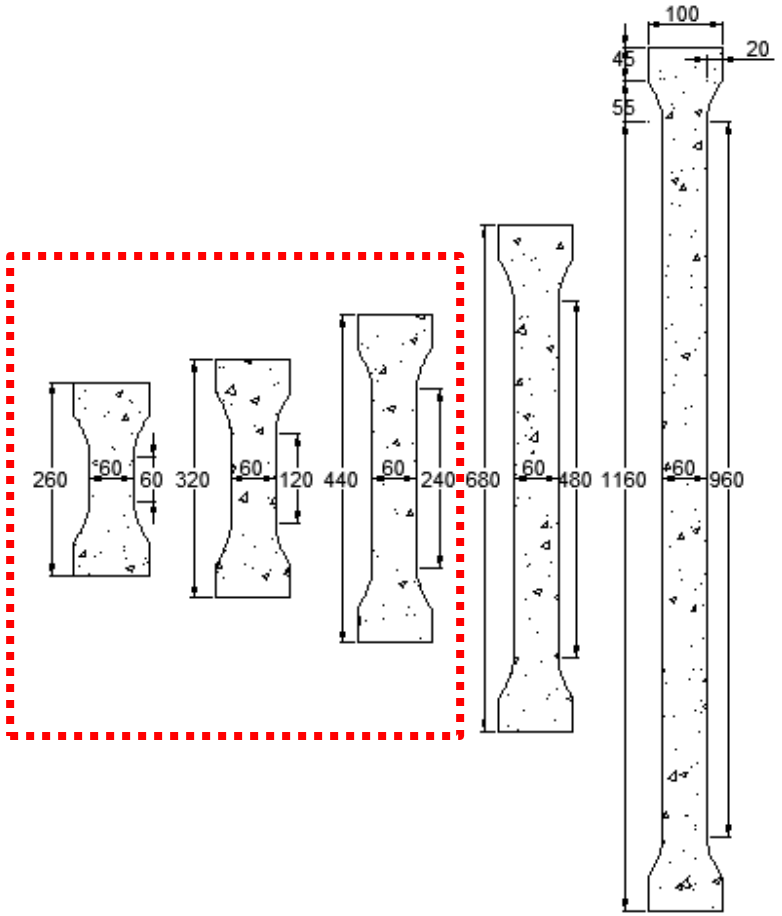

TRC and UHPFRC: a significant synergistic behaviour

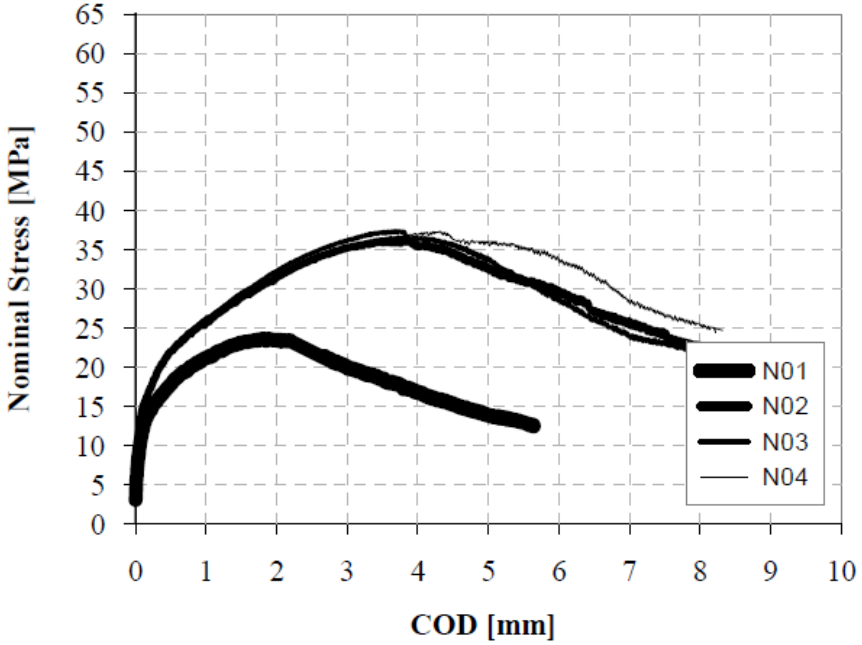

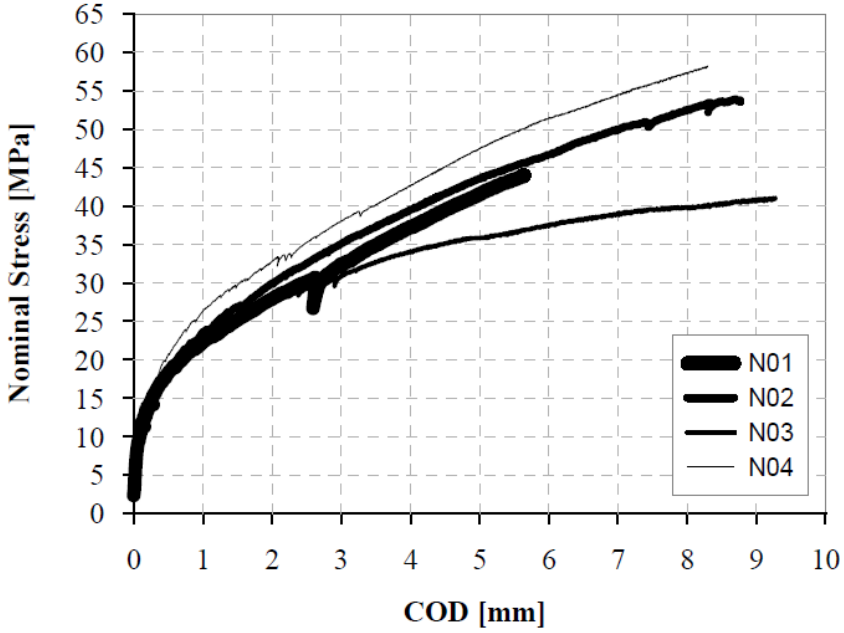

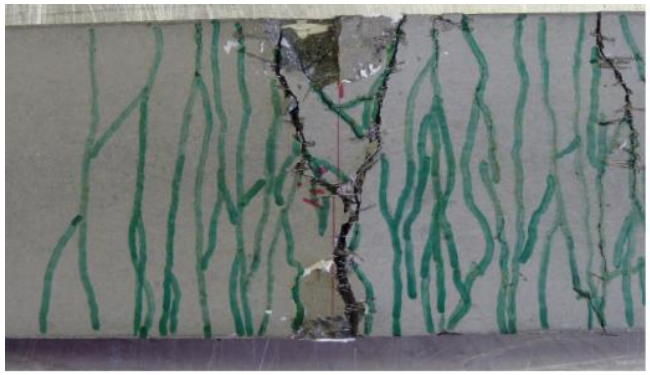

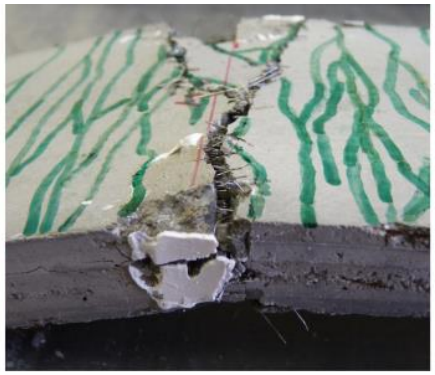

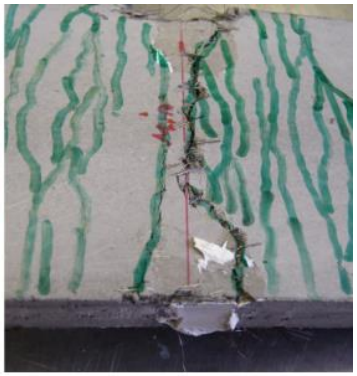

2 layers

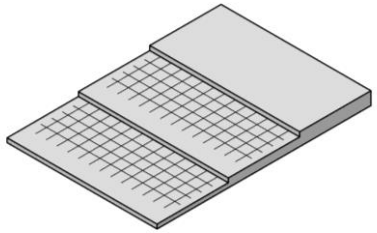

Challenges

✓insulating material: thermal and mechanical performance
✓ compatibility with photovoltaic panels
✓ light structures to reduce the seismic loads and for a sustainable construction
✓ durable & dismountable constructions
✓ fire resistant

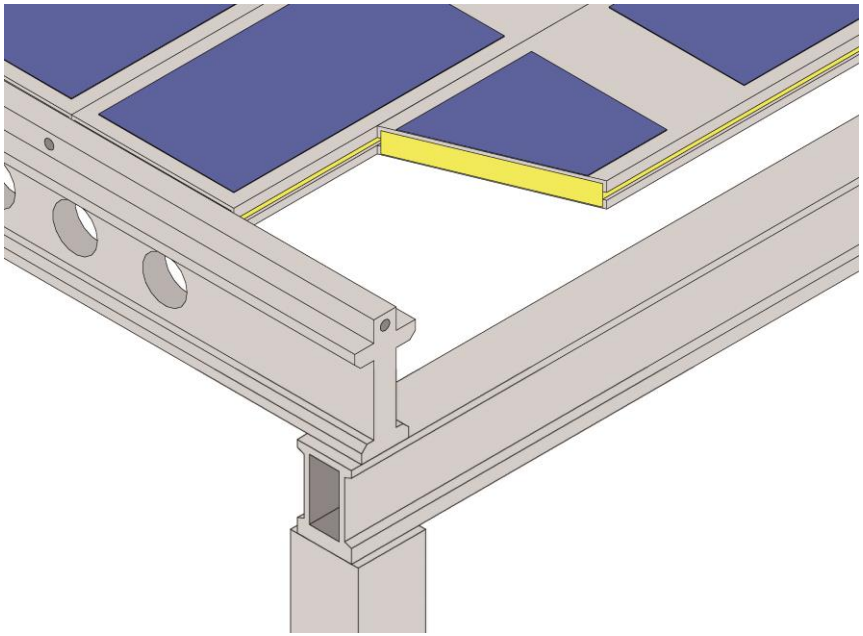

Concluding remarks

✓Thin walled structures represent the future of many solutions for retrofitting and design of roofing and façade systems, due to their ability to reduce the dead weight and to be used in engineered technical solutions aimed at solving at the same time safety, insulation, fire resistance and energy caption

✓Need of “structural” specimens for characterization. The mechanical is not homogeneous and isotropic. If this assumption is forced, a suitable k factor has to be used, especially for local check of safety.

✓The conceptual design requires a global ductile behaviour: if specific bending or axial response is softening, a careful prevision of self-stresses due to shrinkage, thermal loads and boundary conditions must be computed, because if their combination can induce cracking, the crack opening regarded as limit values by Codes can easily be exceeded due to crack opening localization

✓ the addition of a suitable reinforcement as AR glass fabric can simplify the design, guaranteeing a hardening behaviour both in uniaxial tension and in bending. **A special attention to robustness is also absolutely required**

✓the designer has to pay attention to instability and deformability as for steel structures: when precast elements are designed, a special care has to be paid to deformability in the cross section plane, because the shape loss of the cross section can strongly reduce the bearing capacity

✓ In multi-layered solutions a connection between the layers is suggested to prevent the detachment consequent to the buckling of the compressed layer.

✓The in-plane load diffusion can cause a brittle failure in the D-regions, but no needs to reduce the uniaxial compressive force is required if FRC respects the minimum toughness performance requirements expressed in terms of minimum SLS and ULS residual strengths

✓size effect requires further research: the results obtained highlight a weaker size effect dependency of residual strengths even if first cracking strength of FRC seems to be affected as plain concrete. Hybrid solutions with micro-fibres can mitigate also this brittleness effect.

✓A mechanical characterization made at room temperature after a high temp. exposure can give the residual strength variation with temperature, allowing the designer a full fire resistance computation. HPFRCC can represent an interesting solution for fire resistance due to their impressive bending strength up to 400˚C.


Thank you
for your attention